OXI 2018
EUROPEAN OXIDE SCALE CONFERENCE

11-12 / DEC / 2018

Quantitative Description of the Parameters Characterizing Mechanical Failure of Oxides

- *The η - c - Concept* -

Michael Schütze

DECHEMA-Forschungsinstitut

Frankfurt am Main / Germany

Abstract

Stresses in oxide scales can lead to wanted or unwanted mechanical failure of the scales. In thermo-mechanical processing the removal of oxide scales can based on a “wanted” mechanical failure situation. For protective oxide scales in plant operation mechanical failure of the scales is usually unwanted. In either case it would be desirable to have a predictive tool for mechanical scale failure. There is a large amount of scattered information on mechanical scale failure in the literature dating back to as far as the 40ies of the last century. However, only recently a comprehensive concept has been proposed for this situation in the form of the η-c-concept. This concept summarizes the mechanical properties of an oxide scale system by introducing the parameter η and uses as a second parameter the effective physical defect size c. Physical defects are pores, cavities, micro cracks, partial delaminations, etc. Once the parameter η has been established by laboratory measurements the critical strains to scale failure of oxide scale systems of the same type can be assessed merely from metallographic investigations on defect sizes without further work-intensive mechanical testing. In the paper the theory of the η-c-concept is derived and examples of measurement data are presented for Fe-oxide, Ni-oxide and Ti-oxide. Furthermore the industrial potential of the concept is discussed briefly.

Personal data:

- PhD in Materials Science from RWTH Aachen University
- 40 years of research work at DECHEMA-Forschungsinstitut in Frankfurt am Main with 20 years as head of the institute
- In parallel professorship at RWTH Aachen University since 1998
- Past President of the European Federation of Corrosion (EFC) and the World Corrosion Organization (WCO)
- Retired 2018 and now scientific advisor to DECHEMA-Forschungsinstitut
- More than 500 publications and 8 awards

Experimental determination of the critical strain of fracture of oxide scale in hot finishing mill conditions using the sigma test

Wanda Melfo[1], Edoardo Barabino[2]

[1] Tata Steel. R&D, The Netherlands, [2] Eindhoven University. The Netherlands

1. Introduction

The surface quality of steel flat products is one of the main properties demanded by the customers. Surface quality defects are in many occasions originated at the hot finishing mill and are related to the behaviour of the oxide scale during rolling. Rolled-in-scale (RIS) is the collective name for these type of defects. More specifically, the fracture of the oxide before the roll-bite will cause the formation of oxide rafts and the extrusion of the steel during the rolling. At the entry to the roll-bite, a tensile strain is exerted on the oxide layer and the oxide scale will fracture if its critical strain of fracture is surpassed [1][2].

The transition from elasto-plastic to brittle behaviour of the oxide layer is dependent on temperature, adhesion of oxides to the substrate, thickness and proportions of the different (iron) oxide types. Crack formation occurs when the critical strain of fracture in the oxide scale is reached. Authors concur that a critical strain of fracture (ε_c) of the oxide-scale can be defined by:

$$\varepsilon_c = \frac{K}{2E}\frac{1}{\sqrt{c}}$$

This critical strain prediction assumes a void size (c), must know the values of a critical stress intensity factor (K) and the elastic modulus (E) of the oxide-scale [3]–[6]. The expression of K is so far derived from experiments done for one type of steel, and the elastic modulus is derived from generic ceramic mechanical properties, both of which are temperature dependent [7] [6] . However, we have previously demonstrated that the iron oxide proportions are variable depending on the substrate composition [8] and it is well known that the properties of each iron oxide have vast differences and high dependency on the deformation temperature [6] . Therefore, it is fair to assume that K and E are not equal for all oxide scales of iron-based materials.

The information available of the scale fracture is not sufficient to define for industrial off-line models that can help on the designing of both the alloys and the processing. A test to determine experimentally the critical strain of fracture at the conditions of finishing mill rolling, the sigma test, has been developed in our labs [2]. In this paper, the results of the tests for different steel compositions and our interpretation of the relation between oxide composition and critical strain of fracture are presented.

2. Experiment description

The details on the Sigma test design were recently presented in the AISTech 2018 conference [2]. The Sigma test is designed to be able to create a layer of oxide as thin as tertiary scale by resistance heating. Once the oxide is formed, the compression applied is actually a tensile stress on the sample nose, and it is low enough to only fracture the oxide but representative of real strains in the surface of the steel. The moment of the first crack on the oxide is recorded with a high-speed camera and converted to a strain value on the nose. A schematic of the test and shape of the sample is presented in Figure 1.

Four steel compositions, shown in Table 1, were tested . Steel A is a reference low carbon steel and the steels B to D are advanced high strength steels. Strips were taken from cold rolled industrially-processed steels. The nose is deforming at strains below 0.065, which is in the range calculated as the maximum strain in typical HSM conditions

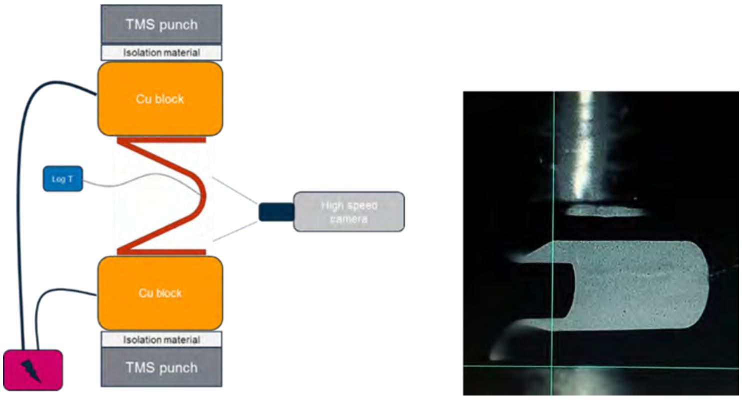

Figure 1. Schematic of the sigma test and image extracted from the high speed camera with the oxide fracturing while the sample was compressed

Table 1. Steels composition (wt%)

Steel	C	Mn	Si	Al	Cr
A	0.03	0.2	0.05	0.03	0.04
B	0.14	2.2	0.1	0.6	0.04
C	0.14	2.1	0.4	0.7	0.2
D	0.14	2.2	0.1	0.03	0.5

Samples were heated to three temperatures: 800, 900 and 1000 ºC, and held for sufficient time to allow oxide formation to occur. The heating rate was adjusted to the final test temperature using either 40 ºC/s for T:1000 ºC or 20 ºC/s for 800 ºC (to avoid overshoot). The expected oxide thickness was calculated with existing constants for low carbon oxide growth and the soaking times adjusted accordingly, the longest test was a total of 50 s until the compression. The aim was to have an oxide thickness of max 8 μm for a short test and 20 μm in a long test. Samples were then deformed at 10 s^{-1}, to a maximum 20 mm (50 %) vertical deformation. Once the sample is compressed, the electrical contact is lost and it starts to cool down, the natural cooling rates were in the order of 12 to 15 ºC/s. The deformed samples were mounted and prepared in cross section to show the centre of the nose. Images were taken with optical microscopy and some with scanning electron microscopy. The thickness and type of oxides were analysed.

3. Main findings

There were many phenomena occurring during the test, such as formation of blisters on different sizes, delamination, and –the expected- fracture of the oxide (see Figure 2). Blisters were forming due to the heating conditions and their onset was related to the steel composition. The control of the test temperature must be improved. Although the temperature at the moment of the compression was the aimed, some samples reached higher temperatures during the test, while others had a different heating rate. These were the first test and an improvement in the method is in progress.

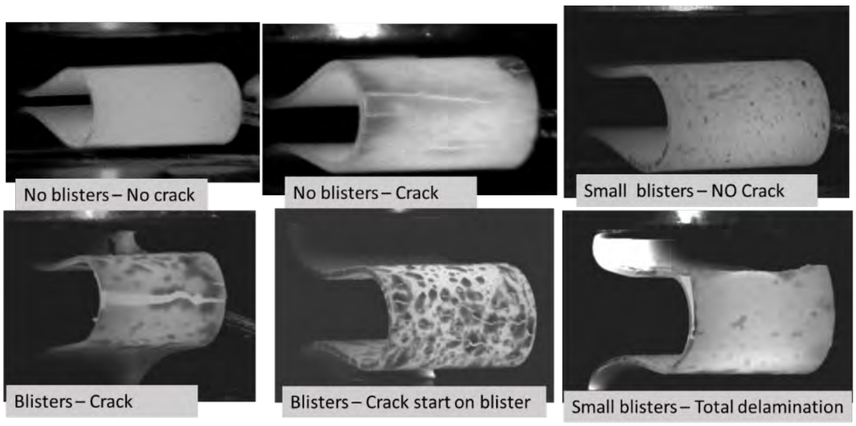

Figure 2. Phenomena occurring pre and during the compression in the sigma test

3.1 Strain of fracture

The results of the strain of fracture are plotted by finding a function that separated obviously the cracked and not cracked samples in at least two of the steels and includes temperature (T) and oxide thickness (X) at the moment of compression: $T^2X^{(-1/2)}10^{-4}$. The results of all tests are shown in Figure 3. These plots show the measured strain when the first crack occurs in the oxide. The dots with a black rim are the samples that blistered. There is an approximate line showing the limit between the crack and not cracked oxides.

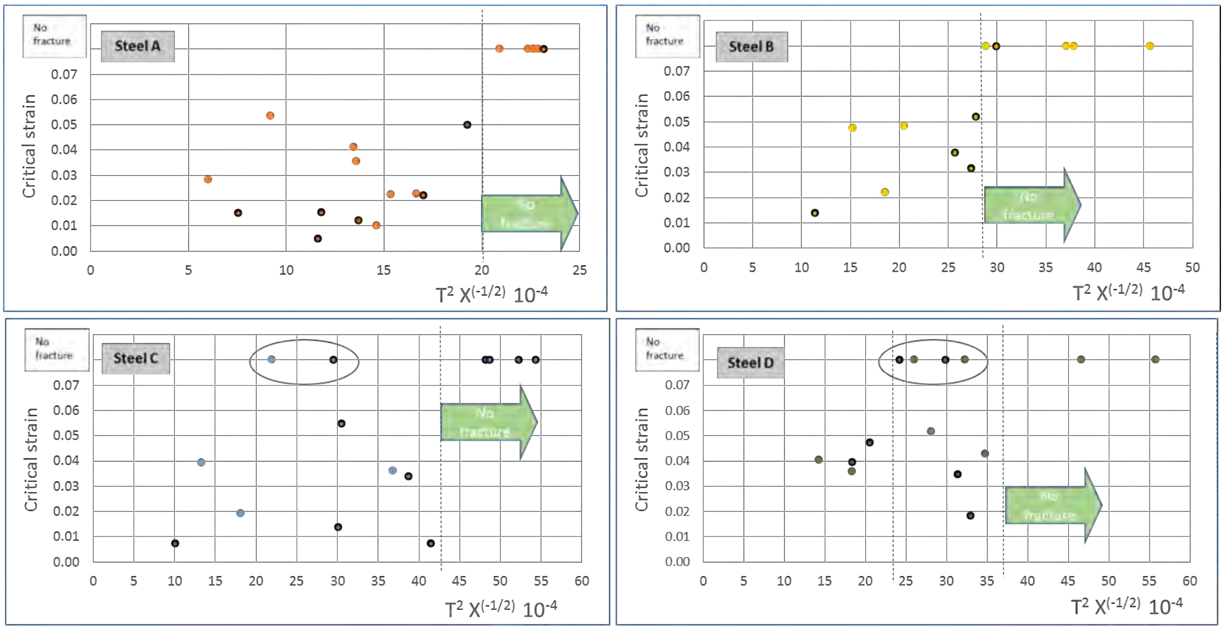

Figure 3. Representation of all experiments as a function of measured strain rate vs temperature and oxide thickness at the time of compression.

3.2 Oxide microstructure

When the samples were examined in cross section, the features of the oxides can be more clearly discerned. It was then revealed that for steel C the oxide has cracked in all tests. Probably because the oxide layer was too thin it was not possible to observe the contrast of the crack with the high speed video camera. For steel D it is also the same case, only on few samples the oxide remain with no cracks.

Steel A: Low carbon

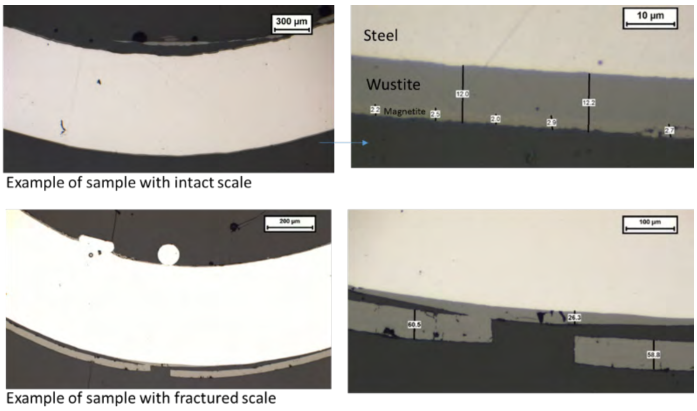

Steel B: Mn + Al

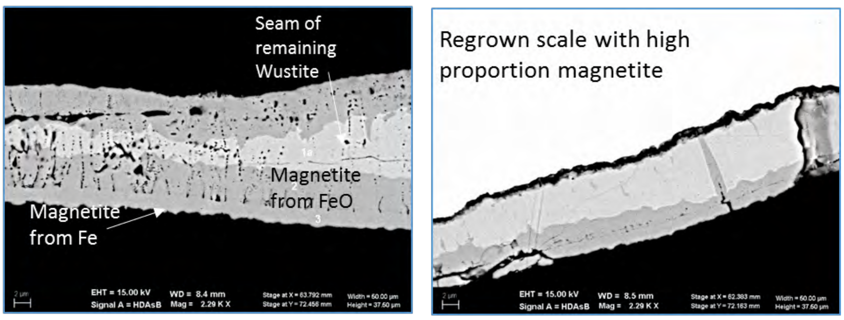

Steel C: Mn+Si+Al

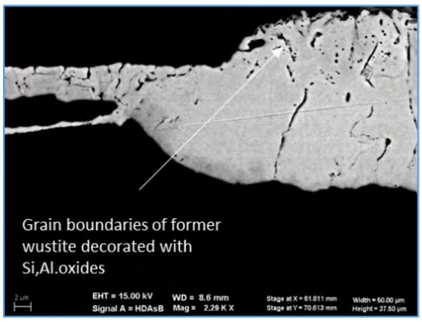

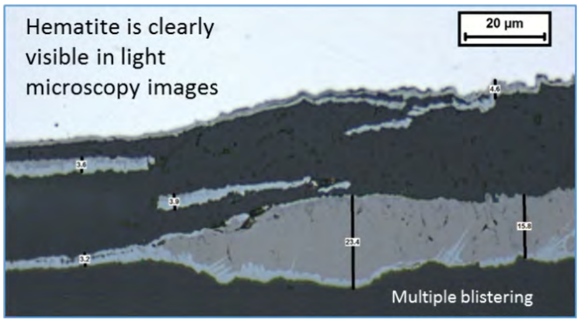

Steel D:

Mn

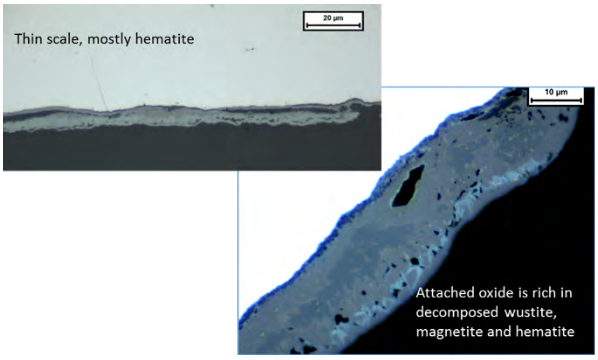

4. Discussion and Conclusions

The critical strain of fracture was determined using the sigma test that allowed the growth of thin enough oxide layers and to apply high strain rates. For low carbon and steel with Mn+Al there is a clear limit between fracture and not fracture and it is related with the temperature and thickness of the oxide. All AHSS steels gave much thinner oxides than calculated for low carbon and the proportions of magnetite and hematite are higher as well. Steel containing Mn+Si+Al forms particularly thin oxides that tend to blister multiple times, the oxide in the conditions tested was always fracturing. The scatter of the test results makes it hard to draw a trend, but it can serve as an alert for the simulation tool of rolling that indicates if the conditions are given for scale fracture yet.

For an accurate prediction of strain of fracturing the blistering onset must be taken into account, once the blister is formed the more rich oxides of iron are formed and fracture will occur earlier than for oxides with same thickness but attached to the steel. We have found the presence of former liquid oxides decorating the wustite grain boundaries. This must hardly occur in the finishing mill conditions, therefore the heating rate should be more accurately controlled to avoid reaching so high temperatures.

The tests show clearly that the behaviour of the oxide is dependent of the steel type, hence the oxide proportions and the adhesion to the substrate. We suggest that any effort to determine fracture behaviour of oxides is done together with kinetic prediction of growth and blister onset.

5. References

[1] M. Krzyzanowski, J. H. Beynon, and C. M. Sellars, "Analysis of secondary oxide-scale failure at entry into the roll-gap," Metall. Mater. Trans. B, vol. 31B, no. 12, pp. 1483–1490, 2000.

[2] W. M. Melfo, J. Wadsworth, and R. Brandon, "Novel Methodology to Determine the Critical Strain of Fracture of Oxide Scale in Hot Finishing Mill Conditions," RS 172296, 2018.

[3] P. Hancock and J. R. Nicholls, "Application of fracture mechanics to failure of surface oxide scales," Mater. Sci. Technol., vol. 4, pp. 398–406, 1988.

[4] J. Robertson and M. I. Manning, "Limits to adherence of oxide scales," Mater. Sci. Technol., vol. 6, pp. 81–91, 1990.

[5] M. Schütze, "Mechanical properties of oxide scales," Oxid. Met., vol. 44, no. 1/2, pp. 29–61, 1995.

[6] Y. Hidaka, T. Anraku, and N. Otsuka, "Deformation of Iron Oxides upon Tensile Tests at 600 – 1250 ° C," Oxid. Met., vol. 59, no. February, pp. 1–8, 2003.

[7] B. Picque, "Experimental study and numerical simulation of iron oxide scales mechanical behaviour in hot rolling," Ecole des Mines de Paris, 2004.

[8] W. M. Melfo, S. Melzer, and P. H. Bolt, "In situ determination of oxides forming in steels containing Mn and Si at finishing mill hot rolling conditions," in European oxide scale conference 2014(OXI 2014), 2014, pp. 79–86.

New Promising Actuators to Control the Cracking Behaviour of Scale During Hot Rolling, Including Enhanced Evaluation Technologies

Diana Espinosa[1], Hugo Uijtdebroeks[1], Jurgen Malbrancke[1]
[1]CRMGroup, Belgium (diana.espinosa@crmgroup.be)

Abstract
In order to control the cracking behaviour and deformation of strip surface scale during rolling a new innovative active actuator is being studied: "micro-dimples indentations". The principle is to induce with textured looper rolls micro-dimples in the strip scale just in front of the roll bite influencing the onset of scale cracks. With the indentations a very fine controlled cracking of scale is obtained in front of the roll bite limiting the metal extrusion through scale cracks during deformation. Different dimple patterns have been studied with and without lubrication. The best result is obtained with 10 µm diameter dimples combined with lubrication, resulting in a controlled cracking of the scale and also an increase of 10% in lubrication efficiency.
Keywords: Scale, Micro-dimples, Hot rolling deformation, Scale cracking

1. Introduction

One of the main concerns of hot strip rolling mills is the occurrence of rolled-in-scale. Even in high performance mills, this defect is still observed on more than 15% of the coils and about 0.1% of critical surface steels are downgraded after pickling due to this defect. During the last decades several studies indicated that the rolled-in-scale defect is linked to an inhomogeneous deformation of the scale layer during rolling. Surface stresses in the scale layer at the entry of the roll bite induce a cracking of the scale layer. In the rolling pass hot metal extrudes through these cracks and capsules scale parts. The severity of rolled-in-scale is related to the friction in the roll bite (e.g. roll wear), the reductions, the scale thickness and the temperature. These rolling parameters are however inherent to the rolling process to obtain the required metallurgical properties. The rolling conditions however can be changed by different existing actuators influencing the friction (e.g. lubrication) and the scale properties (e.g. skin cooling, interstand sprays). In order to control the cracking behaviour and to create a cracking network beneficial for the surface quality at the end of the process, numerous hot rolling trials with several configurations of existing actuators have been performed at CRM. All the actuators have a different effect on cracking as visible in Figure 1.

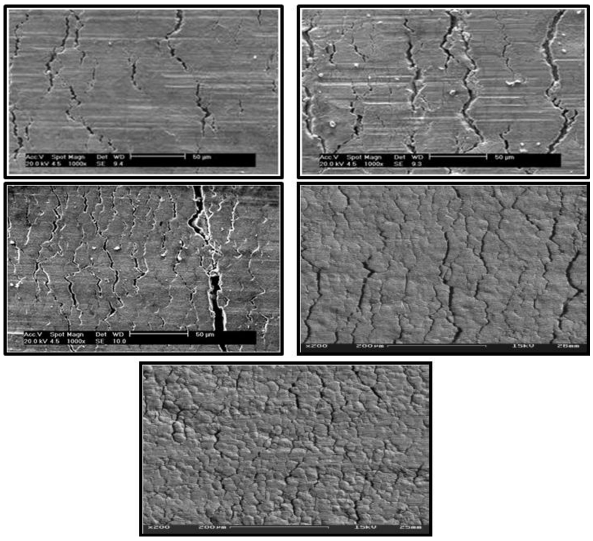

Figure 1 Different crack networks formed by changing external actuators.

It has also been observed that the existence of a fine crack pattern minimises extrusion at the interface steel/scale, changes scale adherence and reduces rolled-in scale defects [1]. As the existing actuators have however also a different main objective (e.g. skin cooling to reduce the heat flux to the work roll). By this, it is difficult to modify these operating conditions in industrial mills. For this reason new external actuators have been studied at CRM (e.g. nitrogen rolling, burning of oxygen in air). One of the most promising actuators was the indentation of micro-dimples in the scale layer just before the rolling pass.

2. Definition of micro-dimples

Many studies show that well-designed dimples or grooves can drastically improve tribological performance of sliding surfaces. The micro-dimples can act as lubricant reservoirs capable of feeding lubricant directly into the contact and initiating micro elasto-hydrodynamic lubrication. [2-6]
However, no previous studies exist how a micro-dimple can influence the cracking behaviour of scale layers when applying a tension.
To perform this experimental study existing micro-dimple patterns to enhance lubrication have been applied.

3. Inducing micro-dimples

For the hot rolling trials at CRM a pinch roll has been designed with different patterns. The objective is to induce the selected patterns of dimples/grooves on the scale layer before the roll bite during hot rolling. To induce the dimples, the pinch roll has peak texture, so it is possible to transfer to the scale layer as dimples. At the roll bite lubrication will be used, so that the dimples work as lubricant reservoir during the rolling reduction.
A pinch roll has been machined by laser texturing with 6 different size and distribution of peaks pattern. The selected patterns are shown in Figure 2.

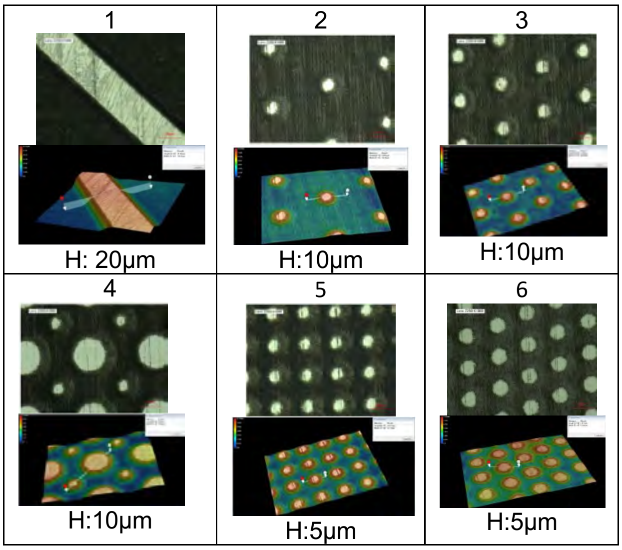

Figure 2 Micro-peak patterns, laser technique

4. Experimental methods: Hot rolling trials

The hot rolling line allows the continuous rolling of a baby-coil with conditions very close to hot rolling process. Furthermore it provides the possibility to change parameters in well controlled conditions. The decoiler furnace is under inert atmosphere at slightly higher pressure than atmospheric in order to avoid oxidation during reheating. The reheating temperature and the distance between the decoiler and the stand are kept constant during the trials. The strip is deformed in the first stand and it is quenched right after the exit of the gap so that the scale evolution is frozen. See Figure 3.

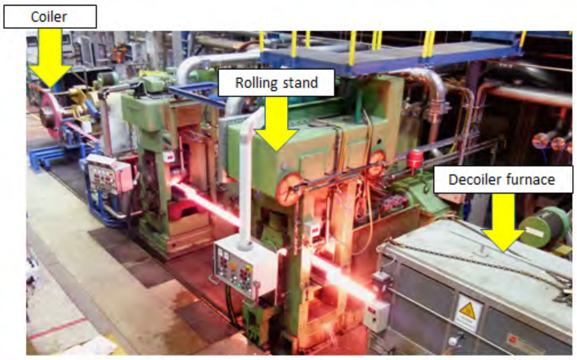

Figure 3 Hot rolling pilot line in CRM Gent

In the trial the pinch roll was installed on the looper roll, fixed to a structure and a compression force was applied on the strip by the piston of the looper, the pressure of the piston was varied during the trial. Figure 4.


Figure 4 Pinch roll with peaks pattern.

The strip is passing by the contact of the pinch and looper roll at around 950°C. The lubrication was set ON and OFF in order to see the behaviour of the dimples in combination with lubrication during rolling. Samples were taken directly after the roll bite and cooling, to analyse the surface offline and to see the effect of the dimples on deformation, scale cracking and interface steel/scale behaviour. See Figure 5.

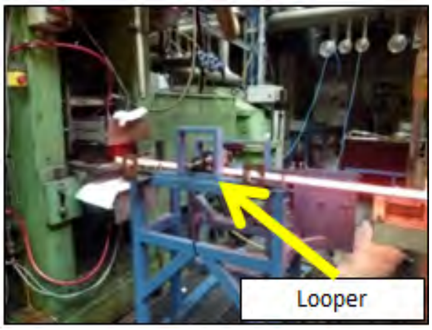

Figure 5 Hot rolling trials using pinch rolls to induce micro-dimples on the oxide layer

5. Results and discussions

5.1 Surface analysis of pinch rolls after hot rolling trials

The pinch roll was analysed after the hot rolling trials to check the degradation of the peaks after contact with strip at high temperature 950°C. The peaks are intact for almost all the patterns, only the pattern #5 and #6 (height 5µm) showed a slightly wear.

5.2 Rolling forces during hot rolling trials

The first surface observations indicated that when lubrication is used, the transference of the pattern is very clear. The lubrication goes into the dimples, working as reservoirs [2], and helps to keep the dimples printed on the strip creating a layer of lubricant that is able to protect them from deformation, Figure 5, giving a smooth surface aspect and reducing rolling forces up to 10%, see Figure 6. This is especially visible on samples rolled at 50% reduction.

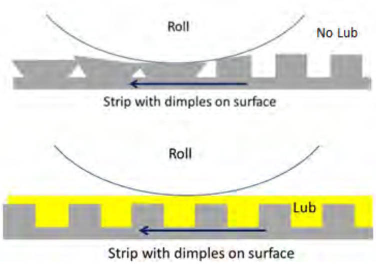

Figure 6 Effect on strip surface when dimples and lubrication are used during hot rolling

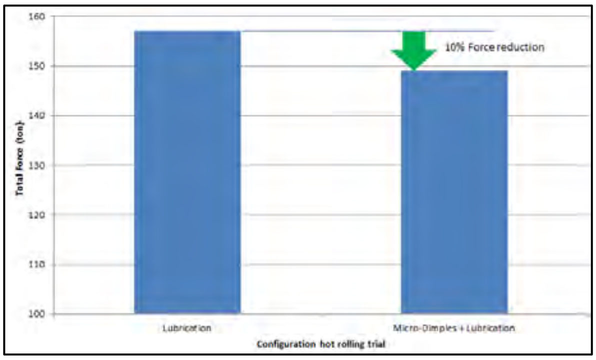

Figure 7. 10% of force reduction when micro-dimple and lubrication are used.

5.3 Surface analysis of pattern on strip material

The analyses of the samples under microscope validate the first observations during the trials. The strip surface rolled with micro-dimples without lubrication shows an arbitrary crack network with large and open cracks. Some dimples are visible but disappears during the rolling reduction. In the other hand the surface rolled with micro-dimples and lubrication clearly shows that the crack network follows the dimples pattern, no deep and large cracks are visible. The pattern printed on the surface is visible after the roll bite for all the 6 patterns when lubrication is ON. In the Figure 7 the cracking induced by pattern #6 is visible.

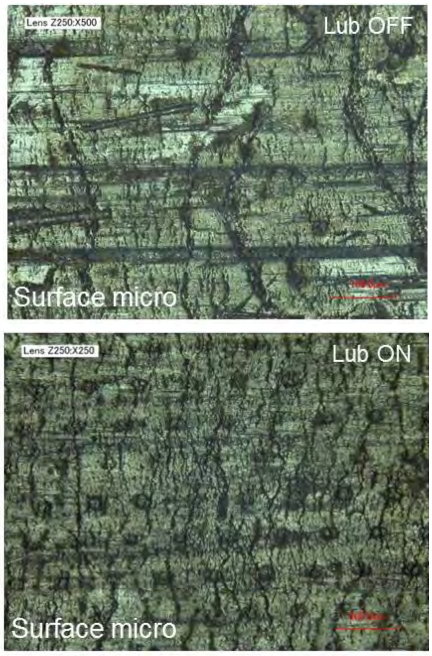

Figure 8 Surface after micro-dimples transfer to the strip and with Lubrication ON/OFF

5.4 Cross section analysis

At 50% of rolling reduction the use of lubrication in combination with micro-dimples showed an effect on the interface scale/steel. The roughness at the interface is much lower when lubrication is used. Low extrusion of fresh metal and a homogenous oxide layer is visible. Figure 8.

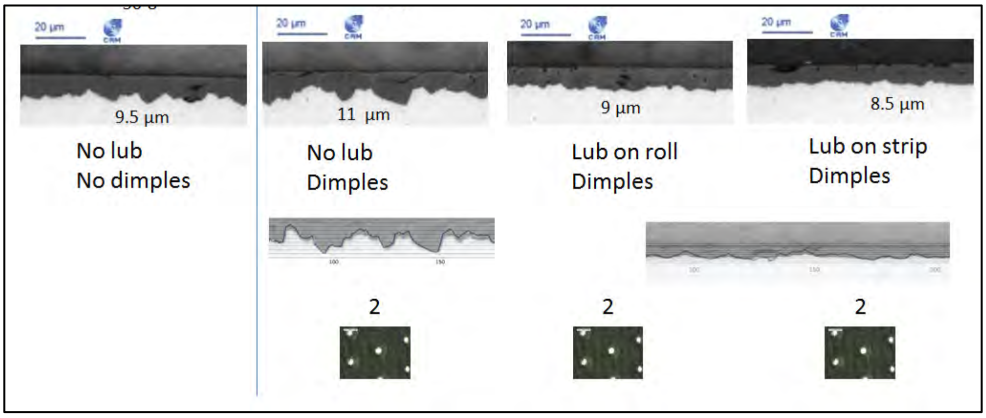

Figure 9. Cross section of samples after rolling at 50% reduction with and without lubrication – Pattern #2

6 Conclusions

The micro-peaks texture obtained by laser ablation is symmetric along the surface of the pinch rolls. The use of the pinch roll with micro peaks printing micro dimples on the strip reduces force up to 10% during deformation in combination with lubrication compared to lubrication without dimples application.

The dimples are visible on strip after roll bite when reduction is applied. This effect is especially visible when lubrication is used. The lubrication goes into the dimples, working as reservoirs, and helps to keep the dimples printed on the strip creating a layer of lubricant that is able to protect them from deformation giving a smooth surface aspect.

The best result is obtained with pattern #6, 10 µm diameter dimples combined with lubrication, resulting in a controlled cracking of the scale and also an increase of 10% in lubrication efficiency.

The surface rolled at 50% with dimples and lubrication is smoother and homogenous along the length, the interface compared to the surface rolled without lubrication which is opaque and rough.

7 Acknowledgments

Grateful acknowledgements are made to the CRM members: ArcelorMittal and TataSteel.

8 References

[1]M. Picard, C. Brunon, J.L Borean, “Rolled-in scale indicator based on description of scale physics under the roll bite”. La Revue de Métallurgie - ATS – JSI 2007

[2]L.M. Vilhena, B. Podgornik, J. Vižintin, J. Možina, “Influence of texturing parameters and contact conditions on tribological behaviour of laser textured surfaces”, Meccanica (2011) 46, pp 567–575

[3] S. Yuan, W. Huang, X. Wang, “Orientation effects of micro-grooves on sliding surfaces”, Tribology International, Volume 44, Issue 9, August 2011, pp 1047–1054

[4] T. Matsumura, S. Takahashi, “Micro dimple milling on cylinder surfaces”, Journal of Manufacturing Processes 14 (2012), pp 135–140

[5] X. Wang, W. Liu, F. Zhou, D. Zhu, “Preliminary investigation of the effect of dimple size on friction in line contacts”, Tribology International 42 (2009), pp 1118–1123

[6] W. Huang, L. Jiang, Ch. Zhou, X. Wang, “The lubricant retaining effect of micro-dimples on the sliding surface of PDMS”, Tribology International 52 (2012), pp 87–93

Grain boundary oxidation of highly alloyed carbon steels at coiling temperature

L. Agrizzi Ronqueti[1,3], M. Picard[1], J.M. Mataigne[2], J. Favergeon[3], M. Risbet[3]

[1] *ArcelorMittal R&D Maizières Process;* [2] *ArcelorMittal R&D Maizières Automotive,*
[3] *Université de Technologie de Compiègne*

ABSTRACT

We studied the selective oxidation of alloying elements in steels in the temperature range of 530C to 700°C in oxygen lean atmospheres. The oxidation regime evolves from bulk oxidation (BO) at the higher temperature, to grain boundary oxidation for the lower ones (GBO). Basically, the GBO depth observed at low temperature can be described making use of the Wagner's model when oxygen is the only diffusing element. Such a description allows estimating the value of the GB oxygen diffusion coefficient at that temperature.

Silicon diffusion evolves according to temperature: while negligible at 530°C, it happened in the GB only at 600°C, and in the bulk at higher temperature. The Manganese content of the Fe-Mn binary alloys was always high enough to promote Mn diffusion in all experiments. A Mn depletion zone was so always detected in the vicinity of oxidized GB.

GB oxidation was not homogeneous: oxidation preferentially occurred in high -angle grain boundary misorientations (higher than 15° misorientation).

INTRODUCTION

At the exit of the hot mill, coils cool down for several hours. During cooling, the metal surface inside wraps are no longer exposed to the atmosphere. However, the scale present on the steel surfaces acts as an oxygen reservoir and releases a tiny amount of oxygen into the metal. The local oxygen potential is sufficient to induce selective oxidation of the alloying elements notably carbon, silicon and manganese.

Except for carbon whose oxides are gaseous, the other alloying elements develop selective oxides inside the steel matrix, which may exhibit different shapes. One of them is grain boundary oxidation (GBO) which can be detrimental to fatigue resistance. So, it must be removed during pickling, which is currently one of the major complications to produce new highly alloyed steels.

The aim of this work was to increase the knowledge of internal selective oxidation (mainly GBO) in new steels with complex alloy compositions.

EXPERIMENTAL PROTOCOL

The experiments were carried out in a furnace with controlled temperatures ranging from 450 °C to 700 °C, and atmosphere being 95%N_2 - 5%H_2 with controlled moisture. The weight changes during oxidation tests were recorded, but not used for this analysis.

Two sets of steels were used in this research. The first set are iron based model alloys. The scale was removed to avoid any effect induced by the movement of the scale/steel interface. The alloying elements were limited to silicon and manganese (and some carbon) to avoid complex behaviors.

The second set consisted in an industrial steel (Dual Phase 600), whose scale was either removed (naked) either kept.

The localization of oxides inside the samples was measured by using SEM/EDS, SIMS and NanoSIMS techniques.

Table 1 - Chemical compositions showing silicon, manganese and carbon contents [wt%] of the steels used in this study.

	Si	Mn	C	Fe
Fe-0.2%Si	0.209	0.010	0.013	Bal.
Fe-0.5%Si	0.496	0.003	0.012	Bal.
Fe-1.5%Si	1.55	0.001	0.002	Bal.
Fe-2%Mn	0.028	2.013	0.150	Bal.
Fe-5%Mn	0.036	5.069	0.153	Bal.
Fe- 0.4%Si- 1%Mn	0.398	1.07	0.320	Bal.
DP600	0.237	1.97	0.083	

DECARBURIZATION IS DEEPER THAN OXIDATION ALONG GRAIN BOUNDARIES

During the thermogravimetric experiments, a mass loss was first recorded before observing the mass gain. This is due to decarburization occurring in parallel to grain boundary oxidation.

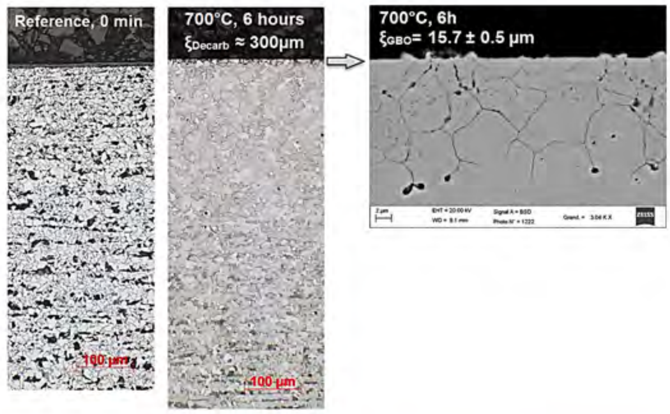

Figure 1 – Optical and SEM micrograph showing decarburization and grain boundary oxidation depths
DP600 at 700°C for 6 h and -5°C dew point.

For all studied samples, both decarburization and grain boundary oxidation occurred simultaneously. However, decarburization depths were always much deeper than grain boundary oxidation (Figure 1).

Figure 2 shows the carbon monoxide content recorded in the exhaust gas (blue line). Decarburization was important during the first 15 minutes but, as it is controlled by carbon solid state diffusion, it decelerated quickly and the CO emission came down after about 30 minutes. During that period, the dew point (red line) was modified by the CO evolution ($H_2O + CO \rightarrow H_2 + CO_2$) before reaching its nominal value afterwards.

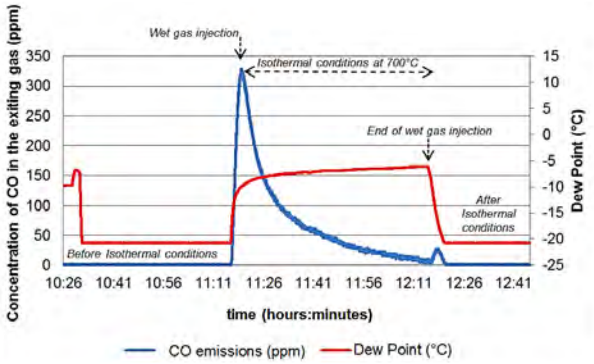

Figure 2 – CO emissions (blue line) and dew point (red line) during tests (700°C for 1 hour in N_2-5%H_2) DP600 no mill scale.

Cross section of this sample (etched with nital solution) showed a 200 µm depth decarburization layer while oxidation depth was only 15 µm. As most of the tests lasted more than six hours, the disturbance induced by decarburization remained negligible.

SCALE IS THE OXYGEN SOURCE FOR INTERNAL OXIDATION

We performed tests with either naked samples or scaled ones. For the naked samples, the oxygen potential was imposed by the furnace atmosphere by controlling the moisture content. The P_{O2} was chosen to match the wüstite-iron equilibrium at the test temperature.

For the scaled samples the oxygen potential was set at wüstite-magnetite equilibrium over 570°C or at the magnetite-hematite equilibrium below. This ensured that the furnace atmosphere remained neutral regarding the scale, inducing no unwanted oxidation nor reduction.

For both naked and scaled samples, the grain boundary oxidation depths were similar (Figure 3 at 530°C and Figure 4 at 600°C). This proves that the oxygen potentials at the metal surface was the same for both situations.

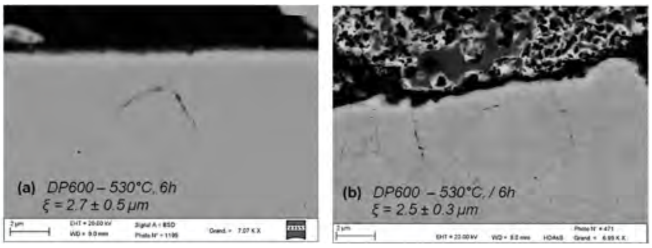

Figure 3 –same GBO for DP600 without scale (a) vs; with mill scale (b) for oxidation tests at 530°C

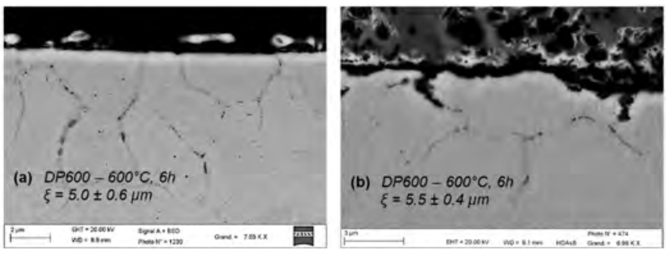

Figure 4 – Internal oxidation depths for DP600 naked samples (a) and with rolled scale (b) for tests at 600°C

MORPHOLOGY OF INTERNAL OXIDATION

According to Harrisons, diffusion inside poly crystal can be classified into three regimes depicted in figure 5.

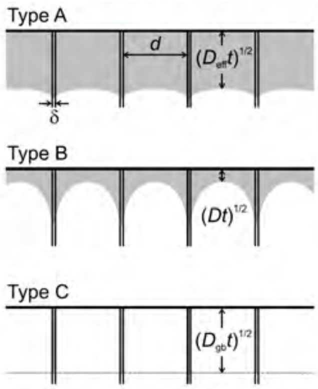

Figure 5 - A, B, and C diffusion regimes in a polycrystal according to Harrisons [Har-1961].

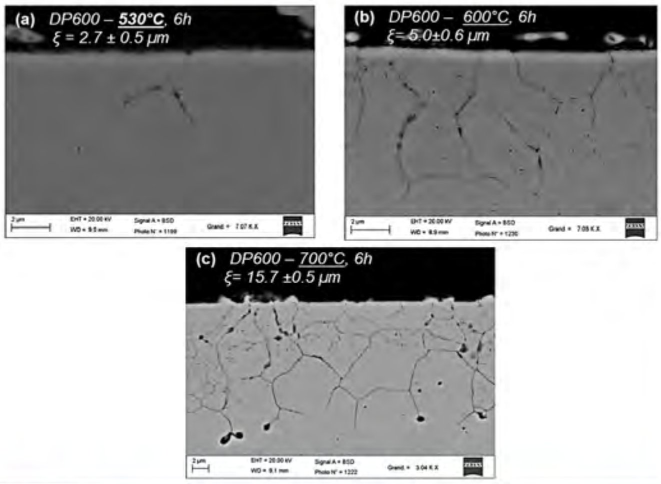

Figure 6 – The internal oxidation depths increase with temperature. Samples studied: DP600 in the absence of mill scale after oxidation tests during 6 h at 530, 600 and 700°C.

When oxidizing DP600 and Si model alloys, all the three patterns where found depending on the treatment temperature. At 530°C only scarce pure GBO was observed while both intra and inter granular oxidation occurred at 700°C.

The same observation could be done when rising the silicon content for treatments at 600°C. For the 0.2% and 0,5%Si alloys, only GBO was detected, while some intra-granular oxide was present with the 1.5%Si samples.

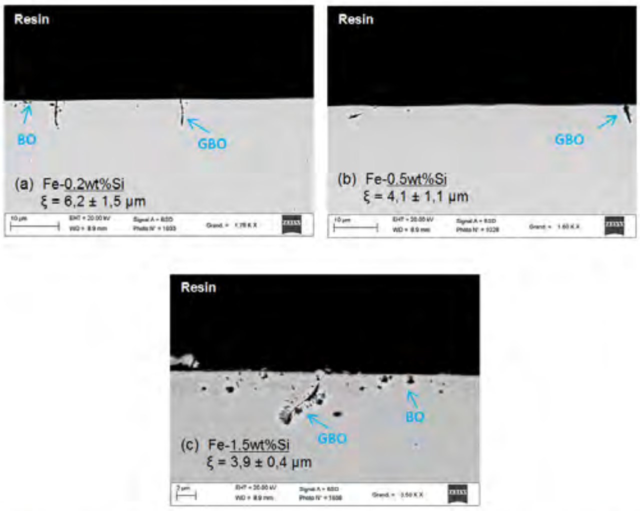

Figure 7 – (a) Fe-0.2wt%Si, (b) Fe-0.5wt%Si and (c) Fe-1.5wt%Si, showing the decrease of the internal oxidation depth with an increase of the silicon content; 600°C 26 hours [Agr-2018a]

SILICON DIFFUSION

NanoSIMS analyses were carried out on cross sections in order to detect possible diffusion of silicon.

The results showed three different silicon diffusion behaviors at three coiling temperatures [Agr-2018a].

- At 530°C, no silicon depletion could be detected neither around neither along grain boundary (Figure 8).
- At 600°C, no Si depletion was detected in the bulk, but depletion of Si in the GB, just below the oxidation depth, was detected.
- At 630°C, a silicon depletion was detected in both along the GB and in the bulk near the grain boundary (Figure 10).

As no depletion of Si could be detected at 530°C, the Wagner's formalism of pure internal oxidation was used to assess the value of the oxygen diffusion coefficient in the GB. The results give: Do in GB = 52±42 µm²/s [Agr-2018a]
Such a value is about 100 times greater than the oxygen bulk diffusion at the same temperature as assessed by Swisher and Turdogan [SWI-1967].

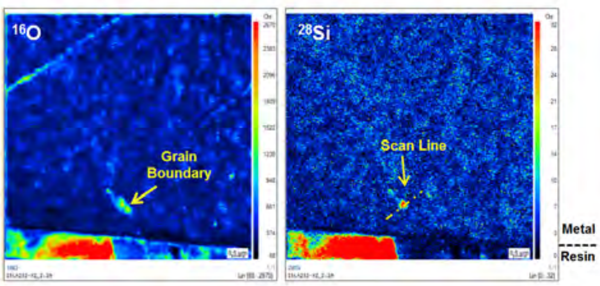

Figure 8 – NanoSIMS cartographies showing no evidence of Si depletion Fe-0.2wt%Si oxidized at 530°C for 6 h [Agr-2018a].

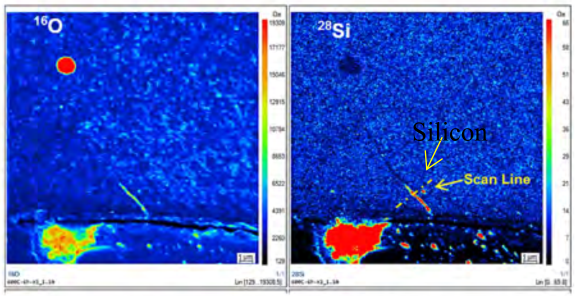

Figure 9 – NanoSIMS cartographies showing Si depletion along GB Fe-0.2wt%Si oxidized at 600°C for 6 h [Agr-2018a].

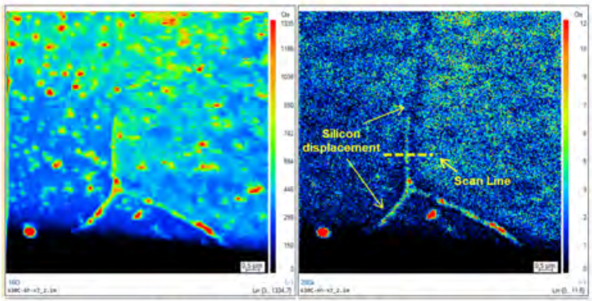

Figure 10 – NanoSIMS cartographies showing Si depletion along and around GB Fe-0.2wt%Si oxidized at 630°C for 6 h [Agr-2018a].

MANGANESE DIFFUSION

For all the Fe-%Mn alloys studied here, manganese depletion was always observed in the bulk (figure 11). This is probably caused by the high level of the Mn content in all the Fe-Mn samples. Another effect that could play a role in Mn diffusion is the higher solubility product of MnO compared to SiO_2, allowing some Mn to diffuse even within the oxidized zone.

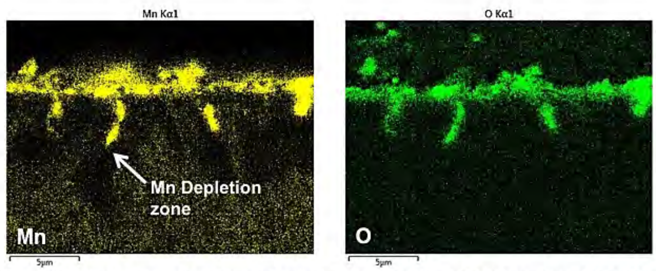

Figure 11 – f Fe-5%Mn showing the strong enrichment of Mn and O inside the grain boundary and a Mn depletion around GB. 600°C, 26 hours dew point –5°C.

INFLUENCE OF MISORIENTATION ON GRAIN BOUNDARY OXIDATION

The influence of grain boundary misorientation on GBO was proved by correlating SIMS and EBSD results. Low-angle grain misorientations (< 15°) were almost immune to GBO whereas high-angle grain misorientations (> 15°) usually exhibited GBO [Agr-2018b].

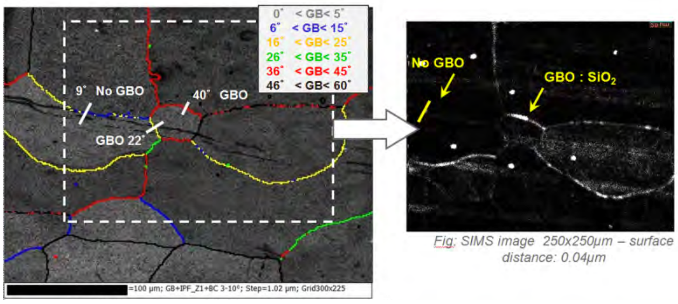

Figure 12 –EBSD (left) and SIMS (right) results. GBO is present for high misorientation-angle (> 15°) while low misorientation angle (< 15°) seems to be free of GBO.
Fe-0.2wt%Si, at 600°C, 6 h and DP = -5°C [Agr-2018b].

This can be explained mainly in terms of grain boundary energy. High-angle boundaries contain large areas of poor fit and have a relatively open structure [Meh-2007]. Moreover, the greater atoms disorder provides many gaps to facilitate the oxygen and/or alloying elements diffusion, thereby reducing the constraints on oxides precipitation.

GENERAL CONCLUSION

The main conclusions obtained throughout this PhD work are summarized below.

- An experimental setup to study selective oxidation in laboratory was developed well representative of industrial coil cooling.

- During oxidation tests, both decarburization and selective internal oxidation occurred, but decarburization only played a role for a short period of time and did not impair the development of GBO

- Scale acted as an oxygen source, sufficient to induce selective internal oxidation.

- Grain boundary oxidation depths increased with temperature indicating conditions where the counter diffusion of the alloying element did not play a major role compared to in depth diffusion of oxygen. At 530 ° C, on Fe-Si binary alloys, no Si depletion was observed so that it was possible to assess the O GB diffusion coefficient at that temperature; its value was 100 times greater that its value in the bulk; for higher temperatures, nano-sims results revealed the existence of Si depletion

- For Fe-Mn alloys, manganese depletion zones were always observed, probably because of the high Mn content of these samples.

- Grain boundary misorientations play has an important role on GBO development. High-angle grain misorientations (>15°) are preferential oxides precipitation sites. On the contrary, a low-angle grain misorientations (<15°) were found almost free of GBO.

The knowledge developed in this work will help to mitigate the consequences of the selective internal oxidation (mainly GBO) in the production of the new steels with complex alloy compositions.

REFERENCES

[Agr-2018a] Agrizzi-Ronqueti, L., Favergeon, J., Risbet, M., Picard, M., & Mataigne, J.M. (2018). Silicon internal selective oxidation of Fe-x%Si model alloys at high temperatures - Effect of Si content and temperature. Submitted in Oxidation of Metals

[Agr-2018b] Agrizzi-Ronqueti, L., Risbet, M., Favergeon, J., Picard, M., Mataigne, J.M. (2018). Effect of grain boundary misorientations on the Si and Mn selective grain boudary oxidation in a □-ferrite matrix. Submitted in Oxidation of Metals

[Hui-2005] Huin, D., Flauder, P., & Leblond, J. B. (2005). Numerical simulation of internal oxidation of steels during annealing treatments. Oxidation of metals, 64(1), 131-167.

[Hui[A]-2016] Huin, D., Bertrand, F., (2016). An available tool to evaluate selective oxidation phenomena: OMEGA - Oxidation Modeling in finite Elements for Galvanizing Annealing lines. ArcelorMittal Global R&D Ref: 2016 23936 RDMA.

[Hui[B]-2016] Huin, D., Huin, T., (2016). First simulations of inter-granular oxidation using OMEGA (selective oxidation model in Sysweld environment). ArcelorMittal Global R&D Ref: 2016 24028 RDMA.

[Liu-2011] Liu, H., He, Y., Swaminathan, S., Rohwerder, M., & Li, L. (2011). Effect of dew point on the surface selective oxidation and subsurface microstructure of TRIP-aided steel. Surface and Coatings Technology, 206(6), 1237-1243.

[Meh-2007] Mehrer, H. (2007). Diffusion in solids: fundamentals, methods, materials, diffusion-controlled processes (Vol. 155). Springer Science & Business Media.

[Swi-1967] Swisher, J.H. Turkdogan E.T. (1967) Solubility, permeability and diffusivity of oxygen in solid iron. AIME MET SOC TRANS, 239(4), pp 426-431

[Tan-2013] Tang, B., Jiang, L., Hu, R., & Li, Q. (2013). Correlation between grain boundary misorientation and M 23 C 6 precipitation behaviors in a wrought Ni-based superalloy. Materials Characterization, 78, 144-150.

[Wag-1959] Wagner C., (1959). Reaktionstypen bei der Oxydation von Legierungen. Zeitschrift für Elektrochemie, 63, 772-782.

Influence of the oxide layer on the spray cooling intensity

M. Chabicovsky, O. Resl, M. Raudensky
Brno University of Technology, Heat Transfer and Fluid Flow Laboratory, Brno, Czech Republic

Abstract

Formation of oxide layers on the surface is inherent part of the steel production. The oxide layer primarily affects the surface quality and material losses during the steel processing. The influence of the oxide layer on the cooling intensity is not frequently reported but even thin layers of oxides can significantly modify the cooling intensity. The oxide layer factor is not as important as the water flow rate but it should be also considered for optimal regulation of the cooling process. The influence of the oxide layer on the heat transfer coefficient and Leidenfrost temperature is investigated in this paper. Laboratory measurement compares the spray cooling of oxide-free steel surface and oxidized steel surface. It shows significant change of the Leidenfrost temperature and heat transfer coefficient due to the oxide layer.

Keywords: Scale, oxide layer, heat transfer coefficient, spray cooling, Leidenfrost temperature

INTRODUCTION

Water spray cooling is a common cooling method used in many high temperature industrial applications, such as metal processing or electronics cooling. Continuous casting and hot rolling of the steel includes the formation of oxides on the surface. These oxides form a porous layer. The oxide layer has a very low thermal conductivity compared to the steel and acts as a thermal barrier. This thermal barrier lowers the heat flux from the metal surface to the surroundings when the air cools it. The use of the water can cause a shift of the Leidenfrost temperature and intensify the cooling for a short time period [1]. The oxide layer also affects the cooled surface roughness, which is another factor influencing cooling [2].

The heat transfer coefficient and the Leidenfrost temperature (temperature at which the minimum heat flux occurs) are mainly influenced by the water impingement (spray) density and by the surface temperature [2]. The influence of the oxide layer is not as significant as previous factors, but it should not be neglected in models for better temperature control.

HEAT TRANSFER COEFFICIENT MEASUREMENT

Four test samples with dimensions 155x60x25 mm were prepared from the spring steel 54SiCr6 (1.7102). Two holes for thermocouples (diameter 1.5 mm, type K) were drilled from the top side in the positions [-30,0] (position T1) and [30, 0] (position T2) to each sample. The position [0, 0] is in the centre of the sample (Figure 1).

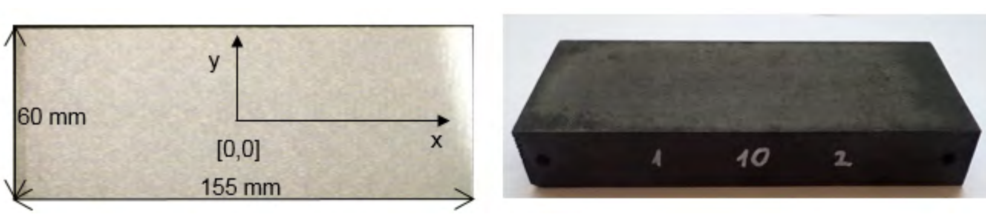

Figure 1 Test samples: clean - bottom side (left) and oxidized (right)

The test bench is shown in Figure 2. It consists of an electric furnace, covering sheet, hot test sample, moveable mechanism with nozzle and nozzle's deflector. The flat jet nozzle (SS.CO 8006) with spray angle 80° was positioned 300 mm under the test sample. The water pressure was set at 2 bars during the experiment and measured flow rate was 0.0317 l/s.

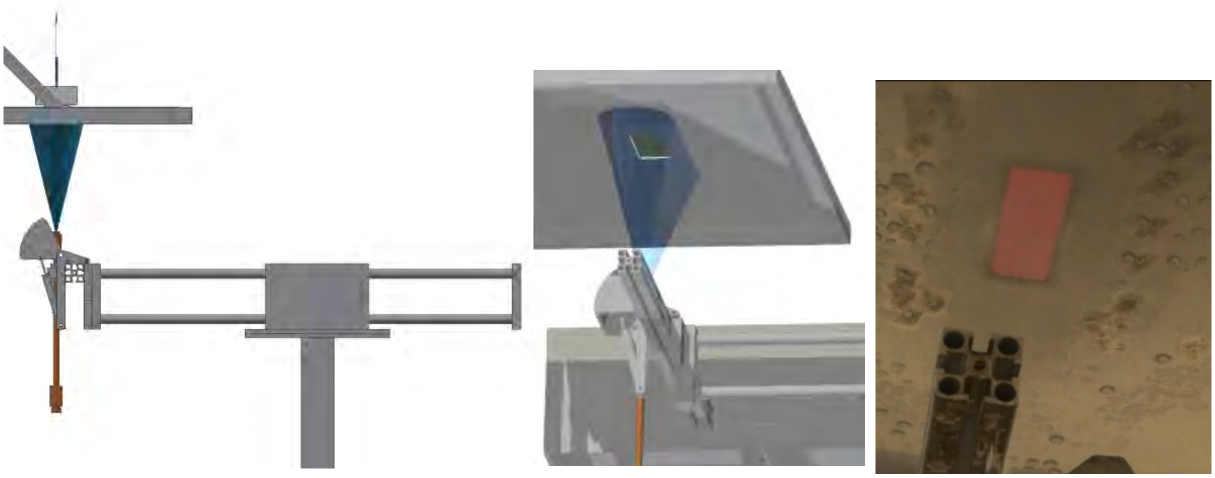

Figure 2 Test bench

Two samples (A and B) were oxidized in an electric furnace and two samples (C and D) were remained clean (without oxides). Sample A and B were oxidized at a temperature of 900 °C for 60 minutes. Holes for thermocouples were cleaned (the formed oxides were removed) and shielded grounded thermocouples were positioned 2 mm from the bottom (spray cooled) surface before the measurement. Each sample was isolated from the top side and was heated in an electric furnace at a temperature 760 °C in a protective nitrogen atmosphere (avoiding of the oxidation). Then, the sample was removed from the furnace and it was positioned on the test bench. The deflector was opened, and the cooling started.

Samples A (oxidized) and C (clean) were cooled by static nozzle (the centre of the nozzle was positioned under centre of the test sample and samples B (oxidized) and D (clean) were cooled by moveable nozzle. The nozzle passes under the test sample with the velocity 4 m/min. The deflector was opened (the sample was cooled by spray) in one direction and the deflector was closed (no spray cooling) in backwards direction. The oxide layer was unchanged (undestroyed) during the spray cooling. Samples were cut after the experiment and the oxide layer was observed in positions of thermocouples on the optical microscope (Figure 3). The thickness of the oxide layer on the samples A and B was approx. 100 µm with deviation approx. 20 µm.

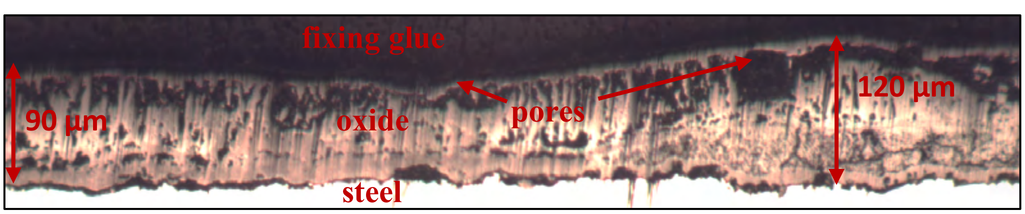

Figure 3 Example of the oxide layer formed on the sample A – position T1

RESULTS

The inverse heat conduction problem was used to compute the time dependent boundary conditions (heat transfer coefficient (HTC), heat flux, and surface temperature from measured temperatures. Beck's sequential approach, which uses a sequential estimation of the time varying boundary conditions and future time steps, was employed. The dependence of the HTC on the surface temperature was directly obtained from the inverse calculation for static experiments. This dependence is obtained by averaging along the position (interval 10 mm around the thermocouple position) for the measurements with moveable nozzle. Comparison of measured temperatures in thermocouple position T1 is shown in Figure 4Figure 3.

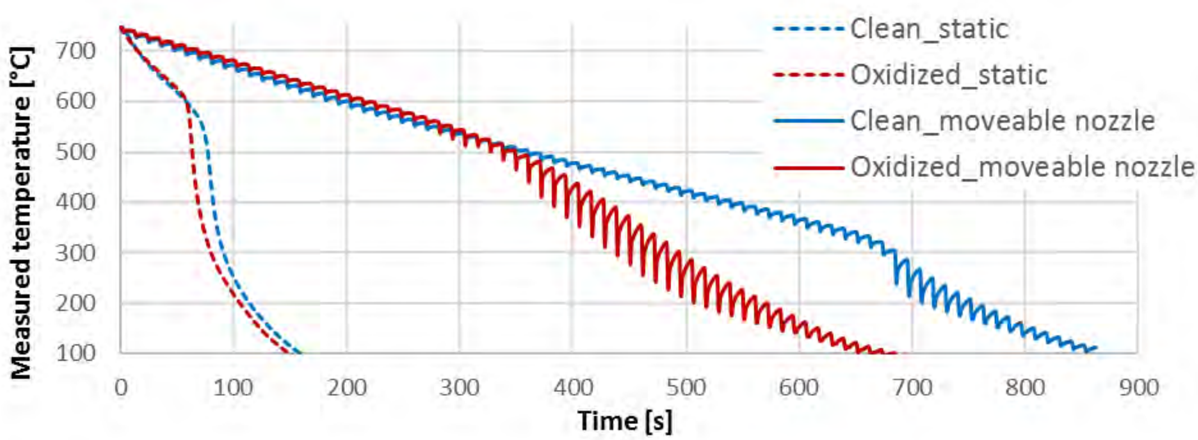

Figure 4 Comparison of measured temperatures for clean surface and oxidized surface in thermocouple position T1 (solid line – moveable nozzle, dashed – static nozzle)

The comparison of heat transfer coefficients (dependent on the surface temperature) for oxidized samples and clean samples are in Figure 5 (static nozzle) and in Figure 6 (moveable nozzle). It is evident, the Leidenfrost temperature for clean surfaces is lower than for oxidized surfaces. It is around 600 °C for clean surface and 540 °C for oxidized sample for tests with static nozzle. The difference between clean and oxidized sample is significantly higher in a case of moveable nozzle. The Leidenfrost temperature is 450 °C for the clean surface and around 600°C for oxidized surface. The heat transfer coefficient is slightly higher for clean surfaces for high surface temperatures (higher than 600 °C) and it is in average higher for clean surfaces for low surface temperatures (lower than 300 °C).

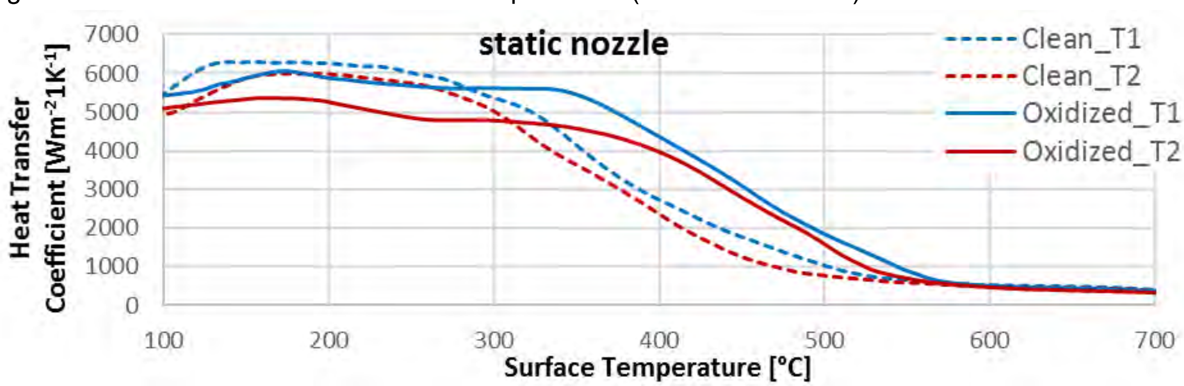

Figure 5 Comparison of clean surface and oxidized surface for static nozzle (solid line – oxidized surface, dashed line– clean surface)

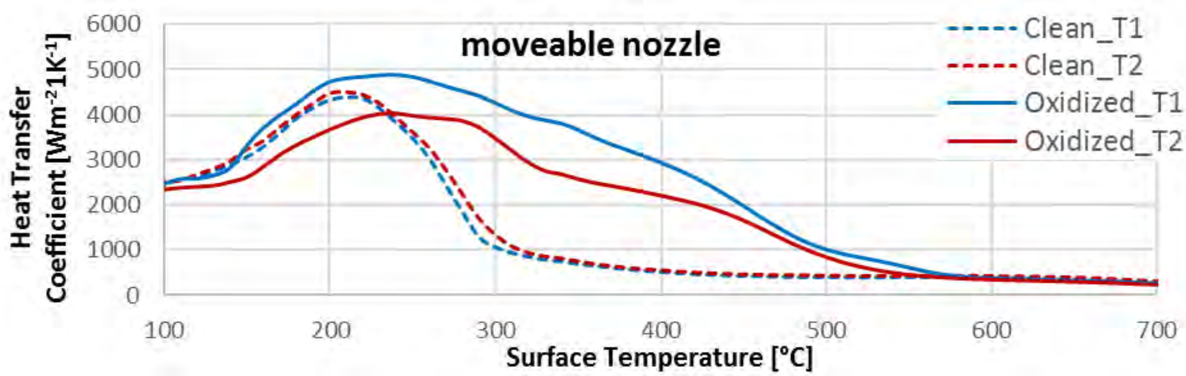

Figure 6 Comparison of clean surface and oxidized surface for moveable nozzle (solid line – oxidized surface, dashed line– clean surface)

CONCLUSION

Laboratory measurements showed influence of the oxide layer on the heat transfer coefficient and especially on the Leidenfrost temperature. The presence of the oxide layer shifts the Leidenfrost temperature to higher values and slightly decreases the heat transfer coefficient during film and nucleate boiling regime. The influence of the oxide layer on the shift of the Leidenfrost temperature is significantly higher for moveable nozzle than for static nozzle.

ACKNOWLEDGEMENT

The research leading to these results received funding from the MEYS under the National Sustainability Programme I (Project LO1202) and from an internal grant from the Brno University of Technology focused on specific research and development No. FSI-S-17-4346.

REFERENCES

[1] CHABICOVSKY, M., HNIZDIL, M., TSENG, A.A., RAUDENSKY, M. Effects of oxide layer on Leidenfrost temperature during spray cooling of steel at high temperatures. *Int. Journal of Heat and Mass Transfer*, 2015, vol. 88, pp. 236-246.

[2] CHABICOVSKY, M., HORSKY, J. Factors influencing spray cooling of hot steel surfaces. In *METAL 2017: 26th International Conference on Metallurgy and Materials*. Ostrava: TANGER, 2017, pp. 77-82.

Through Process Scale; Influence and Control

John Hinton[1, a] and Ian Robinson[1, b]

[1]Primetals Technologies Ltd. Sheffield Business Park, Sheffield S9 1XU, UK

[a]john.hinton@primetals.com, [b]robinson.ian@primetals.com

Abstract

Whenever hot steel is exposed to oxygen-bearing gases it reacts to form a surface oxide (scale). During steel production, the development of the scale layer extends from the reheat furnace through to the cooling bed. This can have a direct influence, for example the final surface quality or the work roll friction or an indirect effect such as variations in recording real time temperature measurements. During processing, the dynamic environment creates transient conditions i.e. the plate surface evolves through complex cycles of oxide scale growth, deformation and removal. Steel producers aim to achieve process consistency and a reproducible final surface quality. The realisation of this requires an appreciation of a number of complex through process variables on a microscopic and macroscopic level, including the scale interface metallurgy and the descaling system set up. This paper summarises the challenges associated with these aims.

Keywords: Through Process, Scale Morphology, Metallurgy, Descaling System Parameters

1. Introduction

Although significant progress has been made in steel plate process technology, the occurrence of surface defects in the final rolled product cannot be excluded. Through process detection and identification of defects is challenging and this is before the subjective visual interpretation of the final surface quality is considered. The acceptability of a surface quality depends on the downstream processing and may be defined by a specification. End use steel plate applications have traditionally allowed the intermediate surface quality to be less than critical. State-of-the-art Plate Mill installations now deliver accurate geometric tolerances and process consistency. Recent market forces have challenged steel plate producers to achieve good uniform surface finishes prior to downstream processing.

2. Through Process Scale

The secondary processing of plate steel requires slabs to be reheated to temperatures above 1100°C before being rolled into a semi-finished product. The exposure to oxygen bearing gases at high temperatures causes a surface reaction leading to the build-up of oxide scale over time. On discharge from the reheat furnace (RHF), the slab is transferred from a relatively stable environment, to a transient, locally inhomogeneous one as the slab is hydraulically and mechanically descaled and re-oxidised during rolling.

Plate steel compositions normally include small silicon and nickel additions (a fraction of a percent) that can lead to generous improvements in toughness and strength. It is well-known that these elements also have detrimental effect on the surface quality; decreasing the descalability (the ease with which the scale can be removed during descaling) and potentially leading to striping on the final plate surface [1 – 3]. The through process nature of descaling is highlighted by the fact that the occurrence of black and red stripes has been associated to poor descaling efficiency of primary oxides [1]. Fig. 1a compares top surface of two slabs exiting a Primary Descaler on a plate mill. For a similar high pressure water (HPW) descaling set up, the descaling performance on the second slab is not as efficient. One of the key differences was found to be in the composition, with the second slab containing a larger, but still relatively small amount, of nickel. Since nickel has a lower oxygen affinity than iron, nickel-rich nodules increase the entanglement between the scale and steel, enhancing the surface roughness of the interface and thus making complete removal of the primary scale more difficult [3].

Downstream from the Primary Descaler, the newly descaled surface layer evolves through the re-growth, deformation and removal cycles as secondary descaling events occur. These cycles create dynamic and transient surface conditions which result in the final plate surface. Other processing effects that create surface temperature inhomogeneity, that will influence the local conditions for scale growth, become more apparent downstream. These include RHF skid marks and roller table oscillation marks. An example is shown in Fig. 1b, taken from the entry and exit scanning pyrometers on the Primetals' MULPIC® plate cooling machine. On entry deviations in the surface temperature are recorded, which become more apparent on exit after cooling. This example, with two identifiable cooler areas (white boxes), is most likely to be skid marks from the RHF. Determination of the final plate temperature is important for developing the structure properties of the plate and for validation, feedback and tuning of the cooling models. A scaled surface influences the temperature feedback and Primetals Technologies Ltd. has developed several analysis techniques to address this.

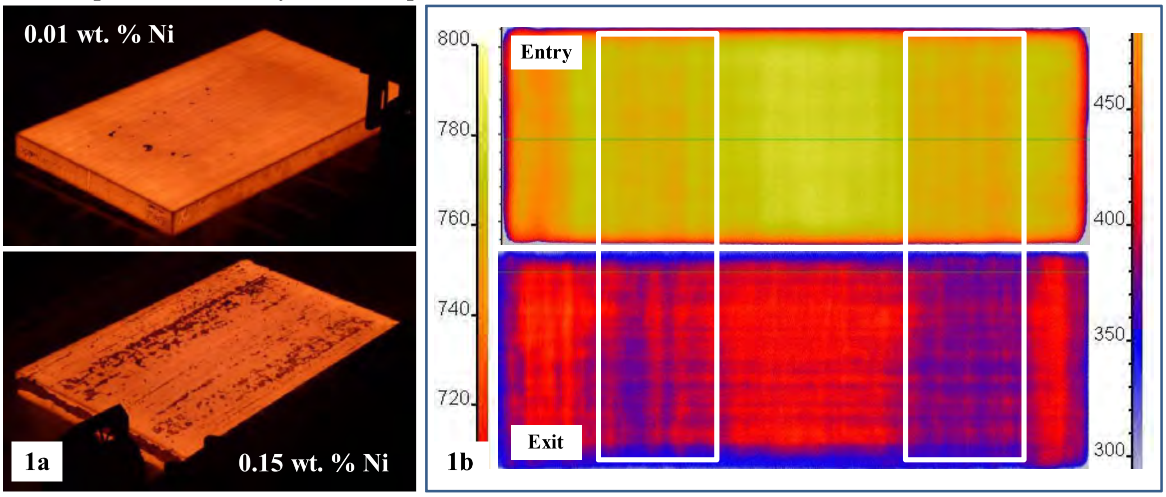

Figure 1 a) Comparison of primary descaling performance; illustration of composition effects and b) plate cooling; the downstream influence of scale through the process [4].

3. High Pressure Water (HPW) Descaling

HPW descaling can be described as the process of removing oxide scale by spraying the passing hot steel surface with moderate to high pressure water from stationary flat jet nozzles or rotary systems [5]. The aim is to remove loose to sticky primary, secondary and tertiary scale using the optimum setup of the descaling system. The goal to achieve excellent and uniform surface finish on the cooling bed relies on the consideration and integration of the following key areas:

1) Descaling Setup
   - Process optimisation through header geometry (design of spray angle, pitch, stand-off etc.) and usage within the limits of the hydraulic system.
2) Metallurgy
   - Appreciation of the influence of composition and atmosphere on the scale morphology, particularly at the interface of the scale and the slab. This directly impacts local dynamic conditions for secondary/tertiary growth layer during processing.
3) Evolution
   - Through process interaction between the descaling strategy and rolling schedule on the local dynamic conditions for secondary/tertiary growth.
4) Characterisation
   - Understanding the influence of the descaling strategy on the final plate surface quality through determination of acceptable quality control standards.

It is generally accepted that HPW descalability is linked to four concepts [5]. These are summarised in Table 1. Each concept is briefly described and linked to geometry, system or process variables. Results of extensive laboratory tests [6] demonstrated that both Specific Impingement Rate (SIR; how much water) and Impact Pressure (IP; how hard the water contacts the surface) are key to ensure efficient descaling.

Over a range of conditions, comparing SIR and IP with descaling efficiency, will identify limits above which descaling performance will be acceptable. The descaling limits are different for different steel grades and also depend on the RHF conditions and furnace atmosphere i.e. the influence of scale metallurgy at the interface on the adherence, ‘stickiness’ and descalability of a product.

Since both SIR and IP are important, further assessment proposed that this combination was best defined by Descaling Energy (DE), a product of SIR and IP [7]. This concept proposes that a limiting level of DE should be exceeded to ensure efficient removal of the scale layer. Given the complex scale metallurgy at the interface, this seems reasonable. Therefore providing that the chosen DE is exceeded, any combination of SIR and IP may be used. As described in section 2, composition influences descalability and can be used as an input to define a required DE. Previous work has suggested that for a base CMn grade, a DE of approx. 20kJ/m^2 should be targeted. Conversely, to descale high alloyed grades that include small be significant levels of Si and Ni then a DE 2 to 2.5 times greater should be targeted [5, 7].

Table 1 HPW Descaling Concepts

Concept		Units	Description	Geometry	System	Process
1)	Impact Force Impact Pressure (IP)	N MPa of N/mm^2	Force of a spray jet Force over impingement area	Header Design	Fluid Properties	
2)	Specific Impingement Rate (SIR)	l/m^2	Area of feedstock covered in volume of water per unit area	Header Design	Flow Rate	Slab Speed
3)	Descaling Energy	kJ/m^2	IP x SIR	Header Design	Flow Rate Impact Force	Slab Speed
4)	Coverage	mm	Spray width, overlap, wash	Header Design		

4 Descaling Energy basis for a Primary Descaling Process Window

As the basis for a Primary Descaling upgrade, a steel producer might specify a target static IP for a new Primary Descaler, achieved by the right combination of header geometry and hydraulic system parameters. HPW descaling concepts can be used to assess this static IP requirement in terms of the expected dynamic descaling performance. Water usage considerations have seen a demand to increase the IP whilst maintaining the consumption. This has generally seen system pressures increase to around 250bar whilst the header stand-off has generally decreased towards 100mm.

As shown in Table 1, the slab speed is an important process parameter in dynamic descaling. The DE concept can be used to estimate a performance range for a given header setup by considering a variety of descaling speeds. An example is shown in Fig. 2a, where for a given static IP, a reduction in the slab speed increases the SIR and therefore increases the DE. At very slow slab speeds, the dashed line in Fig. 2a indicates the conditions under which surface saturation should be considered i.e. the point at which a further speed reduction does not realise an increase in DE. In this example, surface saturation has been assumed when the SIR is > 40l/m^2 [5]. During production descaling speeds are typically between 0.50 to 1.50m/s but saturation is a consideration where the header water consumption is large.

As described in section 3, the DE concept may be used to define a limit level to efficiently descale certain grades or classes of steels. For example in Fig. 2a, if a minimum DE of 40kJ/m^2 is required for steels containing > 0.5wt. % Si + Ni, then the maximum speed through the Primary Descaler is approx. 1.0m/s. Equally, for lower alloy compositions, more typical of base CMn steel grades, a lower DE may be acceptable. In this scenario, the slab speed may be increased or, preferably, the header pressure decreased to reduce the SIR and IP. This option could also potentially offer energy savings by using the descaling system more efficiently. Using Fig. 2a as a basis, a more comprehensive assessment can be completed for different descaling speeds and header pressures. This enables a Primary Descaling Process Window to be defined. An example is shown in Fig. 2b. The limits of the window are given as follows:

- A min. DE of 20kJ/m^2; i.e. that required for low CMn grades.
- A max. header pressure of 230 bar when the system is fully charged.

• A descaling speed that ranges from 0.50 to 1.50 m/s.

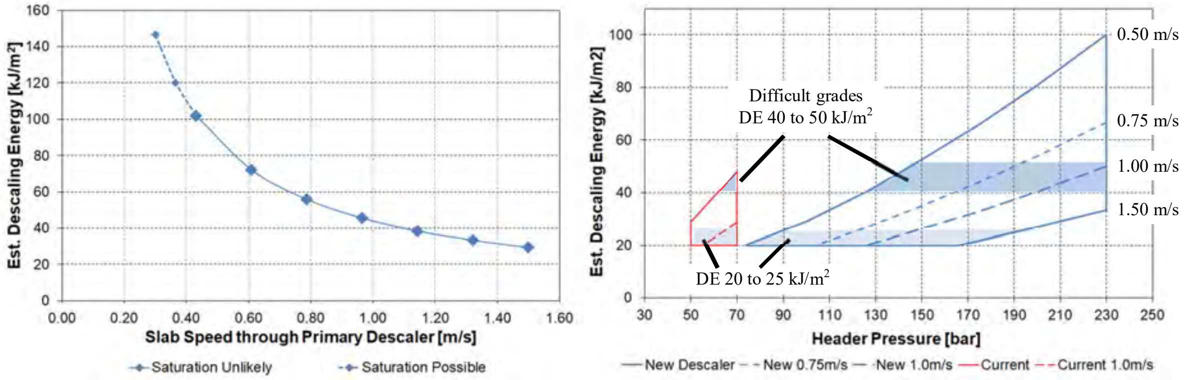

Figure 2 a) For a given IP, the estimated DE range for a variety of slab speeds and b) Process Window for Primary Descaling, targeting a min. DE of 20kJ/m2, and descaling speed ranging from 0.50 and 1.50m/s.

In Fig. 2b, DEs achieved at constant intermediate descaling speeds for a range of header pressure are indicated by the dashed lines. The two shaded areas show example DE target ranges for standard and more difficult to descale grades. For comparison the red outline is the estimated Process Window for a current Primary Descaler. This shows that the proposed system pressure upgrade and new header geometry combine to deliver a large Primary Descaling Process Window that offers a wide range of DEs. For future grade development, this proposal also has the capacity to increase the DE further, to > 50kJ/m^2 when a high header pressure and slow descaling speed are selected.

Fig. 2b also suggests a possible Primary Descaling strategy to reduce energy consumption. Using a constant descaling speed, the header pressure can be adjusted to establish the required DE to achieve efficient descaling. This will develop steel grade groupings (based on composition) that can be used in the future set up of the Primary Descaler, thereby only requesting as much pressure as required. This optimises the energy consumption of the Descaling System. For this proposal, Fig. 2b suggests that a descaling speed around 0.75 to 1.0m/s offers a good range of DE, but also spare capacity where greater DE can be achieve if the speed is reduced further.

5. Conclusions

Final plate surface quality is inherently linked to the local environmental conditions during processing; controlled by temperature, composition and setup of the complete mill descaling system, with through process effects visible. Standalone Primary Descaling has the potential to offer process optimisation by selecting appropriate setup parameters based on the steel composition and RHF practice.

6. References

[1] T. Fukagawa, H. Okada and Y. Maehara; Mechanism of Red Scale Defect Formation in Si-added Hot Rolled Steel Sheets, ISIJ International 34(1994) no. 11 p906.

[2] T. Asai, T. Soshiroda and M. Miyahara; Influence of Ni Impurity in Steel on the Removability of Primary Scale in Hydraulic Descaling, ISIJ International 37(1997) no. 3 p272.

[3] W. Melfo et al.; Experimental Study on Primary Scale Formation and Descalability on Steels containing Ni and Ni + Si, ISIJ International, 53(2013), No. 5 p866.

[4] J. Hinton, I. Robinson and M. Clark; Scale Formation During Reheat and Descaler Practices; European Oxide Scale Conference 2014 (Oxi 2014), 12th – 13th Feb, IOM3, London.

[5] D. Farrugia et al.; Innovative High Temperature and Mechanical Descaling for long products (HIDES), RFCS Project Reference No. RFSR-CT-2009-00009 (2009-2012).

[6] A.T. Sheridan and P. Simon; Descaling of Steels in Rolling Mills, Proc. Of the Forum on European Steelmaking Developments and Perspectives, p233, Luxembourg, February 1995.

[7] N.J. Silk; The Impact Energy Concept for Primary Descaling, Steel Times, 1999 No. 5, p184.

New trends and developments in linear high pressure descaling

Jochen Munz
Co-author: Jürgen Frick
Lechler GmbH

Abstract
During the process of hot rolling of steel, descaling has a decisive influence to the final product and surface quality. New steel grades, higher quality standards and demand-adapted descaling require more detailed investigations on the nozzle installation parameters.
The overlap area of two adjacent nozzle sprays is considered as one of the most important factors for a uniform descaling result over the entire strip or slab width. Enabled by the new Lechler High Pressure Spray Lab it's now possible to investigate the effects in the overlap area more accurately than ever before. An offset angle of 15° has been established almost as an industrial standard during the last decades. This paper focuses on different settings for the offset angle and shows different testing methods for evaluation. An impact measurement with embedded sensor is a fundamental tool and basis for all further steps to elaborate the most effective and efficient nozzle arrangement for the specific boundary conditions.
Innovative approaches could initiate the future direction leading to a modern descaling concept.

Keywords
Descaling, hot rolling, nozzle arrangement, overlap area, offset angle

Introduction
Modern hot rolling mills have to be extremely flexible regarding a wide range of different steel grades, product geometries and rolling speeds. Hence, descaling must be adaptable to fulfill all requirements and ideally to be most efficient at the same.
A well-adjusted descaling is essential for all subsequent process steps in the production chain of rolled steel products. In order to find appropriate installation parameters, it's indispensable to examine the specific situation in detail by initially defining the required main parameters, such as the desired impact pressure and specific water impingement. Additionally the impact distribution over the entire product width is also crucial for a good and uniform descaling result. Especially the overlap area of two adjacent nozzle sprays has to be carefully investigated at the designated operation conditions in order to elaborate the most suitable solution.

Investigation methods
New and more precise investigation methods are available nowadays due to the latest developments in measurement and sensor technology. By using a complete new measurement device which is shown in figure 1, it's possible to operate two adjacent descaling nozzles at the same time, spraying onto a plate with a plane surface, thereby simulating the reality when descaling. A sensor for measuring the impacting forces is embedded in this

surface. The measurement parameters, or variables, such as the water pressure, spray height, nozzle pitch (nozzle spacing), inclination (lead) and offset (twist) angle can be freely set (see figure 2). This method enables realistic measurements of the impact distribution, especially in the important overlap area (see figure 3 and 4), because the water layer on the plate surface is formed like on a strip or slab surface in a rolling mill. These investigations can be carried out on the Lechler High Pressure Spray Lab prior to the detailed engineering of the industrial system and are very helpful to determine the nozzle setting.

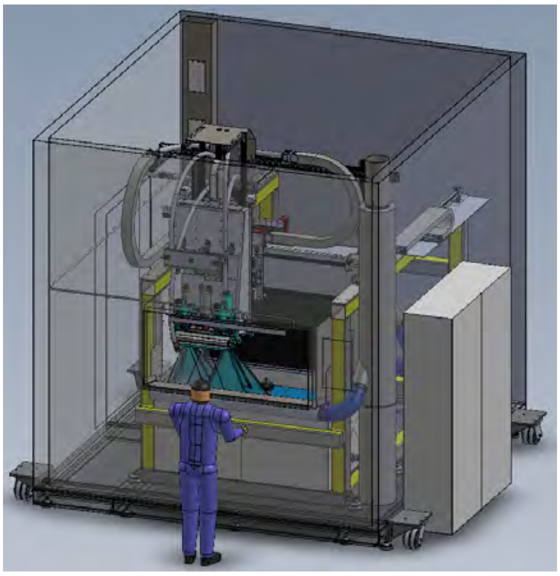

Figure 1: Lechler High Pressure Spray Lab

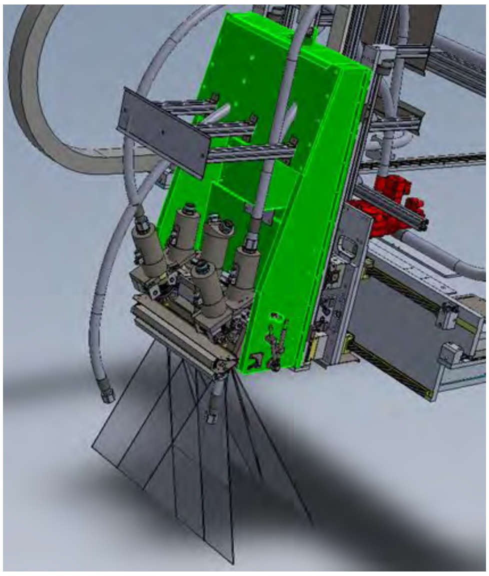

Figure 2: nozzle adjustment

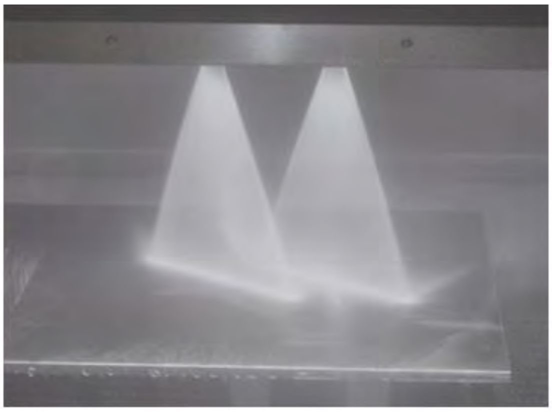

Figure 3: Plate with embedded sensor

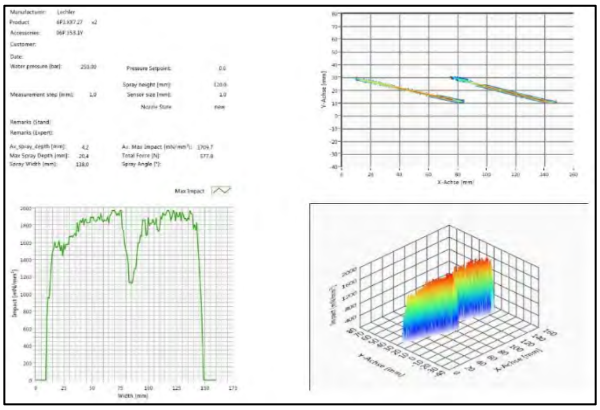

Figure 4: impact measurement protocol

A more common method of investigating the descaling effectiveness, especially the interference of two adjacent nozzle sprays is the Aluminum erosion test (see figure 5). The nozzles are spraying onto the flat surface of an Aluminum plate for a certain amount of time. The crater eroded into the surface by the sprays can be investigated optically and by the weight loss.

In addition to this static method, a new dynamic test can be performed. For this purpose, a special composite sample coated with several color-coded layers travels underneath the nozzle sprays at a controlled velocity. This composite sample has been developed by the Betriebsforschungsinstitut BFI, Germany and is representing the scale behavior very closely.

First results

Below the inclination (lead) angle is maintained 15° against the moving (rolling) direction of the product.

A typical nozzle arrangement at a spray height of 120 mm, a water pressure of 250 bar and a nozzle offset angle of 15° results in an impact distribution as shown in figure 4. Using these parameters the new measurement method reveals an impact ditch in the overlap area. This phenomena can be described as the well-known “wash-out effect” in this zone which is indicated in figure 6.

In order to verify this result by an additional method, an Aluminum erosion test at the identical conditions has been performed and with a similar result as shown in figure 5. Also here a clear band with almost no erosion can be observed at the wash-out area.

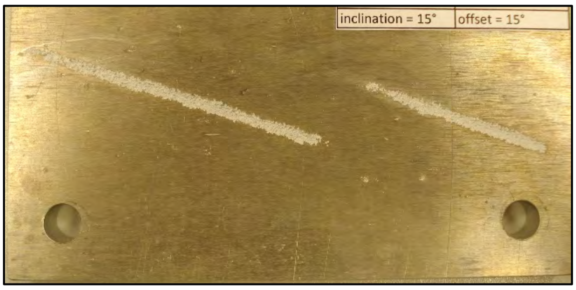

Figure 5: erosion test

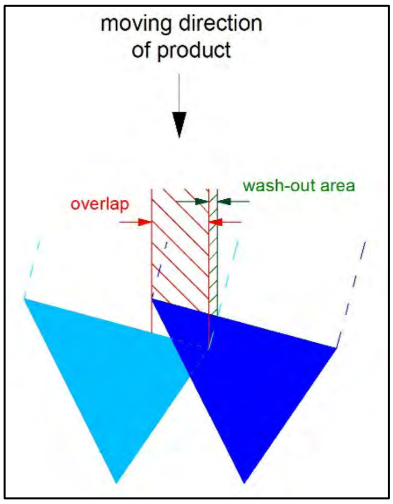

Figure 6: sketch of two adjacent sprays

Having these observations in mind, the new logic approach was to repeat these tests at identical conditions except for the offset angle. The offset angle was modified from 15° to 5° with the intention to reduce the width of the wash-out area. The corresponding measurement is shown in figure 7 and proofs that this reduction of the offset angle helps to reduce both, the depth and the width of the impact ditch. Also the erosion test presents the advantageous behavior when applying smaller offset angles (see figure 8).

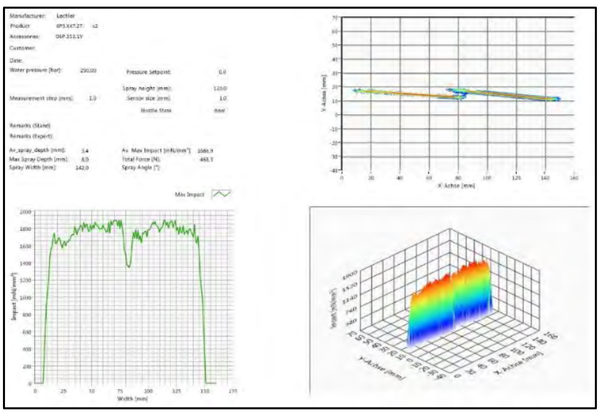

Figure 7: measurement with 5° offset angle

Figure 8: erosion test with 5° offset angle

Besides the offset angle also the size of the overlap influences the impact distribution in the overlap and wash-out area. Theoretical studies supported by impact measurements show a smaller and narrower ditch while increasing the overlapping.
In reality the increase in overlap has to be carefully balanced as there are also good reasons for limiting the overlap. One is that at an excessive overlap could lead to an overcooling of the surface in this area. Depending on steel grade and product thickness, an overcooling could be a potential cause for striping. Another reason is that using excessive overlap requires more total water flow to cover the entire product width as the overlap is creating a double spray. As this has consequences for the sizing of the pump and eventually for the energy consumption, all aspects must be considered for finding the best compromise. On the other hand, an overlap being too short will result in un-descaled stripes on the surface. A reasonable safety margin should also be considered in case of wavy strips or uneven slabs so that enough spray height providing sufficient overlap is always secured.

Summary and outlook

The combination of offset and inclination angle, overlap, single nozzle impact distribution and the specific operation conditions (spray height, water pressure, etc.) are important parameters for an even overall impact distribution.
In reality the best possible compromise has to be determined.
The results of the tests with reduced offset angle are quite promising and show a positive effect to the overall impact distribution as well as to the erosion. With this in mind and by utilizing the new methods on the new Lechler High Pressure Spray Lab further research will be done the bring descaling to the next level.

Maximizing Impact Force from Descale Headers using CFD Analysis

Lesli Peterson[1]
[1]Spraying Systems Co.
PO Box 7900 Wheaton, IL, USA, 60187
Phone: 630-517-1380
Email: Lesli.Peterson@spray.com

Keywords: descale, impact, oxidation, CFD, spray nozzle

INTRODUCTION

Descaling is an important step in the rolling process. Oxide is removed from the surface of the product to improve surface quality and maintain the rolls. Nozzle selection and header design are important parts of an effective descaling system. The nozzles need to be sized and placed so they provide sufficient impact force to remove the oxide with minimal amount of water possible. Headers need to be sized to maximize the impact performance of the nozzles. Impact testing along with CFD (Computational Fluid Dynamics) analysis can help to determine if a header has been properly designed to provide maximum impact force. CFD analysis can determine the fluid approach velocity along with the turbulence level in the header. The spray pattern of the nozzle can then be measured for impact force and distribution under different approach velocities and turbulence levels. Comparing these to a nozzle tested under an ideal no turbulence condition can determine minimum header size requirements based on nozzle capacity and pressure. Optimizing the header can help to improve performance and minimize energy costs.

DISCUSSION

Background

Hot strip mills use high pressure hydraulic nozzles in the descaling process to remove scale from the steel surface. It is important to remove the scale to prevent defects in the material and to increase the life of the rolls. Scale is formed by a direct reaction of metal with oxygen, water and other elements. The type of scale formed will depend on a number of factors including base material, temperature, time in the furnace and type of furnace. In theory the spray cools the outer scale layer causing a temperature difference between the base material and the scale. This causes the scale to create cracks and allow the spray to penetrate through the scale. The water then turns to steam and helps to lift the scale from the base material. Lastly the sprays push the loose scale off of the surface of the steel.

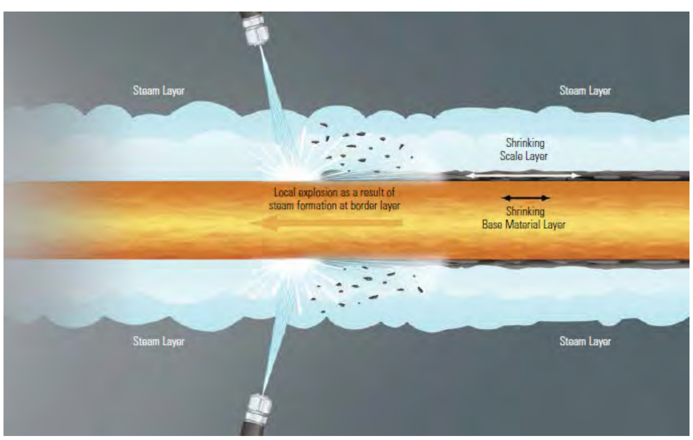

Figure 1. Schematic of descale process

The impact of the nozzles is determined based on the type of scale being removed and the amount of force needed to remove the scale. The maximum impact force can be determined by calculating the reaction force for the nozzle, Eq. 1. The reaction force is then divided by the area of the spray to determine the impact force, Eq. 2.

$$F_T = \rho Q V \qquad (1)$$

$F_T =$ Total Impact Force

$\rho =$ Density

Q= Flow Rate

V= Velocity

$$I_m = F_T / (w * t) \qquad (2)$$

I_m = Impact Force

w = Spray width

t = Spray Thickness

Testing

The previous equations are theoretical only. Experimental testing has been used to determine how the nozzles function in more realistic conditions. Turbulence levels have been divided into three categories and as the approach velocity increases the impact and spray pattern become compromised. Based on experimental testing we know both impact and spray pattern are compromised when the approach velocity meets or exceeds the severe level. As figure 2 shows the pattern shifts from a straight uniform spray to a curved spray and eventually takes on an "S" shape as the approach velocity increases.

Turbulence Level	Approach Velocity
Low	Less than 5 ft/s or 1.5 m/s
Moderate	5-15 ft/s or 1.5 to 4.6 m/s
Severe	Greater than 15 ft/s or 4.6 m/s

Table 1. Turbulence level categories

Figure 2. Spray pattern shape based on turbulence category

Impact testing, where a load cell is moved under the spray in a grid pattern to collect force data, has been used to determine the average impact at various approach velocities. Approach velocities are varied in the header using a set-up similar to figure 3.

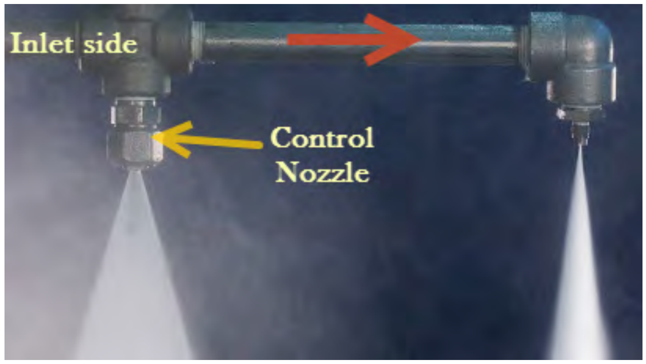

Figure 3. Header manifold for experimental testing

The control nozzle is closest to the inlet and is kept constant while the nozzle furthest from the inlet is varied. The effect is increasing or decreasing the approach velocity through the control nozzle. In the low to moderate range the average impact is relatively flat. As the approach velocity approaches the severe level the average impact begins to drop off significantly.

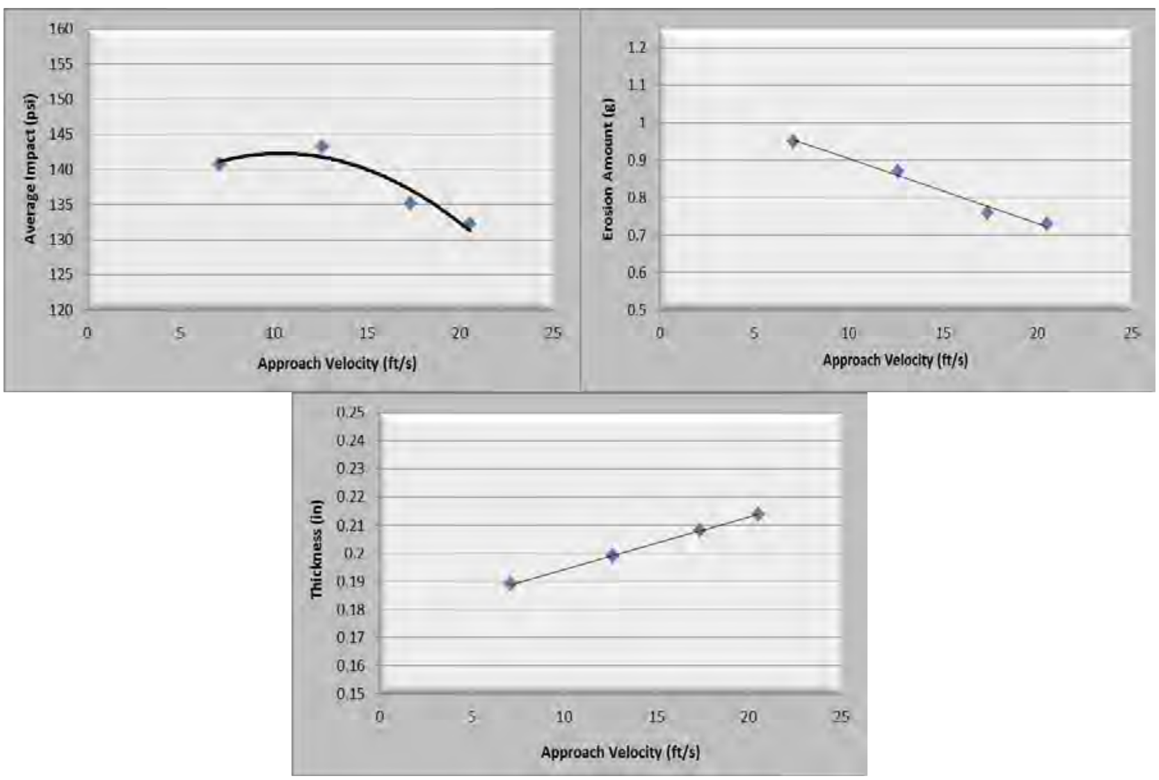

Figure 4. Results of impact and erosion testing

Erosion testing is another method used to examine the integrity of the spray. Erosion testing is the method of spraying onto a plate of soft material for a set amount of time and weighing the plate before and after to determine the amount of material removed. The material used in this test was aluminum. The same header used in the impact testing was used to vary the approach velocities of the liquid.

Figure 5. Erosion test set-up

By doing erosion testing at different approach velocities we noticed a reduction in the amount of material removed and an increase in the thickness as the approach velocity increased. In addition the uniformity of the pattern began to change. At the lower approach velocities the pattern was straight and uniform. As the approach velocity increased the pattern began to take on a more "S" shaped or curved pattern.

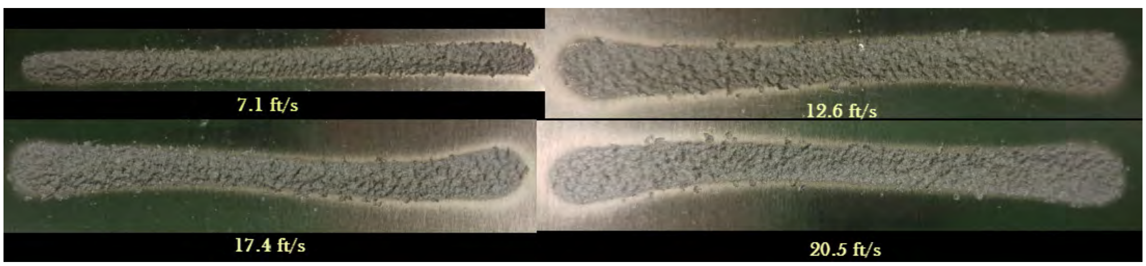

Figure 6. Spray pattern as seen on aluminum plates at various approach velocities

Results

Impact and erosion testing has determined the limits the spray nozzles can handle. CFD analysis can then be used to analyze the header based on the performance limits determined during experimental testing. The following examines three cases. Case 1 is the current mill condition and cases 2 and 3 are two ways of optimizing the header design based on CFD results from case 1. All three cases are based on the same header design in figure 7 using 14 nozzles and an end feed.

	Pressure	Total Flow	Header Size
	psi	gpm	
Case 1	2300	743.1	4" sch. 160
Case 2	2300	530.8	4" sch. 160
Case 3	2300	743.1	6" sch. 160

Table 2. Header details for CFD analysis

Figure 7. Header schematic showing the location of the inlet and number of nozzles

The results from case 1 show velocities on the inlet side of the header in the severe to moderate range. In total six nozzles have approach velocities in the severe range. It would be expected to see spray patterns that have an “S” or curved shape. These non-uniform patterns were observed when board tests were done. Patterns for nozzles further from the inlet were more straight and uniform. This causes uneven descaling on the product surface and is not desired. As the flow moves away from the header inlet the turbulence and the approach velocities are reduced. The turbulence levels on the inlet side of the header are also on the high side and decrease in value further from the inlet of the header. In this case the highest level of turbulence is seen in nozzle #3.

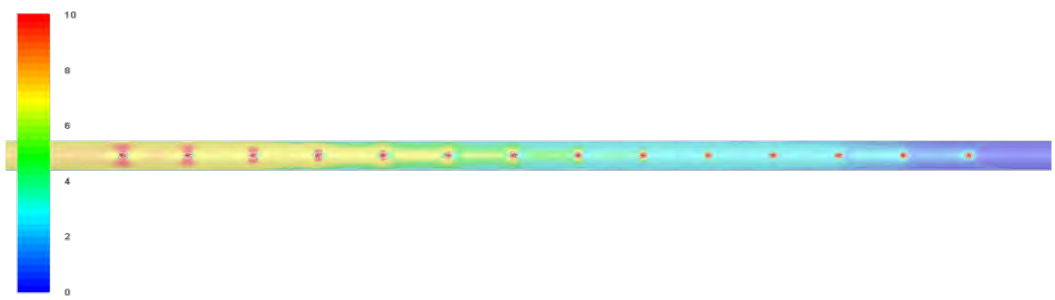

Figure 8. Approach velocity results for Case 1

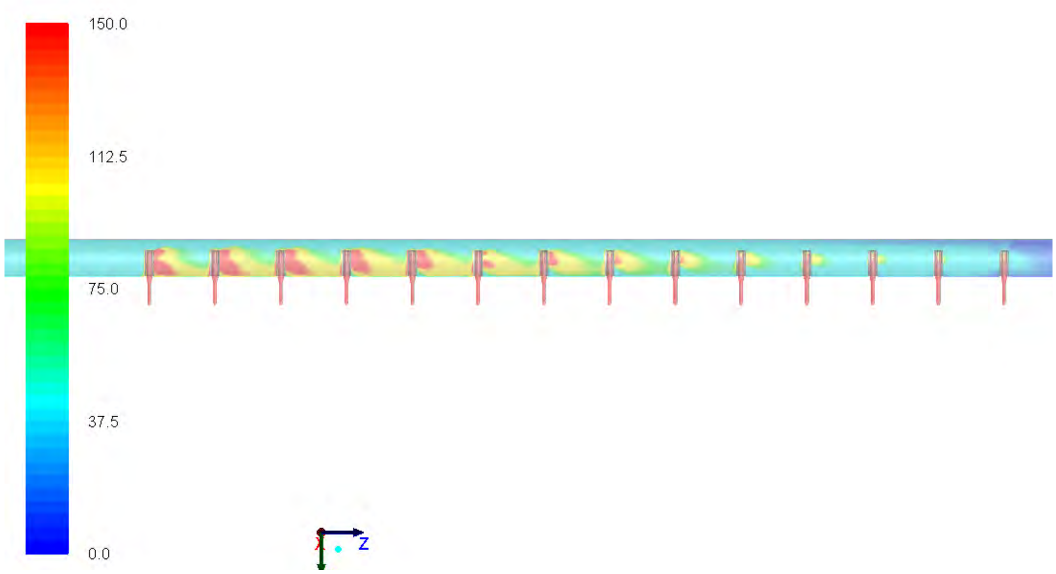

Figure 9. Turbulent intensity results for Case 1

Using CFD two additional options were examined. Case 2 used the same size header but reduced the flow rate by 28%. Case 3 kept the flow rate the same but increase the header size from a 4" sch 160 pipe to a 6" sch 160 pipe.

In case 2 the first two nozzles of the header had approach velocities above the severe level but the turbulence levels were drastically reduced. The number of nozzles above the severe level was reduced by 4 nozzles from case 1. The turbulence intensity was also reduced indicating a smoother approach to each individual nozzle. Case 2 would be the recommended maximum flow for this pipe size and inlet configuration and while the flow rate has been reduced the impact level would be expected to be near the same level as in case 1 because of the lower turbulence level. A change to this option would be a minimal investment for the mill as only a nozzle change is required.

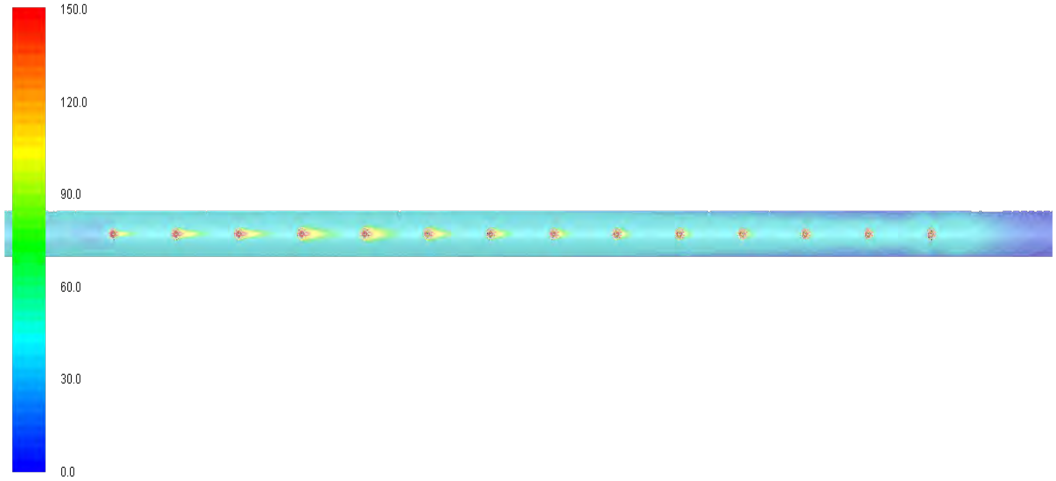

Figure 10. Approach velocity results for Case 2

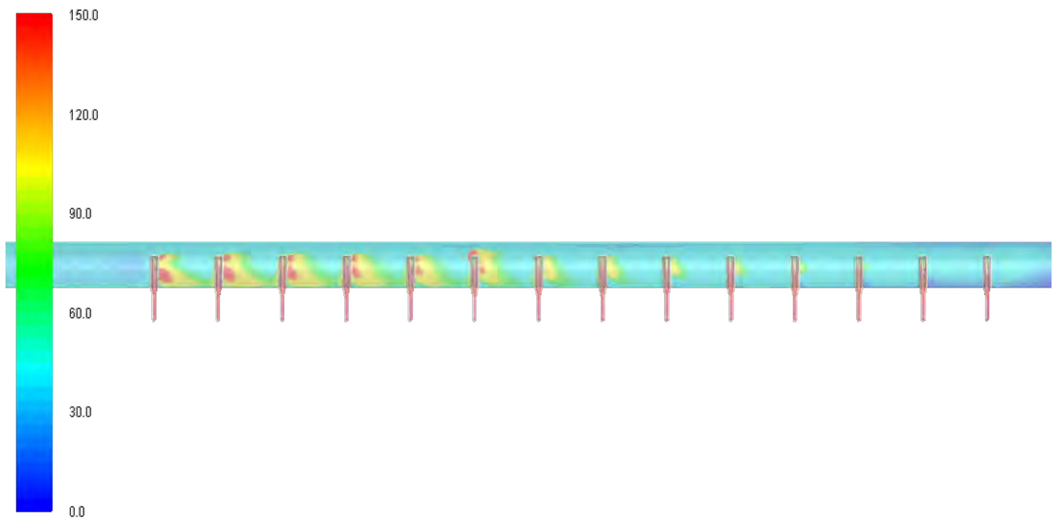

Figure 11. Turbulent intensity results for Case 2

Case 3 drops all approach velocities to the moderate or low level. This is the most ideal case and will provide the most efficient use of the nozzles. The turbulent intensity percentage has also been reduced in this case. The flow rate with the larger header would be the same as the original design and the mill could expect a 10-15% increase in impact. In addition all spray nozzles on the header are expected to produce straight uniform patterns and provide uniform descaling across the width of the strip.

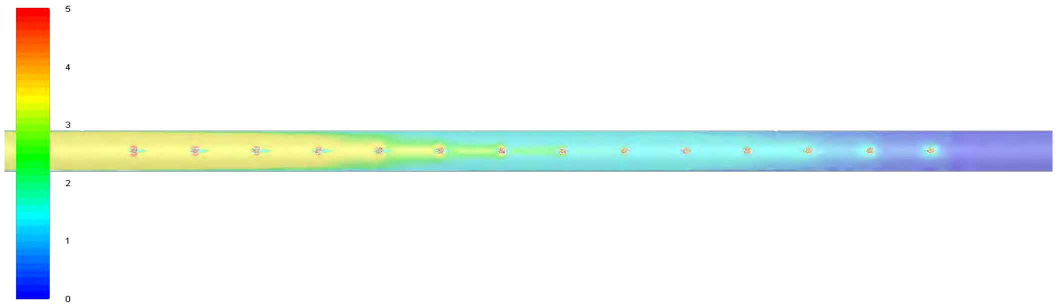

Figure 12. Approach velocity results for Case 3

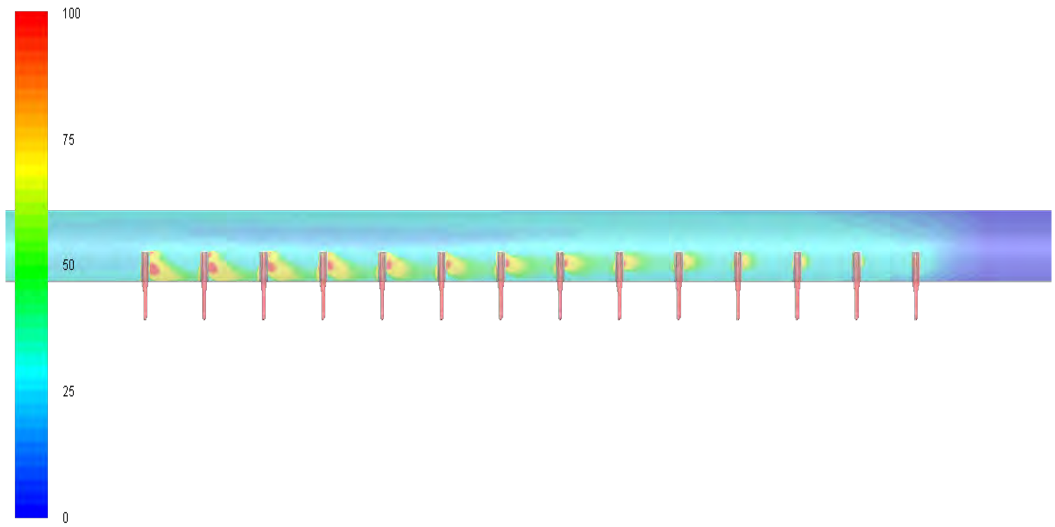

Figure 13. Turbulent intensity results for Case 3

CONCLUSIONS

CFD combined with experimental testing can be used to predict and optimize the performance of the nozzles in descale headers. Experimental studies have shown that turbulence and fluid velocities need to be kept at minimal levels in order to ensure the nozzles are performing efficiently and providing their maximum impact. Spray nozzles that have approach velocities above the moderate level will produce spray patterns with reduced impact and altered spray patterns. CFD can be used to determine approach velocities and turbulence at each nozzle location. Additionally new header designs can easily be modeled and analyzed to ensure any changes provide maximum nozzle performance.

REFERENCES

1. Sheppard T and Steen WM, Hydraulic Descaling of Steel a Preliminary Experimental Study, JISI Septermber 1970
2. Brown GA and Chiang KC, Tools for Hydraulic Descale Nozzle Evaluation, 34th Mechanical Working and Steel Processing Conference Proceedings-1992
3. Silk NF, The Practical Aspects of Hydraulic De-scaling, Steel Times International October 2001
4. Blazevic DT, When to Change Descaling Nozzles and How to Interpret Board Tests, AISTech Conference Proceedings, 2006
5. Yu Q, An Effective Descaling System for Hot Rolling, AISTech Conference Proceedings, 2008
6. Robb L, Effect of Spray Height, Lead Angle and Offset Angle on Impact, AISTech Conference Proceedings, 2005

Systematic development of a rotary descaling device.

Dirk Schulze Schencking, Udo Hertel, *both of Hauhinco GmbH & Co. KG*

The pressure on the steel producing sector in Europe and also in the USA is rising constantly due to a global production of steel and heavy duty products. Even so the costs for energy, employees and XXX effects the earnings. Therefor there is a high requirement to increase the productivity and efficiency of the existing plants and in particular the quality of the product itself.

One of the most effecting devices according the surface quality and even the material structure in the process is the descaling system which takes place at several positions in the process.

The old philosophy of the more the better does not reach the requirements of a highly efficient and reliable process for high quality products. The most important aspect is to completely erase the scale of the product before it is milled, forged or pressed to avoid scarcs and scratches on the surface or even engaged scale into the surface. But also the cooling of the material needs to be considered. With a high water consumption the work pieces are unnecessarily cooled which leads to higher process forces and increased wear. Depending on the alloy or the material width also the metallurgical changes could be caused by an insufficient water impingement. In a certain range the overcooling can be compensated due to a higher furnace temperature which comes along with higher rates of scale and even higher energy consumption.

Besides the view on the product itself also the reliability of the descaling is one of the most important properties of the system.

An up to 100% availability is only achievable if the complete systems follows a straight design concept. Besides a high reliability of the pumps, valves and periphery it is also necessary to provide a monitoring of possible wear of the nozzles or other significant parts of the system. A smart and professional steel work is also needed to ensure a proper wear resistance and robust covering of the header even in cases of accidents.

With knowing all the critical aspects as well as the do's and don'ts Hauhinco developed a straight and highly reliable descaling system concept for the future in the field of hot metal products.

A Conventional descaling system

Most conventional descaling systems can be broken down into the following sub-categories: a water supply, a pump station, a high-pressure plus a low-pressure piping, an accumulator bank with a high-pressure air supply and the descaling devices (Figure 1).

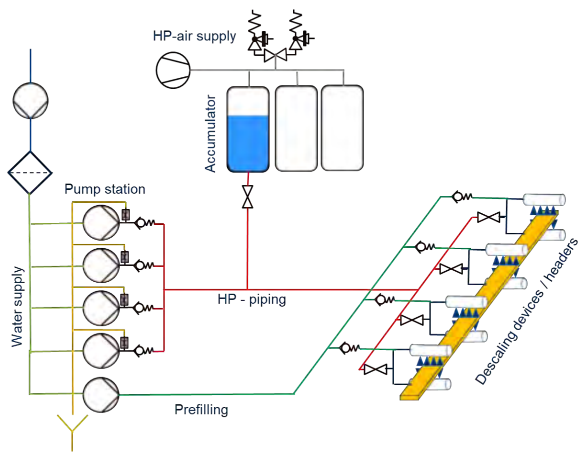

Figure 1: Simplified principle of a centrifugal loaded descaling system

To achieve the benefits of an accumulator driven system all headers/ devices are supplied by one central pump/ accumulator station. This comes along with one pressure level for all headers, disregarding the specific product properties or even the position of the header in the process. Due to the constant high pressure piping shut-off valves closed to each header and even a separate prefilling are needed to prevent the headers being destroyed by a water hammer. Beside the additional pipe work for the prefilling, at minimum a low pressure pump and several additional valves are necessary. The accumulators and the centrifugal pumps have to be designed for the one best efficiency point (BEP) (Figure 2). Therefore, the pump characteristic needs to match the system characteristic. But in most processes, there is no constant system characteristic, so the accumulators have to cover the variation of products (variation of water flow/ consumption). Depending on the capacity of the accumulator bank, the pressure - which is in this case equal to the impact - will significantly vary during the process. A constant descaling quality is not ensured.

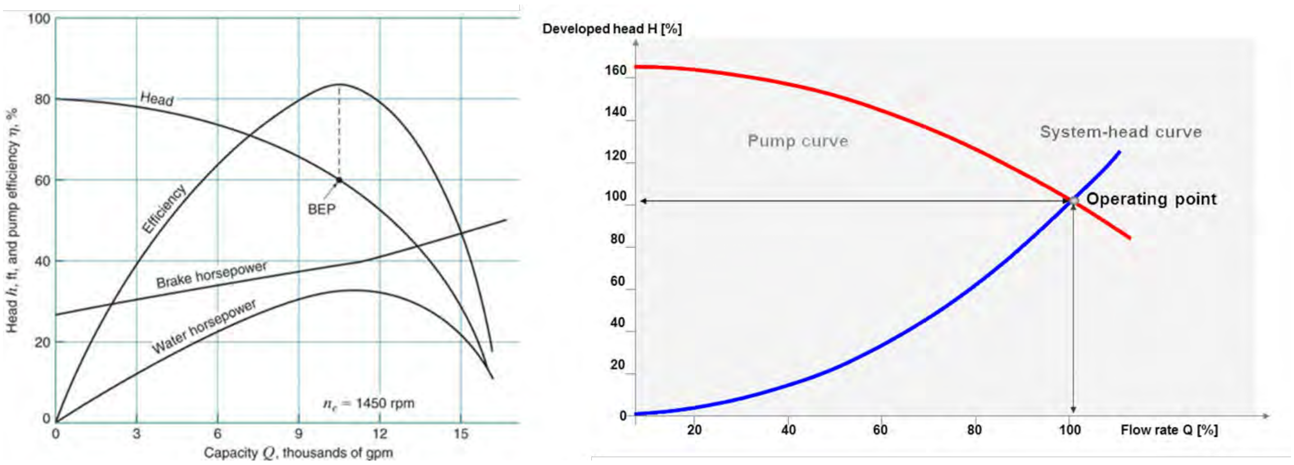

Figure 2: Characteristic diagram of a centrifugal pump (Source: KSB)

Additionally, a variation of the flow rate the system is not running at the BEP anymore. This directly results in a high amount of energy losses due to a very steep slope of the centrifugal pumps efficiency curve (Figure 2).

Because of the varying process parameters, it is also not possible to provide a sufficient monitoring of the nozzles or even the headers. Wear or even worse a plugged nozzle will not be recognized until the product passes the material quality control.

In spite of an elaborate water treatment installed to ensure good water condition, the nozzles and also the periphery will show increased wear or plugging. This is caused by the carbon steel used for the accumulators and the pipe works. Rust and other oxides emerge right after the water treatment equipment and cause expensive reductions on surface quality or down times of the system.

The Hauhinco Descaling System

Due to the negative aspects regarding the pressure driven system with accumulators Hauhinco follows the strategy of pump driven volume flow systems. With direct driven pumps a high degree of efficiency and variability is achieved. This straight architecture also provides a very quick system availability, particularly good monitoring and maintainability.

As shown in Figure 3 each descaling devices is directly connected to one (or more) pump. There is only one pipe necessary for hp and lp due to a new designed pump unloader valve. This descaling unloader valve ensures an adjustable pressure level in the pipe while unloading. Also, the switching times of the valves are adjustable and when combined with the prefilling, a fast but smooth loading without water hammers can be ensured.

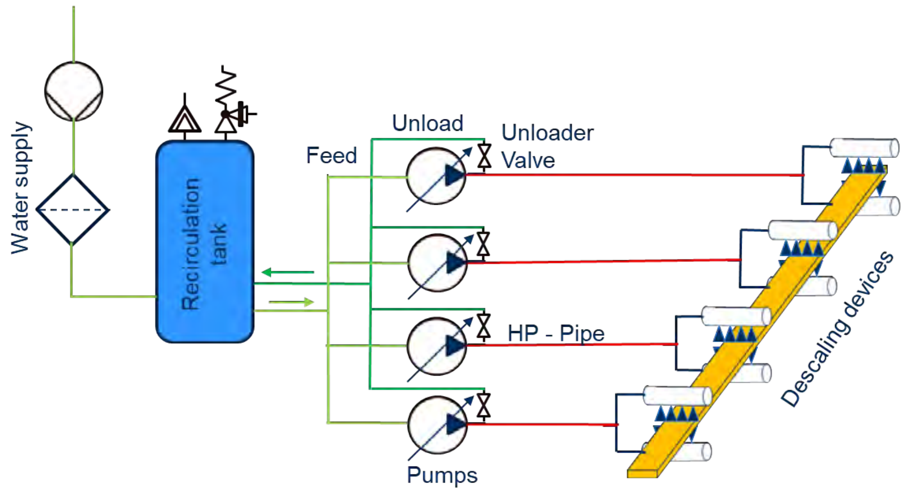

Figure 3: Simplified principle of the HAUHINCO descaling system

Depending on the product interim period the pumps are driven with a decreased rotational speed or are even shut off completely. As soon as the motors stop, the water end of the system is energy-free and the electrical energy consumption reaches almost zero Watts. In terms of the idling power consumption of a centrifugal pump system this yields a high potential of energy savings. Also in the event of emergencies somewhere in the plant, the time to reach a safe state of the descaling system is minimized to guarantee safe working conditions.

While running, the pumps are fed by a low-pressure recirculation tank. This single vessel is much smaller than the accumulator bank and has no air over water chamber. Quite the opposite it includes an air bleed valve to degas the water. Dissolved air in water causes potential cavitation or destroys the water jet after the nozzles which causes a significant decrease of impact. Also the unload water is circulated back to this vessel to keep the filtered water in system.

The water is filtered by maintenance free back flush filters with at least 25 µm fineness. Once the water passed the filter unexceptional high-quality stainless steel is used to avoid self-induced pollution of the water. This ensures a high lifetime and a maximum reliability of the nozzles, as well as the pumps and valves.

Besides the advantages on the hardware, this system structure provides also outstanding controlling and monitoring opportunities. Due to the independant pressure supply of each descaling device, the specific headers are loaded as needed to achieve an specific impact to the product without overcooling. By knowing the pumps volumetric efficiency and the dp/Q curve of the header, a continuously monitoring of the nozzles is available. Wear or fractures at the nozzles will now be noticed early. Plugged nozzles are prevented by the filter and pipe work concept.

Using the Hauhinco system structure the descaling process is already way more reliable and efficient than the conventional. Although the water demand is adapted to the requirements of the product there is still a physical limit for further improvements regarding the descaling results and the material influence with the static nozzle header.

Limits of a static nozzle header and its disadvantages

Besides the attractively simple design of a static nozzle bar there are at least two big disadvantages.

First and even worst is the static position of the nozzle above the workpiece, so the scaled surface is only reached once by the water jet. If the scale isn´t completely removed within the first impingement it will remain on the surface with all its consequences.

Second is the dimensional limit of nozzle density. Due to the geometry of the nozzle body or its carrier, the minimum clearance between the nozzles are predefined. But to achieve a maximal impact without overcooling the workpiece due to massive water flow a small clearance between the surface and the nozzle is essential. Figure 4 shows an conceptual example of the limited space problem. Although the number of nozzles is doubled (and along with it the volume flow!) the designated impact couldn´t be reached.

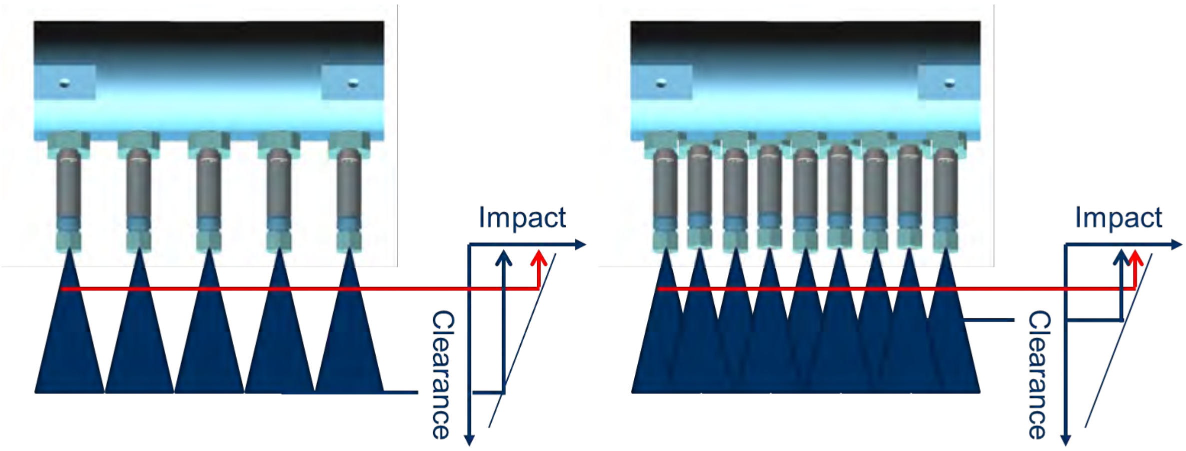

Figure 4: Static nozzle header with the correlating impact (blue) and the designated impact (red);
left original alignment with low impact; right max. packing density and doubled volume flow with increased impact

The advantages of a moving nozzle

To avoid this principle problem of the conventional headers, the nozzles themselves need to be moved. With this additional relative movement of the nozzle to the work piece the limited space problem can be solved. There are two possible kinematics to move the nozzle above a surface. One is oscillating, another is rotating. For both movements the locus is shown in Figure 5. Depending on the relative velocity of the nozzle, the impingement area for both kinematics can be enlarged until the complete surface is covered. But the high non-uniform movement of an oscillating nozzle comes along with high acceleration forces and a costly bearing. When combined with the very tough environmental conditions this kinematic is not a reliable solution. The rotating nozzle with its absolute uniform kinematic is free of transverse acceleration forces and provides a simple way of bearing. There is also a wide range of robust sealing concepts available to protect the bearing and all other sensitive parts against the aggressive environment. Due to this mechanical assessment, the preferred kinematic for a non-static descaling header is rotating.

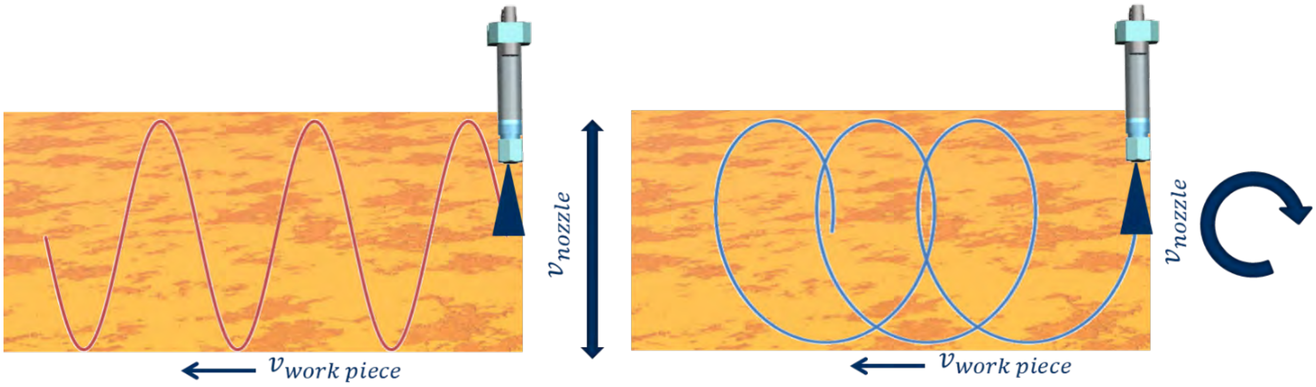

Figure 5: oscillating (left) and rotating (right) movement of a nozzle relatively to the surface of a work piece

In addition to the mechanical benefit, the first and worst disadvantage of the static header can be solved with the rotating header. As shown in Figure 5 there are certain areas which are reached twice by the same nozzle. That means, with a rotating header a redundancy of decaling is already obtained with one single nozzle!

The analytical determination of the kinematic which is used to create the shown slope also provides important process data like the relative velocities in work piece direction as well as in transverse. Also, the ratio of rotational speed (nozzle velocity) and work piece velocity can be used to calculate the minimum overlay of separate spray tracks in order to guarantee full surface descaling.

For a first-rate descaling result, including redundancy, thermal interference and efficiency aspects, a profound knowledge of the distribution of multilayers, the impingement of water and above all, the impact are essential. A simple analytic determination of average values does not meet these requirements.

To acquire an optimal design of the rotor header, which houses rotates the nozzles, a simulation tool is compiled by Hauhinco which enables a specific prediction of required coverage for each mm² of the work piece surface. A visualization of a simulating result is shown in Figure 6.

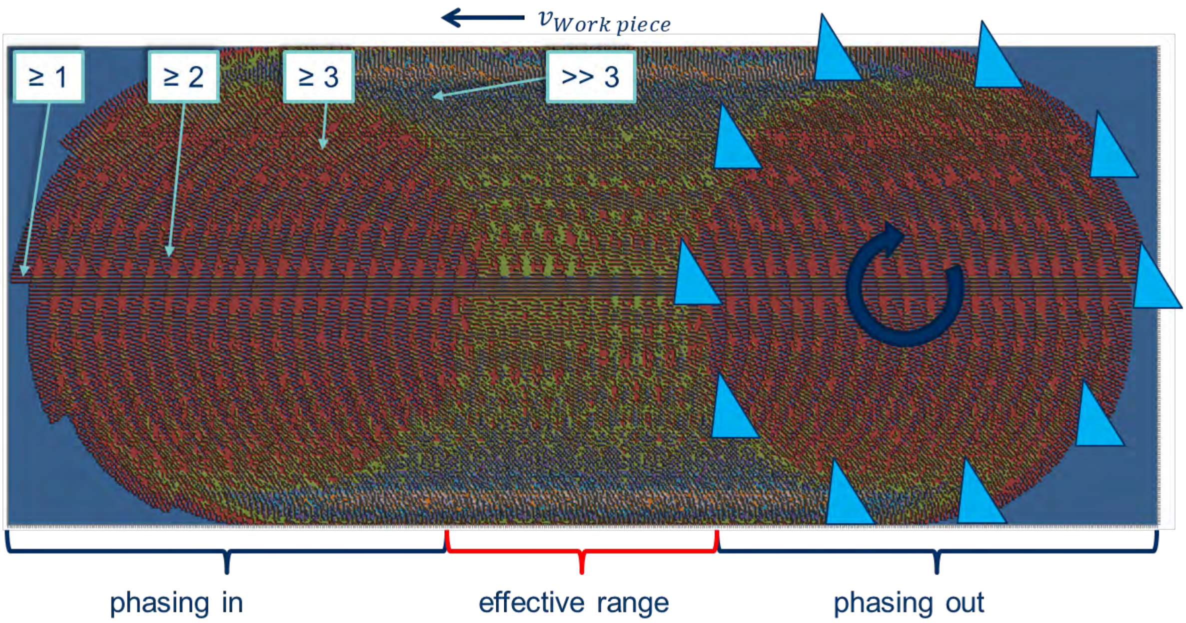

Figure 6: 3D plot of simulation results, numbers of overlays per square millimeter on the work piece surface

In this example the total account of multiple descaling across the surface is evaluated. For a better understanding the blue triangles show the end position of the simulated nozzles above the work piece. The work piece is moving from the right to left while the rotational axis of the header is fixed. Only the effective range is considered to be on the work piece. The color indicates the number of descales per each square millimeter. The value boxes are pointing out certain regions. Within the effective range a multiple descaling of at least 3 to 4 times is ensured (or even more if needed).

Even in cases of a plugged nozzle no descaling gaps occurs as simulated in Figure 7. In the effective range at least a double descaling of the surface can be assured.

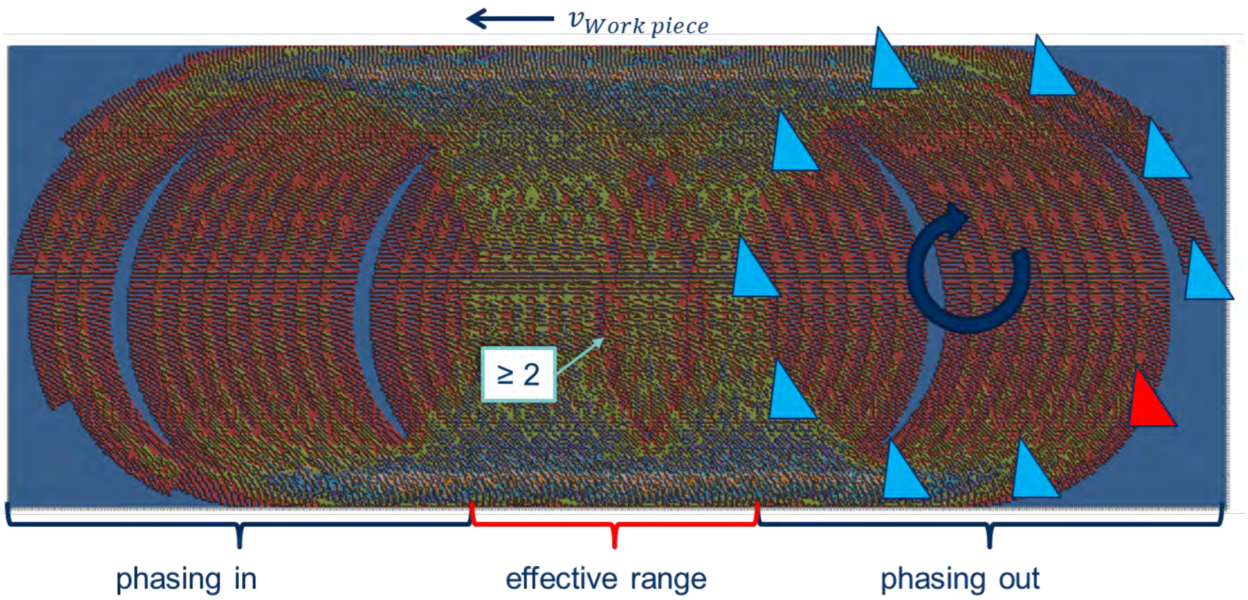

Figure 7: Simulation of multiple descaling in case of a plugged nozzle

Beside the analyses of multiple descaling, also the investigation of impact, relative velocity and the amount of water impingement in a resolution of one times one millimeter is available.

By comparing empirical data of the plant with the results of the new simulation tool a highly efficient customized rotary descaler can be designed for a wide range of products.

Hauhinco's direct drive system structure, along with this cutting edge descaling method, ensure an excellent material quality, high system reliability, and a rapid return on investment.

Optimization of Descaler Nozzle for Reduction of Red Stripe Scale

Sung June Bong, Seoung Yeul Kwak, Seon Yong Choi, Hyeong Jin Kim

ABSTRACT

It is easy to see the news of the global steel industry crisis in various media. This crisis can be overcome by securing excellent quality, different from other companies. Among many quality fields, surface quality can be a biggest appeal to customers.

Surface quality is dominated by control technology of scale occurring in the hot-rolled coil / heavy plate manufacturing process. Since scale growth control is nearly impossible in a high temperature rolling process, it is more important to remove the grown scale. In hot rolled process, high-pressure descalers installed before and after RM/FM effectively remove the scale grown at high temperature by applying a physical / thermal impact. However, unremoved scale is fractured / pressed into the surface of product during the rolling process, so red stripe scales are defected.

In this study, I tried to evaluate and improve the impact pressure of the descaler nozzle for reducing the red stripe scale defect which is a problem in the hot-strip / heavy plate rolling now.

Key words: descaler nozzle, offset angle, lead angle

1. Introduction

In the rapidly accelerating global competition, steel makers are making efforts to reduce production costs and improve product quality.

In particular, surface quality is an essential element to improve customer satisfaction and reliability for steelmakers and to make lower overall production costs.

The surface quality depends on the technique of controlling the scale, and it mainly studied in the way of restraining the scale formation or removing the scales grown during the rolling process. However, in the case of former, there are many cases nearly impossible due to the characteristics of the process, and thus a way of effectively removing the scales grown has been attempting generally.

The descaling is a process that high-pressure water is sprayed from nozzles with regular intervals to remove scale by thermal shock and impact. In order to remove the scale by using high pressure water, many nozzles are installed in the header, and high pressure water transmitted to the surface of the product is changed according to the injection conditions such as lead angle, offset angle, and nozzle spray angle. At this time, if the impact pressure is not uniform and does not reach a certain level of impact pressure, the remaining scales are pressed into the product surface causing a stripe scale problem as shown in Fig.1.

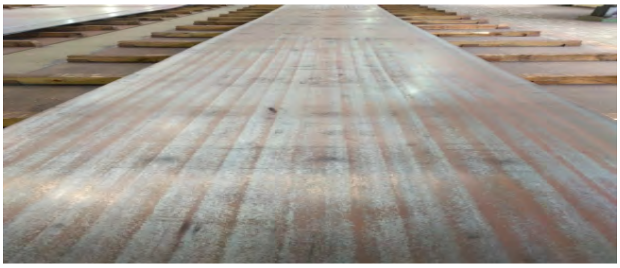

Fig.1 Red Stripe Scales on Heavy Plate

In order to improve the red stripe scale, we modified the distribution of high pressure water and confirmed the improvement of the nozzle by a lab-scale test and on-line test

2. Precede Study

As shown in Fig. 2, a test was conducted using a descaling simulator to confirm the distribution of high pressure water which is one of the factors affecting the non-uniformity descaling.

Fig.2 Descaler simulator & 3D roughness meter

The test results were obtained by measuring the depth of erosion area using a 3D-roughness meter, analyzing the relative pressure, and confirming the non-uniform impact pressure of the existing nozzles.

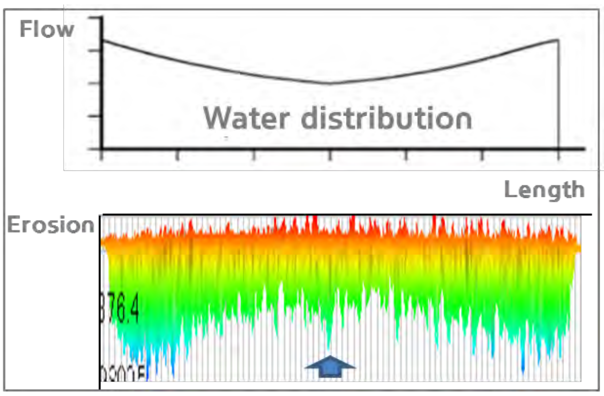

Fig.3 Distribution of erosion(existing nozzle)

As a result, it was confirmed that center impact pressure of the existing nozzle was weaker than edge side as shown in Fig.3. Normally the distribution of high pressure water was designed differently to compensate the impact pressure according to the spray distance between center and edge. But in this case, it was judged that too much compensation was applied for our using nozzles. Therefore we modified the design of the nozzle tip where high pressure water is sprayed to make impact pressure uniform as shown in Fig.4. We attained the result of more uniformed impact pressure compared to the existing one by increasing the flow rate of center area.

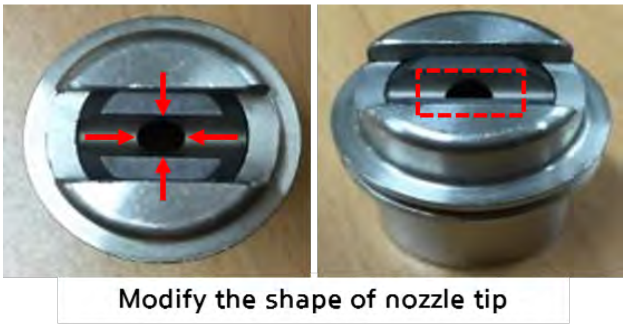

Fig.4 Modification of Nozzle design

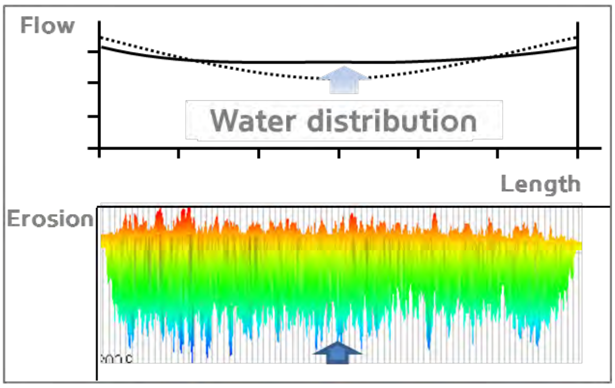

FIg.5 Distribution of erosion(modified nozzle)

3. Experiment Plan

In order to verify the effect of modified nozzle, we installed the nozzles of Finishing Scale Breaker (FSB) at the front and back of the OS(operate side) of finishing mill.

Before comfirming the effect of modified nozzles on the product in on-line, we tried to evaluate the effect quantitatively of uniformed impact pressure of the modified nozzles in the finishing mill. After the Al-plate was attached to the test plate as shown in Fig. 6, high pressure water was sprayed on the Al-plate for 5 seconds to verify the relative impact pressure. Also, we analyzed the impact pressure by measuring erosion depth using 3-D roughness meter at modified nozzles and existing nozzles

Fig.6 FSB spray(erosion) test

For evaluating modified nozzles effect in on-line products, we selected a target steel grade as the low temperature steel that red stripe scale defect easily occurred, and we did test in the same descaling pattern and rolling pass schedule as the existing rolling condition. Test results were analyzed by visual inspection for checking the width and color of red stripe scales and measured by SEM (Scanning Electron Microscope) to compare before and after.

4. Experiment Result

4.1 FSB spray (erosion) test results

First spray test was performed on Al-plate by applying modified nozzle to FSB, and the section shown in Fig. 7 was compared with the result of existing nozzle. As shown in table 1, the amount of erosion at the center was increased. This means that the relative impact pressure is increased and it is confirmed the nozzle has improved.

Fig.7 FSB spray test and analysis position

The impact center pressure was improved by 62% at the maximum even though there is interruption by the high pressure water of nozzle nearby. The impact pressure decreased at both edges of the nozzle because part of the flow on the edge side has been distributed to the center.

Erosion (㎛)	Edge	Center			Edge
	①	②	③	④	⑤
Existing	37	11	33	155	363
Modified	17	12	53	191	385
Change(%)	-54	9	62	23	6

Tabe.1 FSB spray test results

4.2 On-line Product Test Results

As shown in Fig. 8, in the on-line product test results for the modified nozzles, we confirmed that the red stripe scales were significantly reduced in visual inspection. As shown in table 2, the width of red stripe scales were reduced from 25 ~ 40mm to 15 ~ 20mm. The color was improved from dark reddish brown to light brown, and the frequency of red stripe scale generation was also reduced.

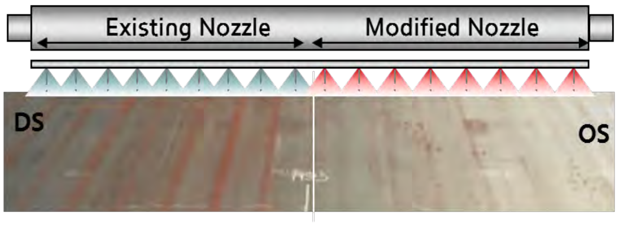

Fig.8 On-line Product Test (visual inspection)

Item	Existing nozzle	Modified Nozzle
Width(mm)	25~40	15~20
Color	dark reddish brown	light brown

Table.2 On-line Product Test Results

In order to analyze the red stripe scales by the modified nozzle application in detailed, SEM analysis was performed.

The red stripe scales are caused by the remaining scales which has been broken and pressed into surface of product during the rolling process. As shown in Fig.9, the red stripe scales were reduced by around 20% by using modified nozzles than using the existing nozzle section.

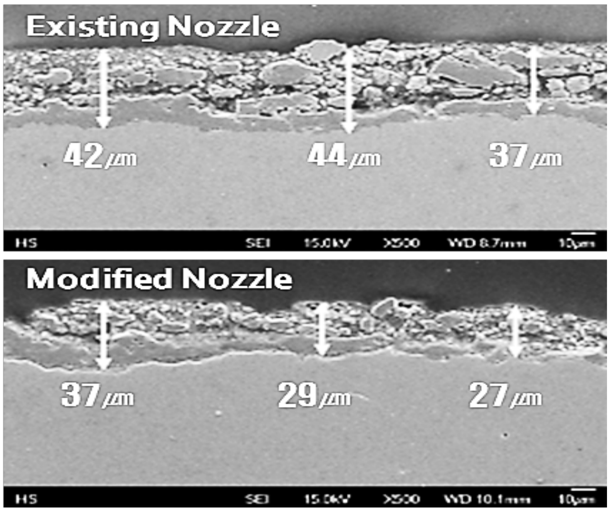

Fig.9 Thickness of red stripe scales by nozzle type

5. Conclusion

In order to improve the surface quality of the steel products, this study was designed to improve the impact pressure uniformity for the high pressure water descaler nozzles. The results are as follow.

1) In the FSB spray (erosion) test, the center impact pressure of the modified nozzle was improved by 62% compared to the existing nozzle.

2) In the on-line product test results, The red stripe scales generated under the modified nozzle section were improved in the width and color of red stripe scales. The width was reduced from 25 ~ 40mm to 15 ~ 20mm, and the color was improved from deep reddish brown to light brown.

3) The red stripe scales were decreased by around 20% by using modified nozzles than using the existing nozzle section.

6. Future Plan

In addition to uniformizing the impact pressure, additional studies are required to eliminate red stripe scale defects, such as “impact pressure reduction at the overlap section due to the offset angle.”, “reducing scale growth in reheating furnace.”

Now, we are conducting further research on offset angle as shown in Fig.10 by our descaler simulator. We are looking for ways to minimize the high pressure water interference between nozzles in overlap sections.

Our continuing research will improve the surface quality of our products.

Fig.10 Overlap difference by offset angle

7. Reference

[1] Sung Cho Kim and Jong Wook Choi, “Method of Setting nozzle intervals at the Finishing Scale Breaker” KSME International Journal, Vol. 17 No. 6, pp. 870~ 878, 2003.

[2] Lothar Bendig, Miroslav Raudensky and Jaroslav Horsky, “Descaling with high pressure nozzles”, ILASS-Europe 2001.

[3] MinJae Park, “The Impact Pressure Distribution of the descaling nozzle and a Major Cause for Stripes”

[4] Lesli Robb Spraying Systems Co. “Effect of Spray Height, Lead angle and Offset Anlge on Impact stripes Mill”

[5]Jong Wook Choi and Jin Wook Choi, "'Convective Heat Transfer Coefficient for High Pressure Water Jet," ISIJ International, vol. 42. No. 3, pp.283~289. 2002.

[6] J.W. Frick, “More efficient hydraulic descaling header design”

Hydraulic descaling of coil of wires during pickling program

Michal Pohanka[1], Milan Hnízdil[1], Petr Kotrbáček[1], Helena Votavová[1]

Keywords: hydraulic; descaling; wire; coil; cold; pickling; long distance

Abstract

An oxide layer is formed on stainless steel wires during the heat treatment process. To remove the layer of scale, the pickling program is used. The wires are treated in coil that is about 1.3 m in diameter. One pass through the pickling program does not result in a scale-free and rust-free surface for all steel grades and the coil has to go through the pickling program again. This results in unwanted double passages that increase the treatment price significantly. Hydraulic descaling of the whole wire coil was inserted into the pickling program to reduce the number of double passages and prolong the life time of pickling baths. This paper presents a study of descaling efficiency for long distances in free space and through wires. Impact pressure distribution measurements are coupled with descaling of wires. Scales on the wire samples were analyzed using optical as well as scanning electron microscopy in combination with energy dispersive x-ray spectroscopy for element analysis before and after descaling.

Introduction

During heat treatment of steel, metal oxides (scale) are formed on the surface of the material. For downstream processing of wire rods or in the metal processing industry, a scale-free surface is essential to avoid excessive tool wear and in particular any impairment of quality and surface properties. The most effective way to perform surface treatment on wire rods is in the coiled form. The coiled wire rod is treated in batches in pickling tanks containing different acids. Depending on the steel grade, the pickling program consists of up to ten steps of pre-treatment, pickling and rinsing.

The pickling line represents a bottleneck in the production of wire rods. To increase productivity a new high pressure water jet treatment is planned to be inserted in the pickling program. Performances of various configurations were studied in laboratory conditions using impact pressure distribution measurements and cold descaling tests.

Measurements

Impact pressure distribution measurements

For a given nozzle configuration, the pressure is measured as a position dependent value while the pressure sensor is slowly moving under the spraying nozzle (see Fig. 1) and pressure values are recorded as a function of position. It is known that the measured impact pressure is positively correlated with cleaning efficiency in most cases (exceptions are pulsating nozzles and in the overlap area because of the different water jet structure). The impact pressure is an average value but the instantaneous pressure varies from values close to zero to a value much higher than the average. Two types of impact pressure distribution measurements were carried out: without and with dummy wires. Examples of experiments with dummy wires are shown in Fig. 2. The water has to go through at least one layer of dummy wires before it reaches the pressure sensor in these cases.

[1] Brno University of Technology, Faculty of Mechanical Engineering, Heat Transfer and Fluid Flow Laboratory
Technická 2896/2, 616 69 Brno, Czech Republic
E-mail: Michal.Pohanka@vut.cz
Internet: http://www.heatlab.cz

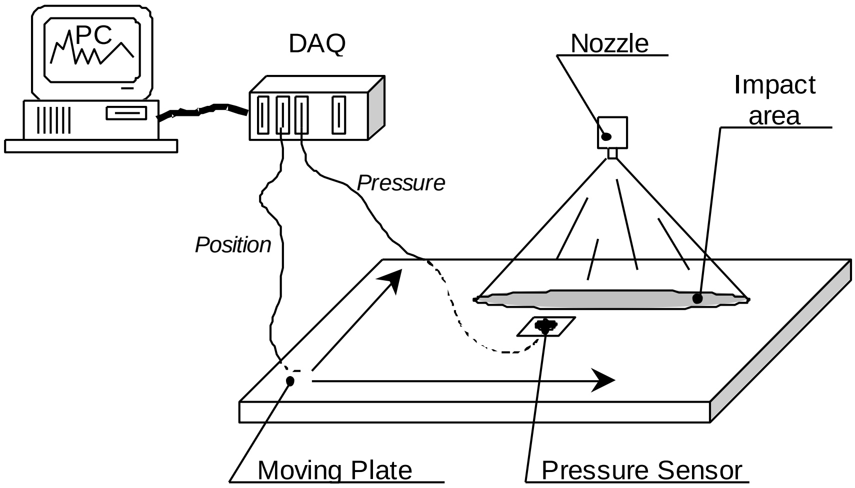

Fig. 1 *Diagram of impact pressure distribution measurements*

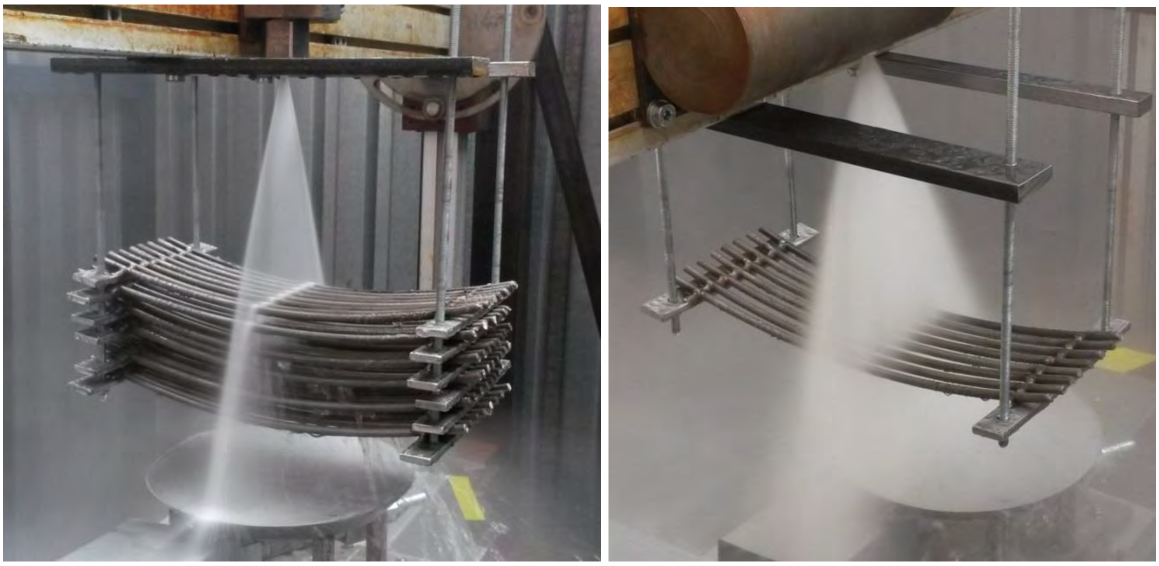

Fig. 2 *Impact pressure distribution through wires (left: six layers of wires; right: one layer of wires)*

Cold descaling tests

The experimental configuration is very similar to the experiments shown in Fig. 2, only the test plate with a pressure sensor was replaced with wire with scales on surface (see Tab. 1). The scaled wire passed through the spray twice with a velocity of 50 mm/s. The descaled surface of the wire was analyzed using photographical, optical and scanning electron microscopy in combination with energy dispersive x-ray spectroscopy for element analysis.

Results

Two types of spray were analyzed. The first one using the bigger "Nozzle A" was done for lower water pressure equal to 5 MPa and the second one using the smaller "Nozzle B" was done for higher water pressure equal to 45 MPa. Both configurations had similar water density equal to 36 l/min/m in the direction of spray width for a spray distance of 300 mm. The spray angle was 40° for nozzle A (see Fig. 2 left picture) and 30° for nozzle B (see Fig. 2 right picture).

Impact pressure distribution measurements without dummy wires showed higher impact pressure can be obtained with bigger nozzle A and a smaller water pressure of 5 MPa for bigger distances as shown in Fig. 3. The water stream does not explode to surrounding air and stays more compact. On the other hand the experiments showed that when smaller nozzle B with a bigger pressure of 45 MPa is used, the water stream breaks up into very small droplets and a highly turbulent water-air mist stream is produced which expands quickly into the surrounding air. The impact pressure drops faster as the distance is increased for nozzle B when no dummy wires are used.

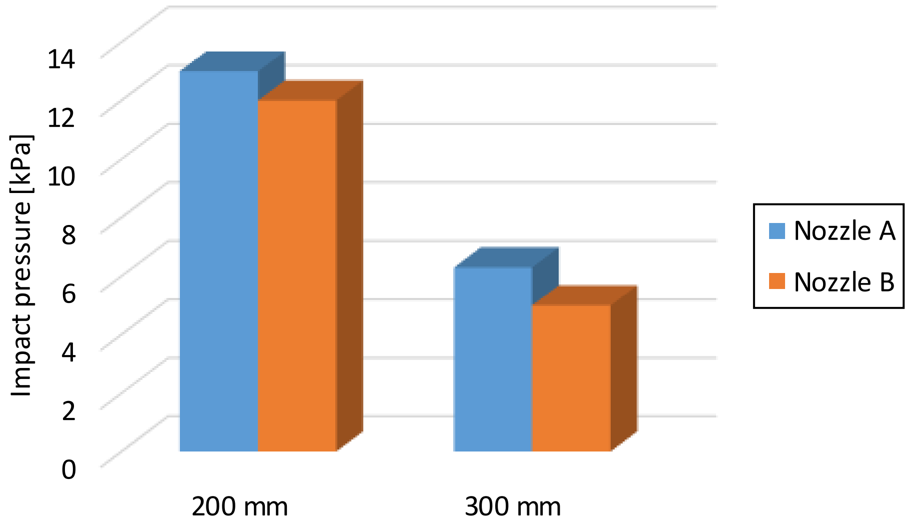

Fig. 3 *Results from impact pressure distribution measurements without dummy wires*

The situation is changed dramatically when dummy wires are used (see Fig. 4). The impact pressure varies extremely with nozzle A. Impact pressure is close to zero under dummy wire but very high under a gap between dummy wires. The local maximum impact pressure is even higher than in the experiment without dummy wires. When four layers of dummy wires are used the water stream is completely destroyed- the water flows on the surface of the wires, drops down randomly, and there is usually zero impact pressure.

The smaller nozzle B with a higher pressure of 45 MPa behaves differently. The highly turbulent water-air mist stream passes around dummy wires and a more homogeneous impact pressure distribution is produced when one layer of dummy wires is used (see Fig. 4 on right). However, the impact pressure decreases rapidly (see Fig. 5) when the number of layers of dummy wires is increased from one to four. With 4 and 6 layers of dummy wires the decrease is significantly slowed down and the impact pressure is similar.

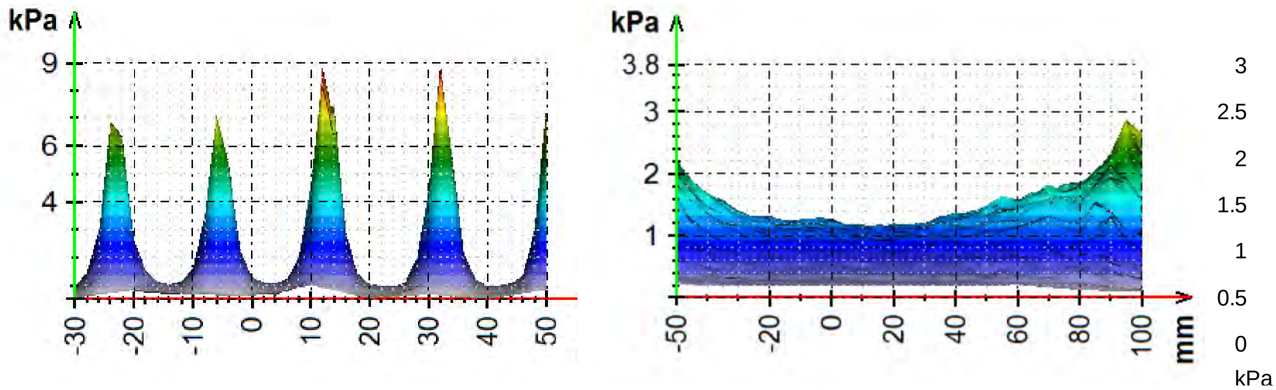

Fig. 4 *Impact pressure distribution for nozzle A at 5 MPa (on left) and nozzle B at 45 MPa (on right) for spray distance 300 mm through one layer of wires*

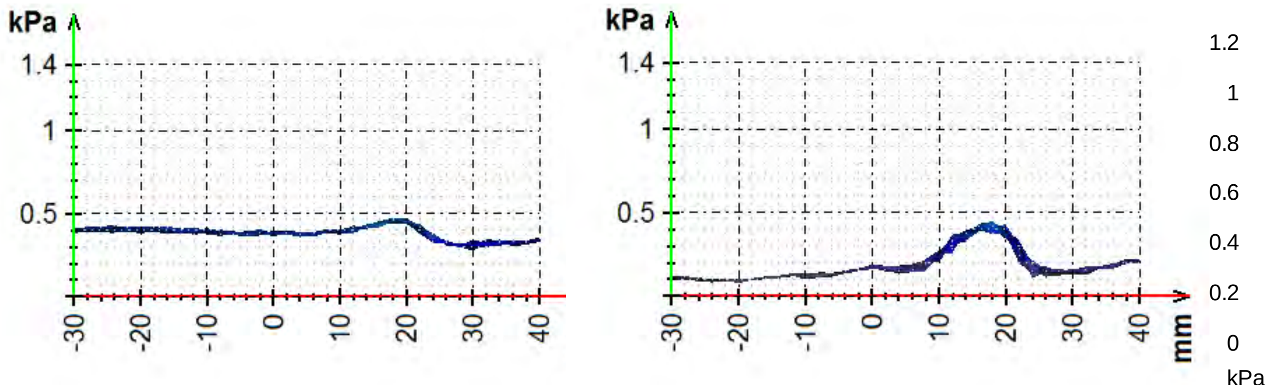

Fig. 5 *Impact pressure for nozzle B at 45 MPa for spray distance 300 mm through 2 layers of wires (left) and 6 layers of wires (right)*

The effectivity of hydraulic descaling through 6 layers of dummy wires was tested with the smaller nozzle B at 45 MPa. Wire rod ⌀13 mm covered with scales (see Tab. 1) was placed at a distance of 300 mm and later at 200 mm from the descaling nozzle. The results obtained in Tab. 1 show that even a very low impact pressure of 0.1–0.4 kPa can help with removing scales from the surface. The effectivity is significantly increased when dummy wires are removed. The scanning electron microscopy in combination with energy dispersive x-ray spectroscopy for element analysis showed that remaining scales contained high content of chromium, nickel, and molybdenum.

Tab. 1 *Wire descaling using nozzle B at 45 MPa for steel grade 1.4571*

before descaling		after descaling from 300 mm	
after descaling through dummy wires from 300 mm		after descaling from 200 mm	

Conclusion

The study of the descaling system showed that a higher impact pressure can be achieved with lower water pressure when a bigger nozzle is used for a bigger standoff of 300 mm. The situation is completely changed when the water has to pass through wires. In this case it is necessary to use a smaller nozzle with a much higher water pressure. The cold descaling tests proved that even very low impact pressure can help with removing scales from wires during the pickling program.

Acknowledgment

The research leading to these results has received funding from the MEYS under the National Sustainability Programme I (Project LO1202) and by the project HIJETROD - Resource-Efficient Hydromechanical Descaling System for Wire Coils, pilot project RFSR 709435, granted by the Research Fund for Steel and Coal.

Comparison of Positive Displacement Pumps vs Centrifugal Pumps for Hydraulic Descaling of Steel in a Rolling Mill - Hardy Siegmund, *HASTEC Group*

The efficient hydraulic descaling of steel in a rolling mill requires that not only quality be achieved but also that the process itself is cost effective and operationally practical. The determining variable in evaluating overall process efficiency is the style of pumps used for the descaling operation. Our discussion will illustrate and compare descale systems using both positive displacement pumps and centrifugal pumps. The functionality of each style of pump will be reviewed along with the associated differences in system design and operational requirements. Further topics like power consumption and maintenance strategies will also be presented. It is important to understand the differences between these systems for decision making when retrofitting existing descaling systems due to reliability or operational cost issues or when new quality requirements present themselves. Some of the retrofitting trends observed on the market in last years will also be shown.

New testing methods for descaling nozzles

Martin Wunde (VDEh-Betriebsforschungsinstitut GmbH (BFI),
Sohnstraße 65, 40237 Düsseldorf, Germany, martin.wunde@bfi.de, +49 211 6707 316)

Summary

Scale must be removed before the first forming step as it leads to product surface defects and tool wear. The complexity and diversity of hot strip production processes require descaling systems to provide optimum performance across a very wide process window. The nozzles are a key factor of descaling plants. Nozzle developers, plant constructors and rolling mill operators can use model tests to estimate the efficiency of descaling nozzles. For these tests the question is remaining how realistic the test conditions are and whether the test results reflect reality closely. Due to these facts, the demands for new possibilities raised to represent the descaleability by cold composites. Therefor, 4 material strategies were followed: Variant A: "Erosion sensitive layers", Variant B: "Imprint sensitive viscoelastic layer", Variant C: "Hardness gradient" and Variant D: “Gradient in stress intensity”.

The properties of variants A and B depend on the expected "usual" impact, descaling energy and specific water impingement. These composites react very sensitive on changes in Impact.

The properties of variants C and D depend on the (fracture-) mechanical properties of scale, as can be expected during a defined hot rolling route. These composites did not react to the water impingements in the experiments.

Keywords

Scale, Mechanical properties, Fracture mechanical properties, Descalability

1 Introduction

Scale must be removed before the first forming step as it leads to product surface defects and tool wear. The conventionally used press water descaling causes quenching, breaking, bursting and rinsing away of the scale[1].

The complexity and diversity of hot strip production processes require descaling systems to provide optimum performance across a very wide process window. The nozzles are a key factor here. For the further development of nozzles and the design of descaling plants, nozzle developers, plant constructors and rolling mill operators can use model tests to estimate the efficiency of descaling nozzles:

Impact measurements: Measurement of the lateral impact pattern over the entire spray pattern,

Aluminium erosion tests: Evaluation of the erosion groove formed in an aluminium plate, and

Hot test: Evaluation of the nozzles using a more realistic hot descaling test.

For all these tests the question is remaining how realistic the test conditions are and whether the test results reflect reality closely. The effectiveness of descaling depends not only on the descaling system but also on the scale properties, e.g. scale thickness, composition, adhesion to the surface, porosity and mechanical properties. These properties are in turn dependent on steel composition, furnace atmosphere, heating time, roller table length and cooling units.

Due to these facts, the demands for new possibilities arised to represent the descaleability by cold composites, which e.g. represent the following properties: (i) the composites should be tested dynamically, thus, in motion, (ii) the results should be evaluated visually, quickly and easily, (iii) the measurements should provide quantifiable results and (iv) the results should reflect the real descaling process.

In the development of the composites four strategies were followed: Variant A: "Erosion sensitive layers", Variant B: "Imprint sensitive viscoelastic layer", Variant C: "Hardness gradient" and Variant D: “Gradient in stress intensity”.

The properties of variants A and B depend on the expected "usual" impact, descaling energy and spec. water impingement. The properties of variants C and D depend on the (fracture-) mechanical properties of scale, as can be expected during a defined hot rolling route.

2 Experimental methods and materials

2.1 Developed composites

The **composite variant A** is intended to provide a quick and convincing alternative to the aluminium erosion test. The strategy is to use the effect of erosion to produce a visually detectable erosion progress very quickly - even in motion. The composite consists of a steel carrier material coated with erosion sensitive layers of different colours. The erosion reacts very sensitively to the impact, the descaling energy and specific water impingement. The erosion resistance is chosen so that minimal deviations of these sizes lead to clearly visible colour gradients.

The objective of **composite variant B** is to deliver quantitative results. For this purpose, a layer sequence has been designed which makes it possible to conserve water impacts in the form of plastic deformation in order to evaluate them by means of topography measurements. The composite consists of an elastic layer applied to a carrier plate. The top layer of aluminium foil ensures the preservation of the impingements caused by the water impact. The properties of the composite are selected in such a way that minimal deviations of the impact are reflected in the permanent impressions, which can subsequently be evaluated with topography measurements.

The strategy for **composite variant C** consists in mapping the pure mechanical properties of the scale according to the calculated temperature profile through a multi-layer structure. The composite consists of a sequence of different polymers, whose hardness corresponds to the hardness curve of a conventional primary scale layer with temperature gradients (**Fig 1**). If the hardness of the scale would be the relevant property for the descaleability, the different coloured polymer layers of the composites would have to react to the water impact by crack formation or spalling.

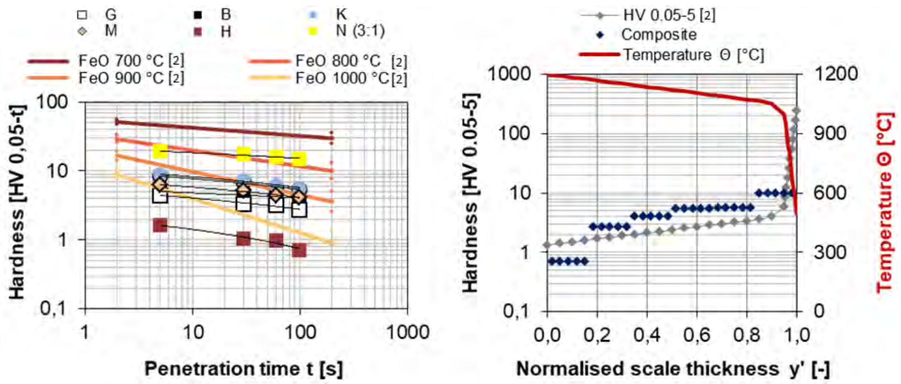

Fig 1: Comparison of hardness curves over the test period of different polymers (dots) and wustite (line) (left) as well as hardness sequence in Composite in comparison to temperature (right)

Composite Variant D: In addition to the mechanical properties - such as hardness and strength - toughness and crack formation play a major role in descaling. The stress state and the existing defect size have a major influence. The strategy for this variant is to reproduce the thermally induced stress state and crack intensity as realistically as possible. This was done on the basis of light microscopic investigations (**Fig 2**) and heat transfer calculations (**Fig 3**), with which the scale morphology and the course of fracture toughness and stress intensity[3] were calculated.

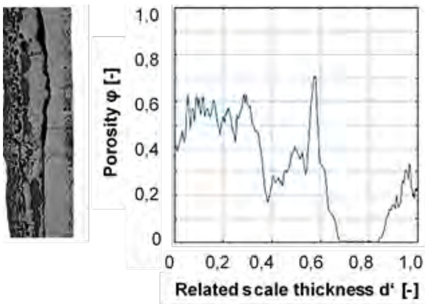

Fig 2: Cross section of the scale (left) and pore distribution of a single measurement (right)

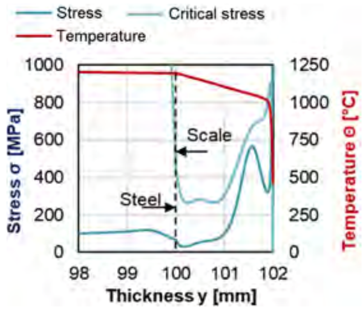

Fig 3: Course of stress, crit. stress and temperature in steel and scale

The composite consists of a carrier material and a porous polymer layer (**Fig 4**), whose stress intensity can be approximated to that of a normal scale layer by bending around the radius ϱ (**Fig 5**).

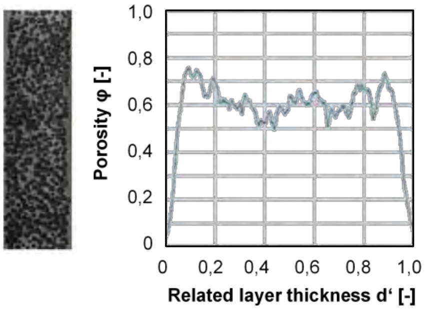

Fig 4: Cross section of the porous polymer layer (left) and pore distribution of a single measurement (right)

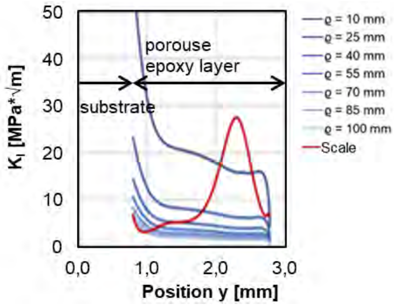

Fig 5: Course of stress intensities in the porous functional layer (blue) and in scale (red)

The defined bending or buckling is applied to the composite in a specimen holder (**Fig 6**).

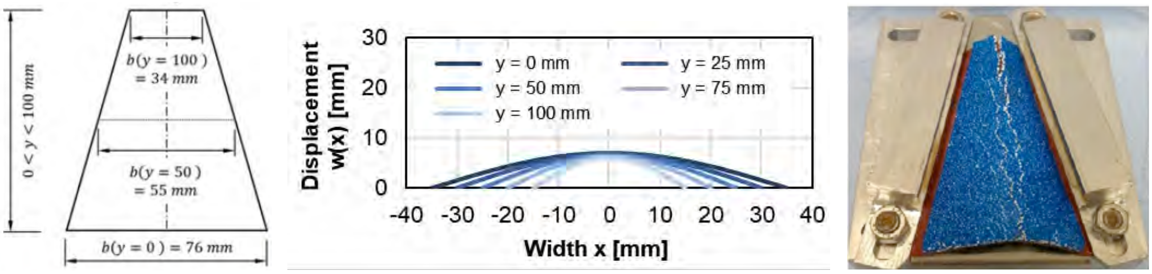

Fig 6: Shape (left), deflections (middle) and mounting (right) of the composite

2.2 Experiments

All developed composites were tested with the descaling test bench installed at BFI. The specification is given in **Table 1**.

Table 1: Specification of the descaling test bench installed at the BFI

Linear drive	max. 4 kg, max. 3 m/s	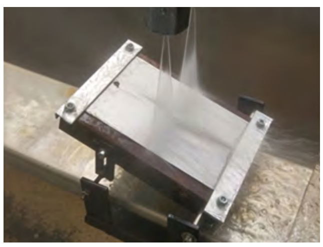
Specimen size	max. 100 x 150 x 35 mm³	
Pump	Speck plunger pump 11 kW max. 50 l/min, max. 220 bar	
Descaling nozzle	Lechler HPS 6P3.495.27 17 l/min at 200 bar 22° nozzle opening angel	
Standoff nights	60 < h_2 < 200 mm	Skew specimen holder for realising different standoff hights in one test

3 Results of selected composites

Table 2 compares selected results of **variant A**. It can be seen that the erosion sensitive layers react very sensitively to impact changes.

Table 2: Selected results of the composite variant A

Test number	**1**	**2**	**3**	**4**
Pressure p [bar]	160	180	200	180
Impact IP [MPa]	0,50 to 0,19	0,56 to 0,21	0,62 to 0,23	0,56 to 0,21
Twist angel γ [°]	0			15
Results				
Further parameters	2 nozzles, specimen speed v = 0,66 m/s, standoff hight h_2 = 80 to 130 mm, inclination angel β = 15 °			

The composites of **variant C and D** did not react to the water impingements in the experiments.

4 Conclusion

The mechanical properties of the scale are sufficiently described. However, the fracture mechanical properties have to be further investigated with a special focus on the influence of pores and cracks as well as the toughness of eutectic structures in the presence of fayalite or other mixed oxides. In the future, high-strength steels will contain more silicon, which will further increase the need for knowledge expansion.

Two variants of a composite (A and B) have been developed that do not reflect the properties of the scale, but can replace the controversially discussed aluminium erosion test or at least make it more quantifiable.

Based on the (fracture-) mechanical properties, a composite (C) was developed to map the technical descaling at room temperature. It was shown that strength and hardness alone are not the decisive factors for spalling and descaling. A further composite (D) was developed, which can be used to map the stress intensities within the scale, taking into account the entire process route. Here, however, it was shown that an important mechanism of descaling - the fast evaporation of water - cannot be reproduced.

5 Acknowledgement

This research was carried out with the financial grant from the RFCS (Research Fund for Coal and Steel of the European community) HiPerScale (RFSR-CT-2014-00010). All financial support is gratefully acknowledged by the authors. The authors gratefully acknowledge the support of the industrial project partners of the above mentioned research projects.

6 Literature

[1] M. Degner: Modern Hot Strip Production - Process and Plant Technology, Verlag Stahleisen GmbH, Düsseldorf, 2013

[2] G. Vagnard, J. Manence; Etude de la plasticite´du protoxyde de fer et de l'oxyde cuivreux, MEMORIES SIENTIFIQUES REV. METALLURG., Vol. 61, No. 11, S. 768 - 776, 1964

[3] Y. Murakami, The Society of Materials Scienc: Stress intensity factors handbook, Pergamon Press, 1987, Vol. 1

THE DESCALING BEHAVIOUR OF OXIDE SCALE IN A ROUGHING MILL

Annika Nilsson[1], Jan Niemi[1], Pasi Lehtikangas[2] and John Niska[1]
[1] *Department of Heating and Metalworking, Swerim, Luleå, Sweden*
[2] *SSAB Europe Oy Raahe, Finland*

SUMMARY

In this work, the changing residual oxide scale appearance and removal was monitored in the roughing mill at SSAB in Raahe. The monitoring of the residual scale was performed using automatically triggered cameras positioned on each side of the roughing mill stand. The evolution of oxide scale during roughing was studied using manual inspection and image processing.

It was possible to follow the behaviour of the oxide scale during hot rolling just from manual observation of the images. It was discovered that residual primary scale often spalls off in the rougher. Even scale that has been rolled-out commonly falls off in subsequent passes. The surface underneath the scale is then clean and hotter than in the surrounding area where secondary scale was not removed. Scale that has a good adhesion and is ductility will be rolled-out so that it becomes thinner and elongates during the rolling passes. Even scale that was elongated often falls off in subsequent passes.

Scale that remains gets rolled into the surface. Rolled-in scale is seen as dark spots on the surface. The appearance of rolled-in scale becomes diffuse so that it is difficult to see in the final passes. From this study it was seen that knowledge about the previous rolling passes is critical for interpreting images correctly.

MEASURING CAMPAIGN AT SSAB

The monitoring system consists of two Sony IMX174 (2.3Mpixels) colour cameras. The cameras were controlled using the SWERIM MEFOS in-house program called MEFScale. The goal was to follow the scale status in the roughing passes. The camera positions are shown in Figure 1. Descaling was used before the first, the third and the seventh pass. Images were taken after each pass so that it is possible to follow the progression of scale status during rolling.

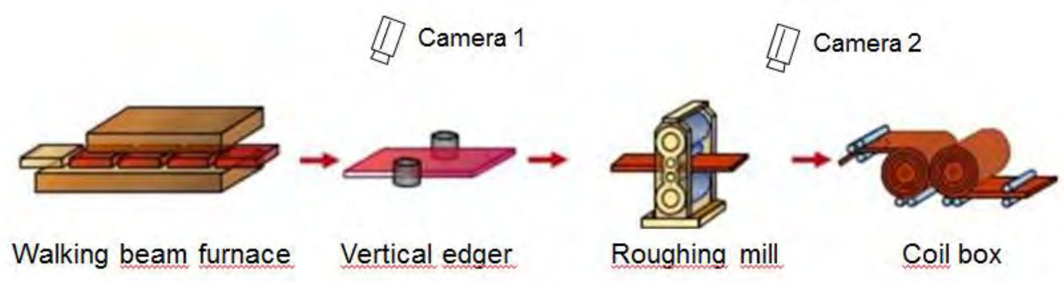

Fig 1. Strip rolling line with the camera positions, one on each side of the rougher

Basically the images show:

- the residual scale after primary descaling
- the growth of secondary scale

- the transformation of the scale (rolled-out or spalling off)
- the formation of rolled-in scale

RESIDUAL SCALE

The images taken before the roughing mill were taken before secondary descaling. The first image shows the residual scale after the primary descaler. Thick scale is dark and thin scale is more transparent. Scale might split up between the scale layers. The variation in the position, thickness and appearance of the residual primary scale can be seen in the surface images. Common types of residual scale include head end scale, tail end scale, local spots, stripy scale, blisters etc.

SCALE BEHAVIOUR

When studying the scale status, interesting changes in the scale appearance were observed. Scale that is hot rolled can elongate depending on the ductility of the scale. According to a summary of data given in Ref [1], oxide scale is ductile and can elongate at high temperatures, that is, above 900°C due to the plastic behaviour of the main component in secondary scale, wustite. Elongated scale gets deformed which in the images is seen as an increased length and increased transparency, see Fig. 2. The scale in Fig 2 b had detached after pass 5 which is also is possible based on the data in Ref [1], since the plasticity of the oxide scale decreases at lower temperatures where the behaviour turns to brittle or less ductile. Even when scale appears to be rolled-in, it can loosen and fall off in subsequent passes. An example is shown in Figure 3.

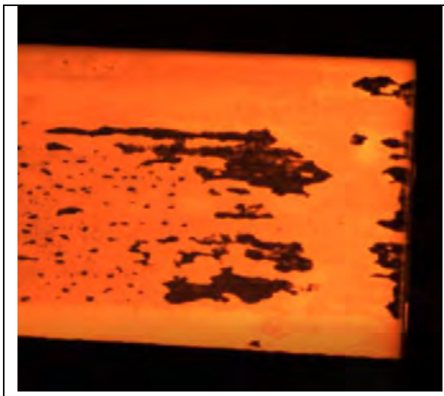	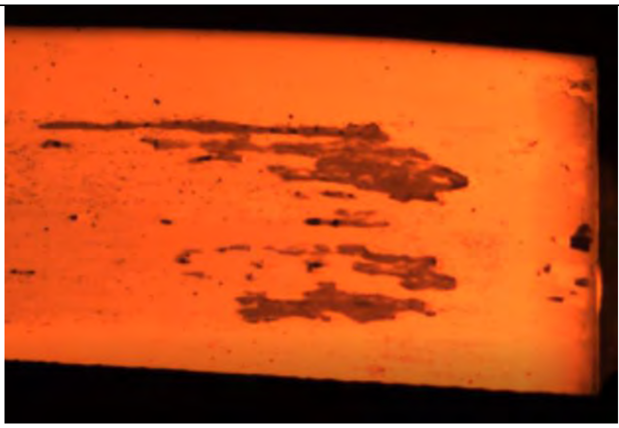
a) Head end after pass 1 remaining scale and blisters	b) Head end after pass 3 elongated scale

Fig 2 Example of elongated seen from an increased length and increased transparency.

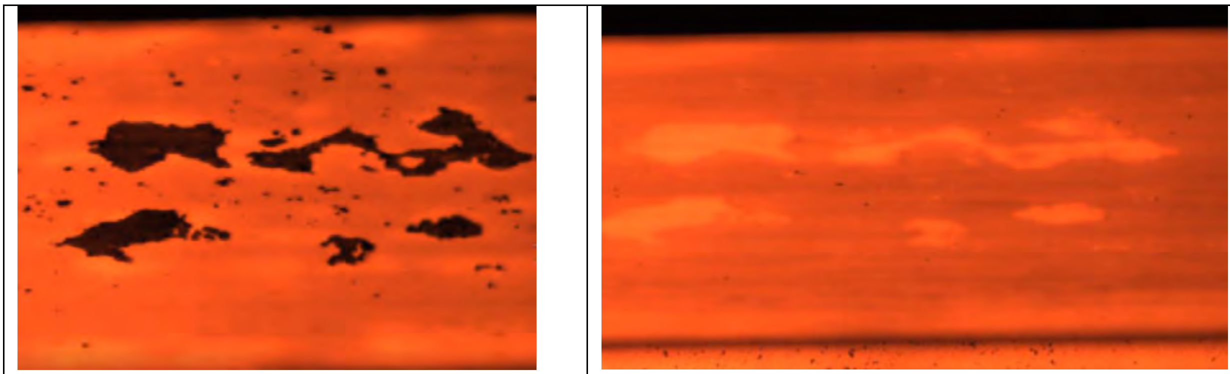

After pass 1. Discharge temp 1140°C The residual scale was hot rolled one pass

b) After pass 3, the residual scale has fallen off leaving behind cleaner spots surrounded by a thicker and darker secondary scale surface.

Fig 3 Initially "dirty" surface becoming cleaner as the scale spalls off.

Figure 4 shows a case where part of the scale has loosened and part remains after the third pass. After the 5th pass the secondary scale layer has cracked forming flakes. After the 7th pass the transfer bar has a nice surface and appears to be clean.

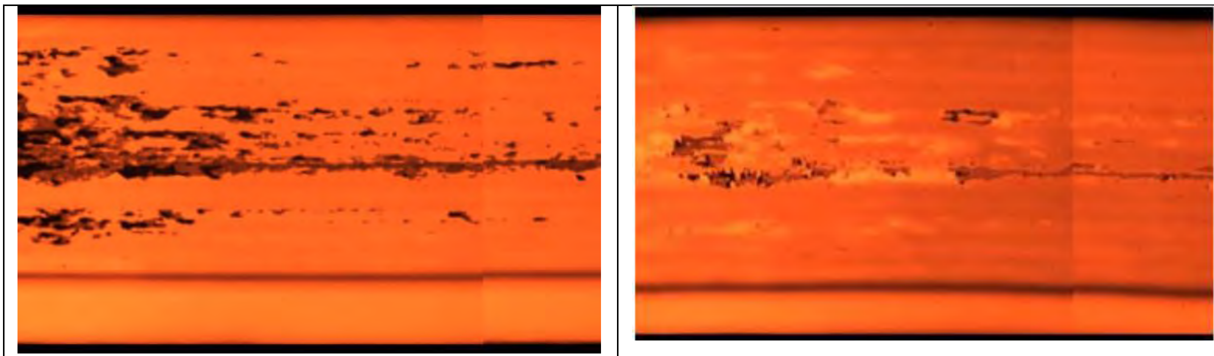

a) After pass 1: Rolled-in scale of varying thickness is seen.

b) After pass 3: A considerable part of the scale has fallen off but some remains. The slab was descaled before this pass.

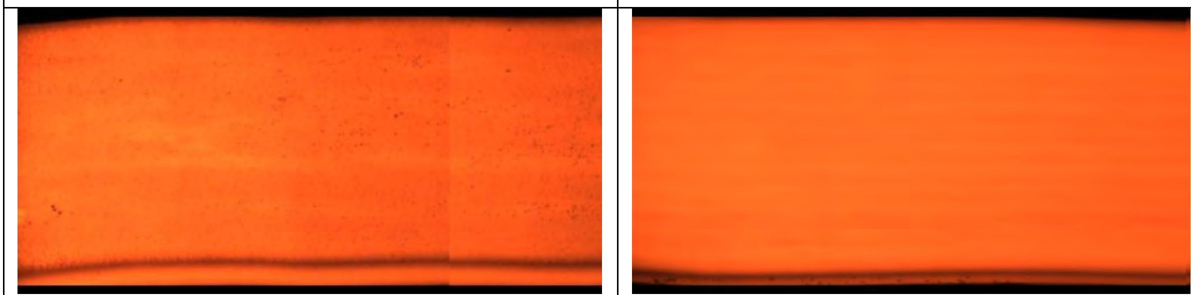

c) After pass 5 A hot spot remaining where the primary scale once was located. Flakes were formed due to a broken secondary scale layer.

d) After pass 7 A nice clean surface with a thin, uniform scale layer is seen.

Figure 4. Progression of the scale morphology during rolling in the rougher for a strip with primary scale left on the center of the slab.

Figure 5 shows the scale development of another transfer bar that was not efficiently descaled. Even though a major part of the scale loosened and fell off in the roughing mill, some was rolled-in.

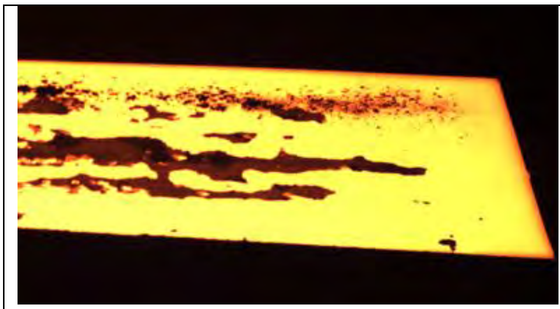

a) Rear end before rolling

b) After pass 2. Scale has broken, off thicker scale spots remain on the surface.

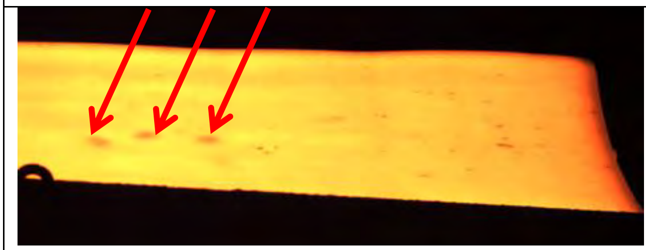

c) After pass 4. Local spots showing scale rolled into the surface.

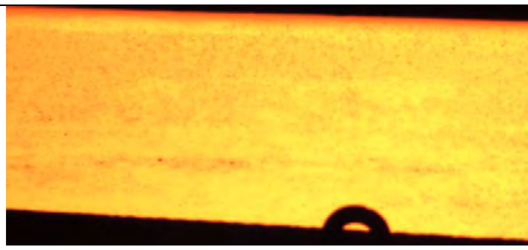

d) After pass 6. A broken secondary scale layer including blurry rolled-in scale spots.

Figure 5. Examples of rolled-in scale on a slab having residual scale near the tail end. The rolled-in scale appears as diffuse dark spots after pass 4.

DISCUSSION

The behaviour of oxide scale during hot rolling is influenced by the material properties of the scale and the adhesion of the scale to the steel surface. A ductile scale will elongate and become thinner and brittle scale will crack. The conditions for spalling off or cracking is believed to be controlled by the relationships presented in Fig 6.

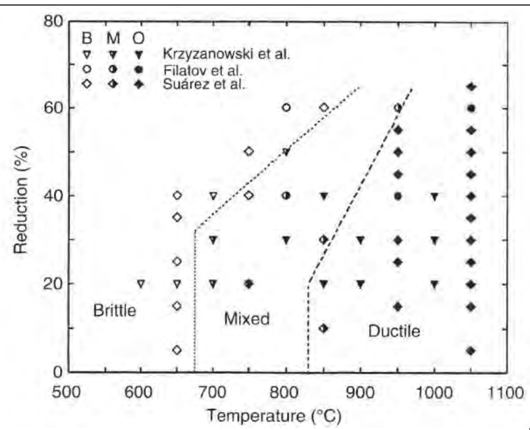

Scale properties at different temperatures and reductions [1]

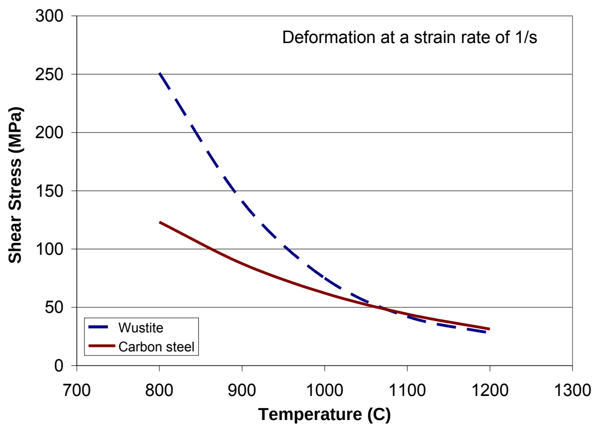

Shear strength for wusite ($Fe_{0.95}O$ [2]) versus a 0.2% carbon mild steel [3]

Figure 6. Properties of scale believed to explain the observations in the rougher.

CONCLUSIONS

Surface inspection during the early hot rolling passes can help identify when the hydraulic descaling is incomplete resulting in residual scale on the surface, and when the residual scale leads to surface defects. Proper temperature control during hot rolling can help avoid rolling in scale by maintaining scale ductility.

ACKNOWLEDGMENT

The research leading to these results has received funding from the European Community's Research Fund for Coal and Steel (RFCS) under grant agreement n° RFSR-CT-2014-00010 [4] and financial support from the steel industry.

REFERENCES

[1] Michal Krzyzanowski, John H. Beynon, Didier C. J. Farrugia, "Oxide Scale Behaviour in High Temperature Metal Processing", Wiley-VCH Verlag GmbH Co. KGaA (2010), p.47

[2] H.J. Frost and M.F. Ashby, "Deformation-mechanism maps, The plasticity and creep of metals and ceramics", Dartmouth College, USA, web version for chapter 12, for wustite with a 10 micron grain size at:

http://engineering.dartmouth.edu/defmech/chapter_12.htm

[3] J-O. Perä, "CONTROLL-Parameteranalys vid valsning" software for carbon steel alloy Nr 3 (0.2C, 0.8Si and 1.2Mn), SWERIM MEFOS, Luleå.

[4] Miriam Sartor, et. al., "High performance hot rolling process through steel grade-dependent influencing of the scale formation and flexible descaling control", RFCS grant agreement RFSR-CT-2014-00010 (2014).

A Methodology for Fine Characterisation of Oxide scale-metal interface

M.Olowe[1], D.Farrugia[2], D. Proprentner[1], M.Auinger[1], B.Shollock[1]

[1]*Advanced Steel Research Centre (ASRC), Warwick Manufacturing Group, University of Warwick, Coventry, CV4 7AL, United Kingdom*

[2]*Swinden Technology Centre, Tata Steel R&D UK, Moorgate Rd, Rotherham, S60 3AR*

ABSTRACT

The attainment of a defect-free surface on fully finished electrical steels is not only an important goal for surface quality but also for the high value, high silicon electrical steel grades; which are considered to be a significant contributor to the achievement of the best possible magnetic properties. The main factors that cause electrical steels to be more prone to surface defects than carbon and alloy steels are related to their oxidation characteristics. The silicon and aluminium alloying additions in electrical steels form much more stable oxides than iron, and the scales are known as 'sticky', i.e. much more adhesive than oxides on more standard steels. In addition, the fayalite (Fe_2SiO_4) eutectic temperature is lowered by addition of aluminium.

The manufacturing of electrical steel follows a complex series of processes starting with continuous casting, reheating (minimum temperature of 1150ºC) and primary descaling. Depending on the hot mill configuration (e.g. conventional Hot Strip Mill or Direct Sheet Plant lines) a series of roughing and finishing mill descaling/deformation steps follows prior to cooling and hot coiling. During reheating, primary oxidation occurs both externally and internally. This has a critical effect on the final performance of the steel if not controlled properly during reheating and subsequent high pressure water (HPW) descaling. The formation of these oxides is dependent on atmosphere and reheating processing conditions, alloy composition (in this case, Al-Si contents), surface state and prior-oxidation which contributes to the oxide growth rate and morphology. Thus, in order to understand the oxide growth (mechanism and kinetics) on these steels, the surface state and metal/oxide interface need to be characterised prior reheating so as to understand the origin of the oxide phases formed post-reheating. In addition, the mechanical properties and kinetic data of oxide growth during reheating must be determined to complement the results obtained.

This paper highlights a strategy for characterising the oxide-steel interface using an array of different techniques. The proposed methodology is based on combining a range of microscopic characterisation at known length scales and lateral resolutions to obtain chemical profiles/phase identification via Scanning Electron Microscope (SEM), Energy dispersive spectroscopy (EDS), Raman spectroscopy and X-ray diffraction (XRD). A fractal approach is taken to quantify 2D profile of oxide-steel interface roughness/waviness and define its degree of complexity. The last method to be explored is X-ray computed tomography (X-ray CT) which provides a 2D and 3D profile of the metal/oxide interface although the methodology for the use of this technique needs to be further developed. Oxide characterisation is then followed by mechanical testing across selected metal/oxide interfaces, initially at room temperature, to qualitatively assess the contributions of types of oxides, morphology of oxide and characteristics of the interface and surface. The aim is to link the data obtained to the descalability of the oxide scale based on the nozzle configuration and descaling impact footprint. This methodology is tested on as-received cast layer of an electrical steel alloy (2.4 % Si) to also study the influence of Si alloying addition during oxidation.

1. INTRODUCTION

Prior to reheating the as-received steels slabs are pre-oxidised. This oxide scale is formed during continuous casting as the steel slab undergoes cooling and re-straightening (see 1-6 in Figure 1). Parameters such as alloy composition, casting speed, cooling rate, mould heat flux, etc., contribute to the formation of the oxide layer during the cooling of the slab; however, the morphology and properties of this newly formed layer are unknown. This paper aims to present a systematic approach to characterising an oxide layer using a number of techniques (Figure 2) which in the past have been primarily used individually [1, 2] at various physical length scales from oscillation marks (mm) to inclusion size (sub-microns). The proposed approach can provide important understanding of the as-cast oxide layer, as little is known about how this oxide layer evolves during reheating and how it contributes to oxide scale properties post-reheating. Characterising these features will allow a better mapping of their physical relationships to the impact force distribution of the descaling nozzle (with spray depth of around 2 to 3 mm.

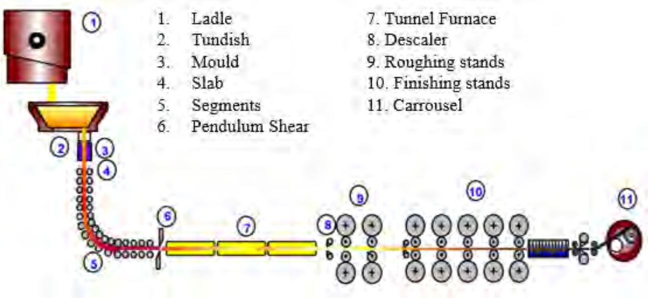

Figure 1: Hot strip mill, Port Talbot

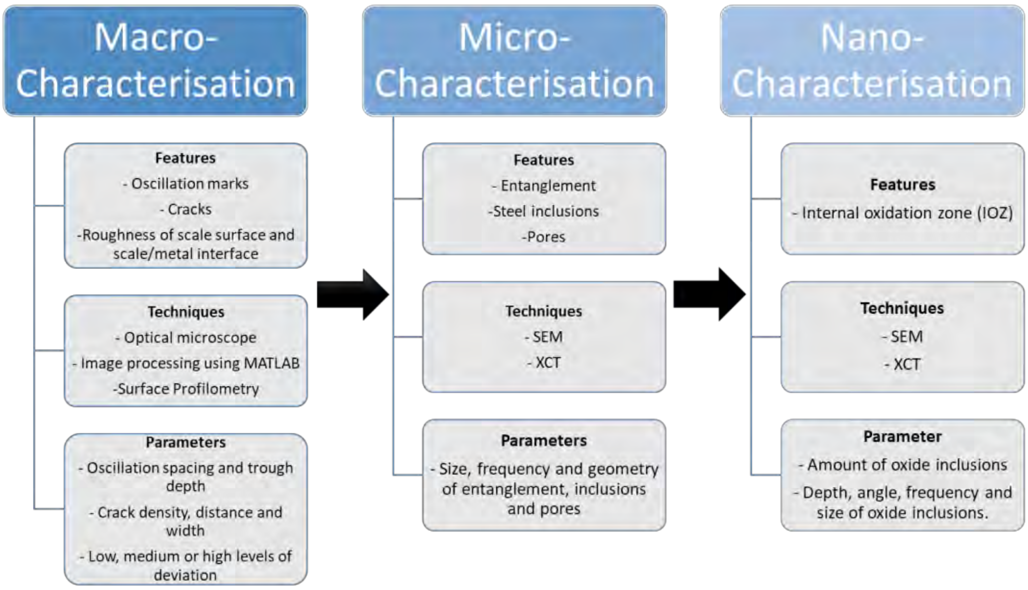

Figure 2: Steel block surface and cross-sectional analysis approach

2. EXPERIMENTAL

2.1 Material

The as-received steel slabs supplied by TATA steel, were cast in the Hot Strip mill (HSM) in Port Talbot. The chemical composition of the alloy is shown in Table 1.

Chemical analysis of the oxide scale was done using EDS. Different oxides across the oxide scale were identified by using a Renishaw inVia Reflex Raman Microscope with 4.5mW helium-neon laser (633 nm) at 10% power.

Table 1: Chemical composition of alloy

Material	Element	Fe	C	Al	Mn	Si	Cr + Cu + Ni
Silicon 1	**Wt. %**	Bal	0.015	0.34	0.184	2.41	<0.09

For electron microscopy, the steel slabs were cut into smaller pieces, and cross-sections metallographically prepared to mirror finish. For X-ray CT, cylindrical samples were cut to 3 mm diameter and 11 mm length using wired electrical discharge machining.

2.2 Oxide Characterisation

Electron microscopy was performed using a Zeiss Sigma scanning electron microscopy fitted with a field emission gun (FEG-SEM) operating at an accelerated voltage of 5 kV for imaging and 20 kV for EDS.

Surface and subsurface oxide phases (100 µm depth) were identified using XRD with Co K_α radiation. This was performed under the following conditions: current, 40 mA; acceleration voltage, 40 kV; step size, 0.013°. X-ray CT samples were scanned using a Zeiss Xradia 520 Versa to obtain a computed tomographic (CT) reconstructions of the oxide scale and scale/metal interface. Measurements of sample porosity and scale thickness were performed using the software packages 'Scout and Scan TM Control System and 'VG Studio MAX', respectively. The parameters for each scan were kept constant as detailed in Table 2.

Table 2. Scanning Parameters

Voltage (kV)	140
Power (W)	9.9
Exposure (s)	10
Projections	1600
Filter (mm, Cu)	HE4
Voxel Size (microns)	1.5476

2.3 Statistical analysis of the oxide interface

A MATLAB code, based on Hotar [3], was developed to extract the oxide/interface from SEM images of the interface collected over 1 mm. Average surface roughness (R_a) value were also calculated.

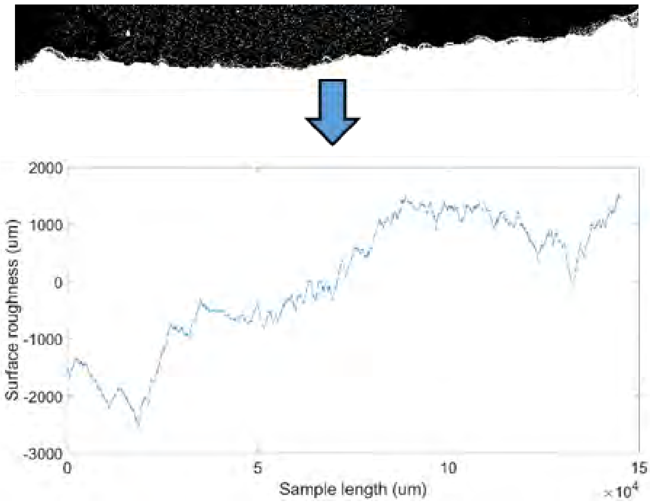

Figure 3: Extracted scale/metal interface profile using MATLAB

Fractal dimension (FD) were employed to quantify the complexity of the oxide/substrate interface using the 'compass method' [4-6] according to:

$$D_r = 1 - s = 1 - \frac{\Delta Log_2 L(r)}{\Delta Log_2 r} \quad (1)$$

where L is the length in i-step of the measurement and r_i is the ruler size. D_R is the fractal dimension when using the compass method. The ratio between $Log_2L(r_i)$ and Log_2r_i is known as the Richardson-Mandelbrot plot. D_r is determined from the gradients of its regression line (s).

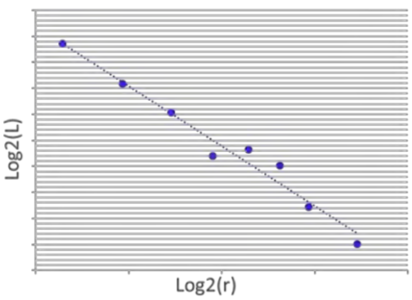

Figure 4: Estimation of the fractal dimension by the 'compass method'

3. RESULTS AND DISCUSSION

The typical cross-section of the as-cast oxide scale is shown in Figure 5.

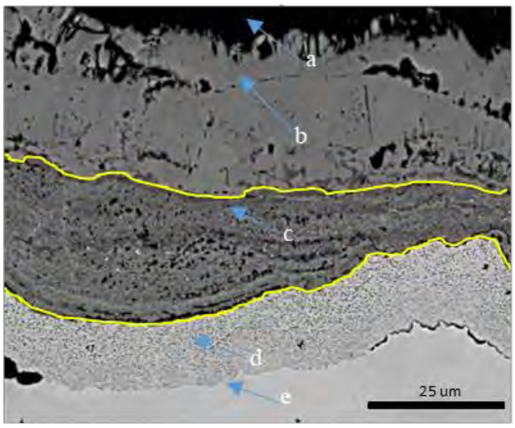

Figure 5: Cross section of As-cast oxide scale. a-mount, b-outer oxide, c-inner oxide, d-subsurface oxide and e-bulk steel.

SEM images coupled with EDS, Raman and XRD analysis, observed three distinct layers, with cracks observed in the outer oxide layers and small pores across the top two layers of the oxide. The maximum oxide thickness was approximately 53 µm. The outer oxide layer (b) typically had a thickness of 25 µm, which allowed for Raman analysis. Raman identified the outer layer as mostly hematite (Fe_2O_3) with strong peaks at 220 cm^{-1}, 290 cm^{-1} and 410 cm^{-1} and weaker peaks at 500 cm^{-1} and 610 cm^{-1} (Figure 7a). EDS analysis (Figure 6) confirmed that the outer oxide layer (b) is an iron oxide which is shown by the area above the yellow line (Figure 5). The inner oxide layer (c) consisted mainly of magnetite (Fe_3O_4) and fayalite (Fe_2SiO_4) (Figure 5), shown by strong peaks at 310 cm^{-1}, 540 cm^{-1} and 610 cm^{-1} and small fayalite peaks at 810 cm^{-1} and 840 cm^{-1}. The presence of fayalite in this area was also confirmed by the EDS analysis (Figure 6) which detected silicon in this region. Below the inner oxide, another subsurface oxide is present (d), where silicon and oxygen has diffused within this region. Although confirmed by EDS, the nature of the oxide is yet to be determined. The XRD surface analysis confirmed the presence of magnetite, hematite and small peaks of fayalite and iron substrate (Figure 7c).

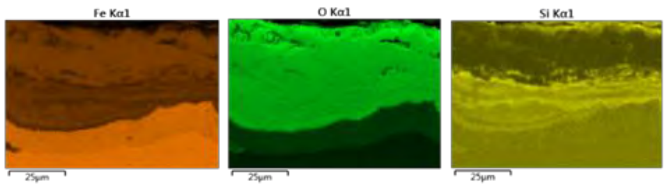

Figure 6: EDS map of oxide scale

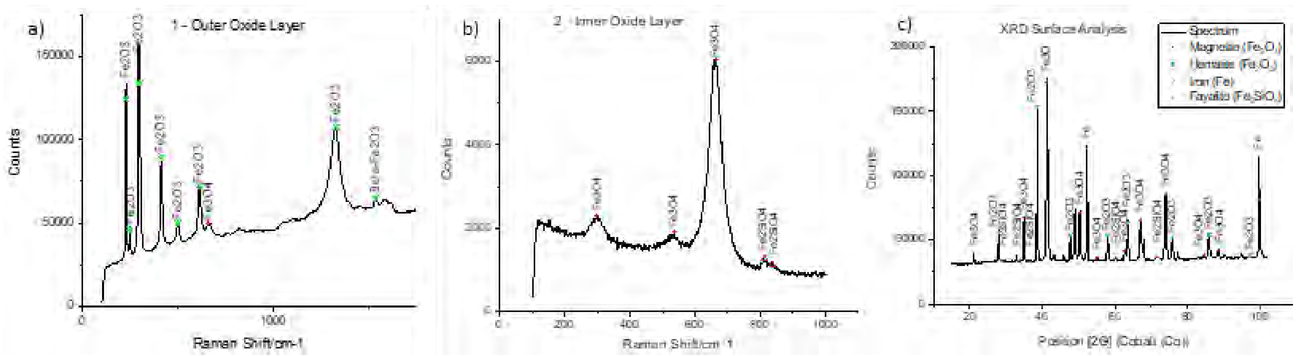

Figure 7: a) Raman Spectroscopy of inner oxide layer, b) outer oxide layer and c) XRD of surface and subsurface analysis of oxide layer

A X-ray CT scan, (Figure 8), showed that the oxide layer is present nearly everywhere on the sample when viewed in 3D (left). In the 2D view (right), one CT scan frame representing a cross-section, revealed non-homogeneity of thickness ranging between 0 to 50 µm.

Figure 8: 2D (right) and 3D (left) of oxide layer using X-ray CT.

3.1 Result of statistical analysis of the interface

The image size and resolution have a huge impact on the surface feature detected. The SEM image stitch provided a more detailed image than the X-ray CT 2D image and hence, a more defined scale/metal interface profile. This effected the calculated roughness but not the FD values (Table 3). When FD equals 1, this would signify that the interface is a straight line although in reality this is not the case. Moreover with a lower spatial resolution, the X-ray CT 2D profile is less defined and interfacial features are lost. By obtaining roughness and FD data (Table 3) in conjunction with other parameters, the methodology has the potential to predict descalability of oxide scale.

Table 3: Surface roughness parameters

	X-ray CT	SEM
FD	1.0	1.1
R_a (um)	9.06	965
Spatial resolution (um)	1.57	0.015
Image size (pixel)	641 x 1502	57344 x 5305

4. CONCLUSION

The combination of SEM, EDS, Raman and XRD have collaboratively aided in confirming the presence of specific iron oxides. X-ray CT results show that when the contrast between the oxide layer and bulk steel is well defined, surface area quantification can be achieved in three dimensions. Roughness and fractal dimensions allow to quantify the complexity of the scale/metal interface and associate the data with potential descalability. This information can aid in identify how this interfacial structure changes upon oxidation although the effects of lateral resolution and contrast settings must be identified before the full potential of the tool can be explored. This is significant in obtaining a true depiction of the interface as low lateral resolution shown (see Figure 8) could skew the data. The strategy of combining these techniques allows a comprehensive characterisation of oxides and interfaces to be developed.

ACKNOWLEDGEMENTS

The authors are extremely gratefully to David Walker for XRD characterisation, B G Breeze (Spectroscopy Research Technology Platform) for Raman characterisation assistance and Remy Guillaume for X-ray CT characterisation.

REFERENCES

1. Ormerod, R., et al., *Effect of process variables on scale formation in steel reheating.* The Canadian Journal of Chemical Engineering, 1997. **75**(2): p. 402-413.
2. Alaoui Mouayd, A., et al., *Effect of silicon content in steel and oxidation temperature on scale growth and morphology.* Materials Chemistry and Physics, 2014. **143**(3): p. 996-1004.
3. Hotař, V. and A. Hotař, *Fractal dimension used for evaluation of oxidation behaviour of Fe-Al-Cr-Zr-C alloys.* Corrosion Science, 2018. **133**: p. 141-149.
4. Peitgen, H.-O., H. Jürgens, and D. Saupe, *Chaos and fractals: new frontiers of science*. 1991, New York: Springer-Verlag.
5. Mandelbrot, B.B., *The fractal geometry of nature*. 1982, San Francisco: W. H. Freeman.
6. Evertsz, C.J.G.E., et al., *Fractal geometry and analysis : the Mandelbrot festschrift*. 1996: World Scientific.

PREVENTING OXIDATION AND CONTROLLING DECARBURISATION IN HOT ROLLING, HOT FORGING AND HEAT TREATMENT

By S.P.Shenoy, Srikar Shenoy**

UNDERSTANDING OXIDATION AND DECARBURIZATION

When steel is heated in an open furnace in the presence of air or products of combustion, two surface phenomena take place: 1. Oxidation 2. Decarburization.

OXIDATION

Oxidation of steel is caused by oxygen, carbon dioxide and/or water-vapour. The general reactions are given below :

$$O_2 + 2\,Fe \rightleftharpoons 2\,FeO$$

$$O_2 + 4\,FeO \rightleftharpoons 2\,Fe_2O_3$$

$$CO_2 + Fe \rightleftharpoons CO + FeO$$

$$CO_2 + 3\,FeO \rightleftharpoons Fe_3O_4 + CO$$

Oxidation of steel may range from a tight, adherent straw-coloured film that forms at a temperature of about 180°C to a loose, blue-black oxide scale that forms at temperature above about 450°C with resultant loss of metal.

DECARBURIZATION

Decarburization or depletion of surface carbon content takes place when steel is heated to temperatures above 650°C. It progresses as a function of time, temperature and furnace atmosphere. Typical reactions involved are:

$$O_2 + C \rightleftharpoons CO_2$$

$$O_2 + Fe_3C \rightleftharpoons 3\,Fe + CO_2$$

$$CO_2 + C \rightleftharpoons 2\,CO$$

$$CO_2 + Fe_3C \rightleftharpoons 2\,CO + 3\,Fe$$

$$H_2O + Fe_3C \rightleftharpoons CO + H_2 + 3\,Fe$$

The equilibrium relationship depends on the ratio of carbon dioxide to carbon monoxide. It is neutral to a given carbon content at a given temperature.

HARMFUL EFFECTS OF OXIDATION AND DECARBURIZATION

Oxidation leads to loss of dimensions and material as extra material allowance needs to be kept for scaling. Often, surface quality is deteriorated due to pitting. Metallurgical transformation during austenitising and quenching may be non-uniform. Surface hardness and strength are also lowered. Fatigue life of heat treated product is reduced. This is especially true in the case of automobile leaf springs.

PREVENTING OXIDATION AND DECARBURIZATION

Prevention of oxidation and decarburization is not only better than cure, it is profitable too. There are several ways to address problems caused by the two harmful phenomena. Decarburized surface removal by machining operations after heat treatment, copper plating of thickness upto 0.025 mm prior to heat treatment or change of heating media to molten salt bath are some ideas. A number of protective atmospheres may be introduced like dissociated ammonia, exothermic gas, nitrogen and endothermic gas. Fluidized bed furnaces and vacuum furnaces are becoming increasingly popular. Switching over to grades which do not require heat treatment is possible in some cases. Availability of capital and highly trained human resource and compliance to stringent safety norms for using high-end furnaces are the major issues. Many small heat treatment shops cannot afford these solutions. Yet they are under mounting pressure to prevent oxidation and decarburization. Use of protective anti-scale coatings has proven to be a logical solution to the problems of scaling and decarburization.

INSIGHTS INTO USE OF PROTECTIVE COATING AND ITS CHARACTERISTICS

An anti-scale coating is applied on components or billets to be heated before charging them into furnace. This anti-scale coating acts as a barrier to diffusion of oxygen and other gases. Care should be taken to apply a uniform, impervious layer of coating. Anti-scale coating also reduces decarburization on billets and ingots during hot forging and hot rolling operations. Heat transfer from heating media to metal is not affected due to anti-scale coating.
No reaction with steel surface, no release of toxic fumes during storage or use, and economical implementation are other required characteristics of the coating. Coated tools and components can be heat treated in air using a box type or bogie hearth; electric, gas or oil fired furnace.

Industrial case studies by the use of protective coatings:

Grade of steel hot rolled: EN-31

Thick adherent scale is observed on billets when coating is not used.

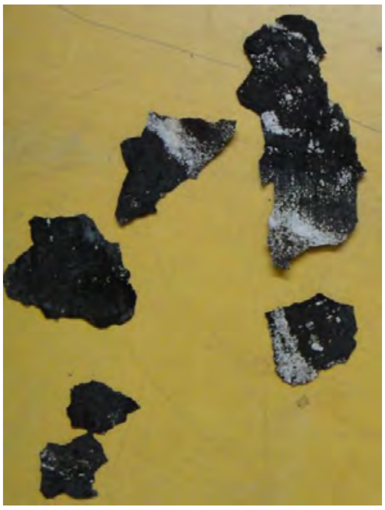

Thin, loose scale is observed on billets when ESPON coating is used. White layer of coating residue is observed on scale. This indicates efficacy of coating.

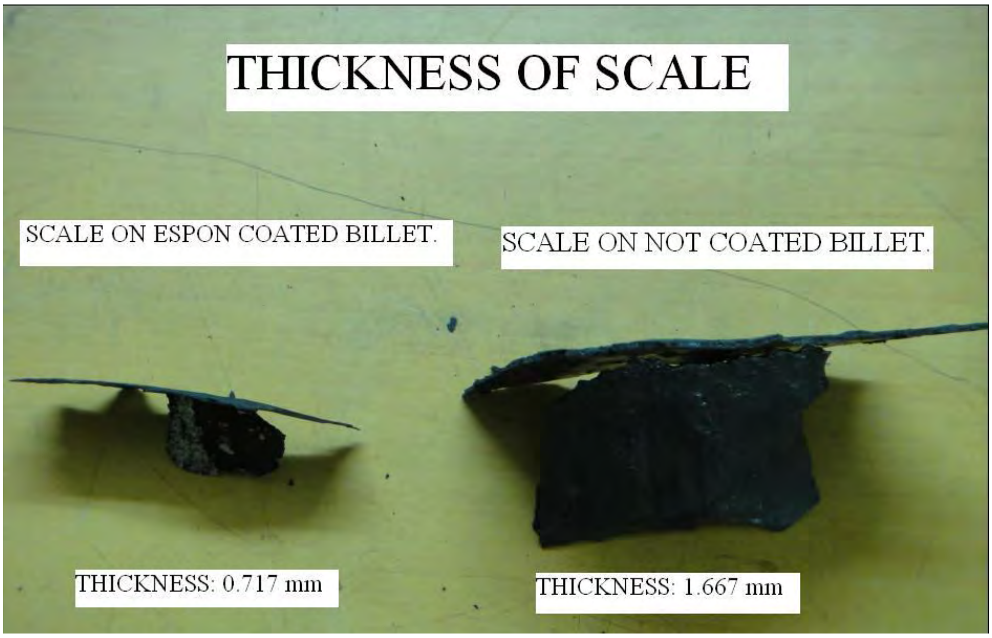

Scale thickness is measured by use of digital vernier calliper.
Total reduction in scale: **0.95 mm.**
Percentage reduction in scale loss: **56.98%**

Grade of steel hot rolled: EN-1A (Leaded)
Thick adherent scale when not coated v/s thin loose scale when coated.

Billet heated without coating:

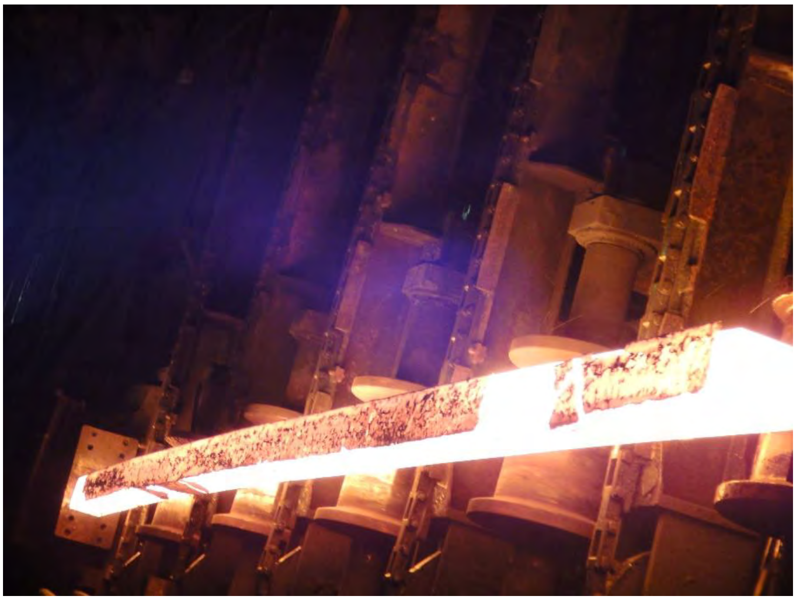

Photograph shows not coated billet on conveyor, discharged from furnace and passed through water de-scaler. As thick, adherent scale was formed, water de-scaling has not been effective. Adherent scale is observed on the top surface and some adherent scale on the left side surface.

Billet heated after protecting with anti-scale coating:

Photograph shows ESPON coated billet on conveyor, discharged from furnace and passed through water de-scaler. Complete scale has fallen off during water de-scaling. This proves that scale loss is reduced. Ease of rolling operation and reduced scale deposits on the rolling mill machinery are ensured.

Other case studies to be presented:

- Scale prevention in hot levelling of critical grade of steel
- Scale prevention in heat treatment
- Salvaging of rejected components by re-heat treatment
- Controlling decarburisation in hot rolling of rail steel and spring steel
- Scale prevention in open and closed-die hot forging

SUMMARY

- Use of anti-scale protective coating is an effective technique of preventing oxidation and decarburization during hot rolling, hot forging and heat treatment.

- It has unleashed a number of benefits like ability to salvage rejected components/forgings by re-heat treatment/re-working, reduction of post heat treatment operations like grinding, shot blasting, acid pickling, etc.

- The coating process has simplified and accelerated many metallurgical heat treatment operations, saving a fortune in capital investment, reducing costs and improving quality.

* Directors, M/s. Steel Plant Specialities LLP, Mumbai, India.

Control of galvanizing process using oxidation thickness measurement inside furnace

C.Plancq, L.Bordignon, G.Monfort, G.Moreas, V.Tusset, X.Vanden Eynde

CRM Group, Liege, Belgium

1. Context

The production of galvanised Advanced High Strength Steels (AHSS), with high Mn, Cr, Al and Si content has significantly increased these last years.
Although adequate mechanical properties are achieved with these grades, the external selective oxidation of alloying elements significantly hampers the reactivity during hot dipping leading to bad liquid zinc wetting which induces the formation of bare spots and/or weak coating adherence.
To solve these problems, the chosen solution consists in the oxidation of the strip during heating or during the fast cooling steps of the process (in this last case an overaging step with high hydrogen content is required for the reduction before the bath). This initial oxidation is necessarily followed by a reduction in a hydrogen-rich atmosphere, resulting into the formation of a pure metallic iron at the uppermost surface level.
For optimised process operation, the expected iron oxide layer must be thick enough to limit further segregation of alloying elements to the top surface and sufficiently thin to avoid iron pick-up on the furnace rolls.
For on-line analysis in industrial lines, CRM Group has developed an on-line sensor, based on reflectance spectroscopy that allows the continuous measurement of this iron oxide layer for most steel grades including AHSS. This continuous measurement leads to a better product quality.

2. Objectives

The control of the oxide and the temperature of the strip are the main objectives of this sensor:

- Measurement of iron oxide thickness on cold or heated metal sheet
- Measurement of the temperature of this sheet

3. Principle

This sensor is based on two measurement methods.

The first technique uses the reflectance spectroscopy. The strip is illuminated by a white light then the reflection of the light on the strip is captured by a spectrometer (see **Figure 1**). The light is partially reflected on the air/oxide interface and partially reflected on the oxide/steel interface.

Those multiple reflections produce constructive and destructive interferences. The interferences induce extrema in the reflectance curve as a function of the wavelength. It can be shown that the thickness of the oxide is linked to the position of the extrema.

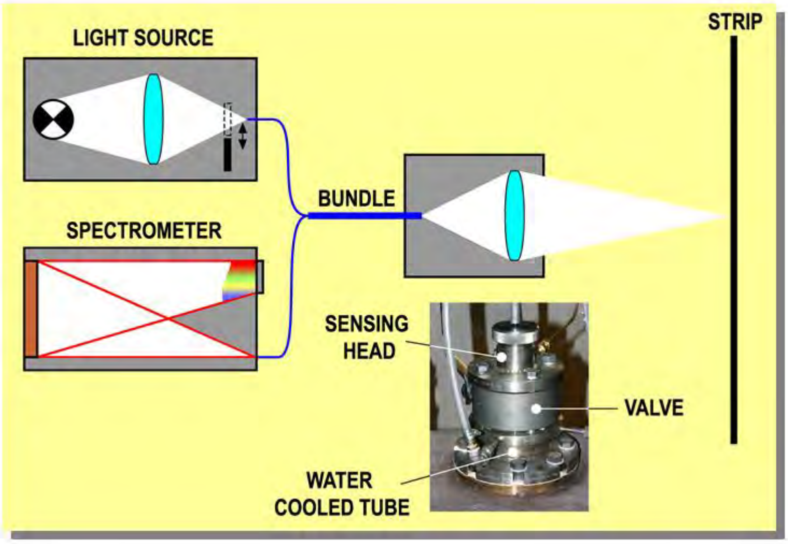

Figure 1: *Layout of the reflectance spectroscopy method*

A simple relationship has been determined and verified between the thickness, the refractive index of the oxide, the position of the extrema and the order of the extrema (see **Figure 2**).

This works well for short distance (270mm) from the strip, even if the sensor has been successfully tested at distances up to 1500 mm. A shutter enables to remove the radiated light coming from the heated strip and consider only the light reflected by the strip.

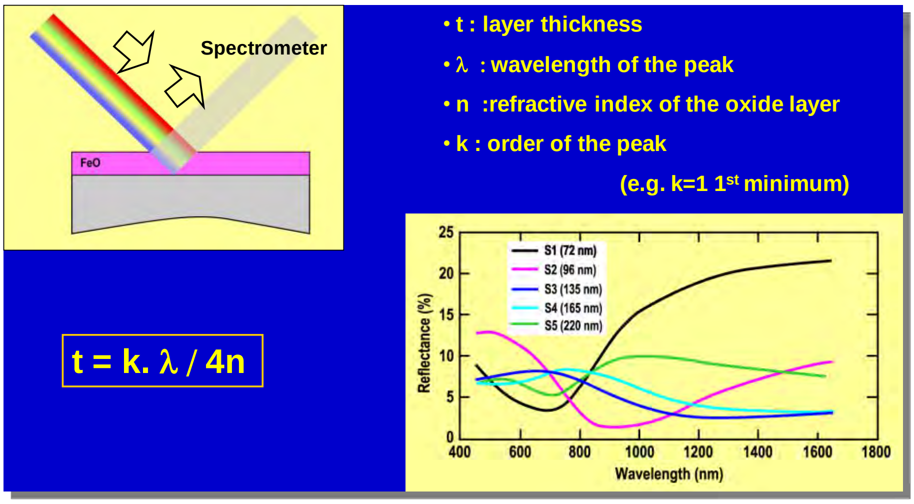

Figure 2: *Principle of the reflectance spectroscopy method*

This simple relation works only for transparent oxides, but other types of oxides or coatings can be measured or at least characterized in the same way using dedicated algorithm.

The second measurement is temperature evaluation. The strip will be considered as a black-body. So the Plank's law (**Figure 3**), giving its spectroscopic thermal radiation, can be directly fitted on the measurement.

This will be used to calculate the local temperature of the strip. Nevertheless, the location and stability of the aimed target point can have a big influence on the results. The interpretation of the measurements has to take this fact into account.

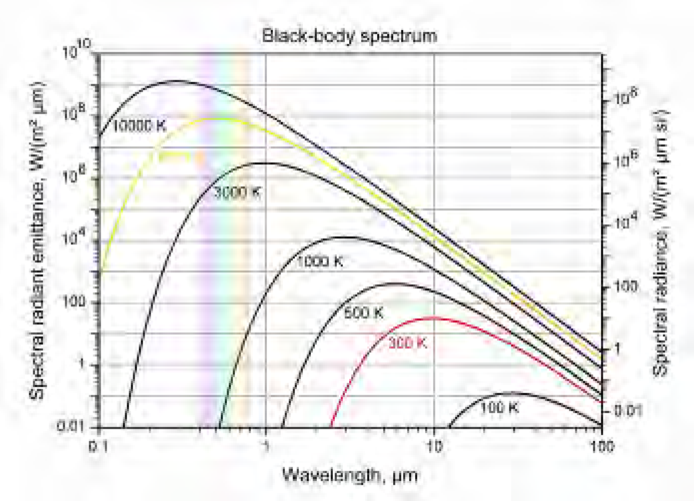

Figure 3: *Thermal radiation emitted from a black-body*

Planck's Law :

$$L^{\circ}_{\Omega,\nu}(\lambda,T) = \frac{2\,hc^2}{\lambda^5}\frac{1}{e^{\frac{hc}{\lambda kT}}-1}$$

Wien approximation :

$$\lambda_{max} = \frac{hc}{4.9651\,kT}$$

λ : wavelength (m)
c : speed light in vacuum = 2.99 10^8 m/s
h : Planck's constant = 6.62 10^{-34} Js
K : Boltzman's Constant = 1.38 10^{-34} J/K
T : Temperature (K)

A calibration has been done in CRM to transform the spectrum into the Planck's law. Once the Planck's Law is known, the maximum is linked to the temperature obtained from the Wien approximation.

4. Measurement results

This sensor is composed of 2 spectrometers, 2 lighting systems, an optical fibre bundle, a PC, an optical lens, a water cooled tube.
- The distance to the sheet must be as short as possible (ideally 270mm)
- No special safety features are required

Working distance	Usually 270mm (but other distances are possible)
Range	70-250 nm thickness 400-800 °C temperature
Precision	+/-10% (thickness)
Frequency	1 measurements/second
Product speed	Measurement up to 1000m/min
Surface type	clean surfaces

Table 1: *OTTM Characteristics*

Figure 4: *OTTM installed on a line*

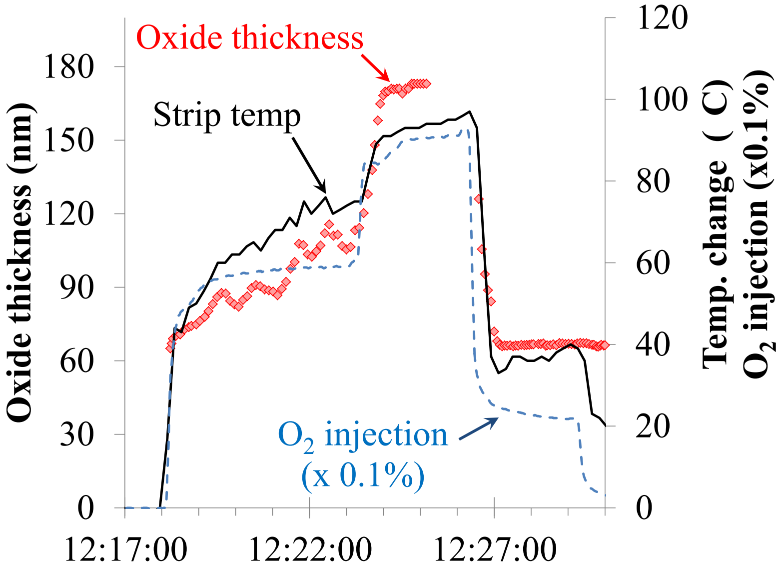

Figure 5: *OTTM measurements*

As shown in Figure 5, related to trials on the CRM pilot line, the strip temperature and the oxide thickness are clearly linked with the O2 percentage. When the oxygen percentage is constant at 2% the thickness is around 60 nm. This Figure shows how the oxide thickness can be monitored.

5. Conclusion

Actual high alloyed steels are difficult to galvanise. They require an oxidation step to selectively oxidise iron and then a reduction of this oxide to let a pure porous iron layer, easy to galvanise. This leads to a better galvanising process

The sensor described here enables an online and real time fine measurement of oxide thickness and temperature of the strip in a furnace (direct fired furnace, inductive...). This enables a fine control of the oxidation step to improve the product quality.

New coatings can be characterized online during the production. This leads to better production repeatability in time, a better homogeneity in the longitudinal direction. If the sensor is placed on a moving support, the transverse homogeneity can be checked. In some cases, the sensor can be inserted in a control loop allowing the regulation of the process.

Interfacial oxidation in processing of nanocrystallised metallic materials using duplex technique - experimental and modelling aspects

Michal Krzyzanowski[1,3], Delphine Retraint[2], Szymon Bajda[1],

[1] AGH University of Science and Technology, Faculty of Metals Engineering and Industrial Computer Science, Mickiewicza 30, Krakow 30-059, Poland.
[2] Institute Charles Delaunay, CNRS UMR 6281, LASMIS, University of Technology of Troyes, 10000 Troyes, France.
[3] Birmingham City University, Faculty Computing, Engineering & the Built Environment, Millennium Point, Curzon Street, Birmingham B4 7XG, UK

Abstract

Duplex techniques are attempted to be developed combining nanocrystallisation processes with a subsequent thermomechanical processing in order to produce multilayered bulk structures with improved yield and ultimate tensile strengths, while conserving an acceptable elongation to failure Fig. 1a and b [1 - 4]. However, bonding imperfections at the interfaces due to interfacial oxidation among other reasons during the duplex process can significantly influence the final properties. Moreover, the interface oxidation occurring during duplex processes influences microstructure development around the interfaces depending on whether the oxide scale is a continuous layer or a layer of discontinuous oxide clusters with heterogeneous thicknesses. Effectively the oxide scale becomes a part of microstructure development in such nano-crystallised multilayered structures. This paper deals with understanding of the underlying events around the highly reactive interfaces explaining the microstructure evolution applying advanced experimental and numerical modelling techniques. The research encompassed surface mechanical attrition treatment followed by constrained compression testing and hot rolling of the assembly of steel strips supported by multilevel numerical analysis using combined finite element (FE) and cellular automata (CA) methods. Shear banding has been observed near metal-metal contact between the oxide clusters at the interfaces (Fig. 1c). The shear banding can be considered as bonding enhancement creating channels for the base metal of the different laminates to come into contact through the oxidised interface. Temperature, texture and grain refining are among the factors influencing the shear banding. In the simulations, the meso-level of the developed multi-level FE-based model is combined with the advanced 3D frontal CA numerical model allowing for both appearance of the new boundaries and rotation of dislocation cells (sub-grains and grains) simultaneously (Fig. 1d).

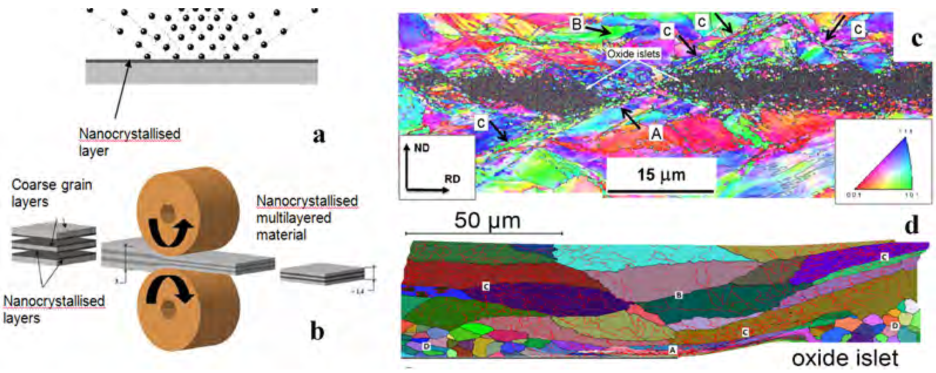

Fig. 1 Duplex technique components (a, b), EBSD orientation map of the cross section (c) and microstructure of 316L predicted near the oxidised interface (c).

References:

1. Bajda S., Svyetlichnyy D., Retraint D. and Krzyzanowski M.: *Int J of Adv Man Technol,* 96(5-8), 2018, 2893-2905.
2. Bajda S., Ratuszek W., Krzyzanowski M. and Retraint D.: *Surf and Coat Technol*, 329, 2017, 202-211.
3. Bajda S., Krzyzanowski M., Kwiecien M., Majta J., Lisiecki L., Sroka J.: *Comp Meth in Mater Sci*, 16(2), 2016, 76-86.
4. Bajda S., Krzyzanowski M., Muszka K. and Rainforth W.M.: *Surf and Coat Technol*, 277, 2015, 170-180.

Understanding Oxide Scale on Nickel Based Superalloys to Help in Life Predictions for Gas Turbine Components

Jonathan Wells, Siemens Industrial Turbomachinery Limited

As operating temps for gas turbines have increased, with the overall aim of increasing turbine efficiency, there has been a greater need to understand oxidation for life limiting hot gas path section components. This paper gives an overview of an industrial methodology for designing and making life calculations for components in extreme environments. The limitations of laboratory testing and extrapolating laboratory data to real service conditions are explored, along with potential techniques for improving correlations.

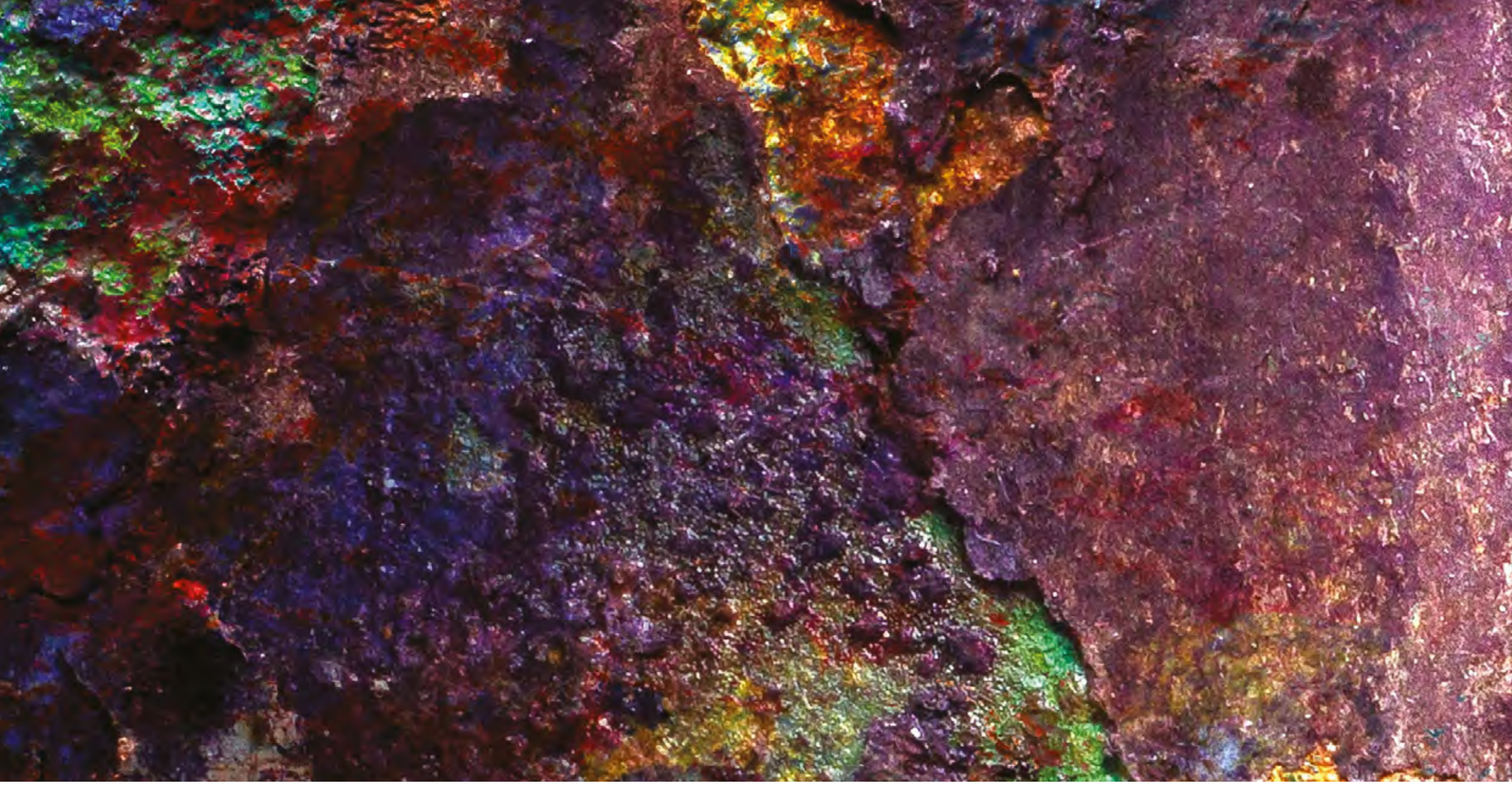

Organised by

Bulk Metal Forming Committee

of the Materials Science and Technology Division

IOM3 The Institute of Materials, Minerals and Mining

With thanks to our sponsors

TATA

HYDROWATT Descaling Pumps

Spraying Systems Co.®

ENGINEERING YOUR SPRAY SOLUTION LECHLER

SPS STEEL PLANT SPECIALITIES LLP

Organised by IOM Communications on behalf of the Institute of Materials, Minerals and Mining (IOM3), Registered Charity No 269275.
IOM3, 297 Euston Road, London NW1 3AD, UK Tel: +44 (0)20 7451 7300 www.iom3.org